Thesis for the Master of Science degree in Molecular Biosciences
Main field of study, Biochemistry

Investigating BEACH domain containing proteins for a role in autophagy

Petter Holland
University of Oslo
June 2012

Department of Molecular Biosciences
Faculty of Mathematics and Natural Sciences
University of Oslo

Department of Biochemistry
Faculty of Medicine
University of Oslo

Acknowledgements

This work was performed in at the Department of Biochemistry, Institute of Basic Medical Sciences at the University of Oslo from January 2011 to June 2012. First and foremost I want to thank my main supervisor, Associate professor Anne Simonsen. You have created a very stimulating environment to learn about both the theoretical and practical sides of science. I am privileged to be training in such an ambitious and helpful research group and I am very grateful for the hard work you put into reviewing and discussing manuscripts, theories and results. I am also grateful to my co-supervisor Serhiy Pankiv for all the help you have given me during day-to-day theoretical and experimental troubles. By giving me assistance when I needed it while also giving me freedom to explore my own ideas you have both allowed me to build confidence in myself as a scientist and given me a great platform for further development. I am also grateful for Kristian Prydz being my internal supervisor at the Department of Molecular Biosciences.

I want to thank the rest of the people in our research group. Even though you are all very busy with your own projects, you always take the time to help when there is need for it. There is a wide range of knowledge in the group to learn from and I greatly appreciate the help I have received in learning various techniques. There is also a great social environment in the group that is appreciated and makes the long days so much more enjoyable.

Friends and family have also been of great support during these years, as they always are. My friends help me separate myself from the world of science every once in a while. My family is always there as support while also pushing me to reach my goals in life. The biggest thanks of all I owe to my girlfriend Malin who allows me the flexibility to put in the necessary hours of work and together with my daughter Synne you create the home that I am always eager to get back to.

Oslo, June 2012
Petter Holland

Table of contents

Abbreviations

AKAP	A-kinase anchor proteins
ALFY	Autophagy-linked FYVE domain containing protein
Ams1	Alpha mannosidase 1
ApeI	Aminopeptidase I
ARG	Autoradiography
Atg	Autophagy-related
Baf A1	Bafilomycin A1
BCL2	B cell lymphoma gene 2
bchs	Blue cheese
BEACH	Beige and Chediak-Higashi
Bph1	BEACH protein homolog 1
BSA	Bovine serum albumin
C-terminal	Carboxy terminal
CD40 (L)	Cell differentiation factor 40 (ligand)
CHS (1)	Chediak-Higashi syndrome (1)
Cvt	Cytoplasm to vacuole targeting
DMEM	Dulbeccos modified eagle medium
DTT	Dithitreitol
EBSS	Earls balanced salt solution
EDTA	Ethylenediaminetetraacetic acid
EGF (R)	Epidermal growth factor (receptor)
ER	Endoplasmatic reticulum
ERK1	Extracellular signal regulated kinase 1
FAN	Factor associated with neural sphingomyelinase
FBS	Fetal bovine serum
FIP200	Focal adhesion kinase family interacting protein of 200kD
FYVE	Fab1 YOTB Vac1 EEA1 domain
GST	Glutathion S-transferase
MBP	Maltose binding protein
MHC	Major histocompatability complex
Keap1	Kelch-like ECH-associated protein 1
KIR	Keap1 interacting region
LB	Liquid broth
LC3	Microtubule-associated protein 1, light chain 3
LvsA/B	Large volume sphere A/B
LYST	Lysosomal trafficking regulator
LIR	LC3-interacting region
LRBA	LPS-responsive and beige-like anchor protein
mTORC1	Mammalian target of ramapycin complex 1
N-terminal	Amino terminal

NBEA	Neurobeachin
NBEAL1	Neurobeachin-like 1
NBEAL2	Neurobeachin-like 2
NBR1	Neighbor of BRCA1 gene protein 1
NDP52	Nuclear domain 10 protein 52
NF-κB	Nuclear factor κB
Nix	NIP3-like protein x
Nrf2	Nuclear factor-like 2
PB1	Phox and Bem1
PBS(-T)	Phosphate buffered saline (with Tween)
PCR	Polymerase chain reaction
PE	Phosphatidylethanolamine
PFA	Paraformaldehyde
PH	Plecstrin homology
PI3K	Phosphoinsositide 3-kinase
PI(2,4)P	Phosphatidylinositol 2,4-phosphate
PI(3)P	Phosphatidylinositol 3-phosphate
PKCζ	Protein kinase C zeta
PTEN	Phosphatase and tensin homolog
RIP	Receptor interacting protein
ROS	Reactive oxygen species
SDS	Sodium dodecyl sulfate
SO B/(C)	Super optimal broth (with catabolite repression)
SQSTM1	Sequestosome 1
Stbd1	Starch-binding domain containing protein 1
TB	TRAF6 binding domain
TBC	Tre-2 BUB2p and Cdc16p domain
TGN	Trans-golgi network
Tm	Melting temperature
TNF	Tumor necrosis factor
TRAF6	TNF receptor associated factor 6
Tris	Tris(hydroxymethyl)aminomethane
TSC1/2	Tuberous sclerosis protein 1/2
UBA	Ubiquitin associated domain
Ulk1	Unc51-like kinase
Vps	Vacuolar protein sorting
WDFY3/4	WD40 and FYVE domain containing protein 3/4
ZZ	Zinc-binding zing finger domain

Summary

The BEACH domain is common for a protein family that has expanded through eukaryotic evolution and contains eight human proteins. These proteins are generally very large and at their C-terminal ends contain a conserved set of domains, a PH-like domain directly followed by a BEACH domain and a WD40 domain. Outside the recognized C-terminal domains, the rest of the proteins are weakly conserved and few functional domains have been recognized. According to their phylogenetic relationship they can be divided into four subfamilies with two closely related proteins in each. ALFY and WDFY4 make up one of these subfamilies where ALFY has been shown to be involved in degradation of protein aggregates, suggesting misregulation of ALFY might contribute to neurodegeneration. NBEAL1 and NBEAL2 form another closely related pair and little is known about these proteins, but recently mutations in NBEAL2 was shown to be causative for the bleeding disorder grey platelets syndrome. LRBA and NBEA are the most studied BEACH proteins and whereas LRBA is implicated in cancers of various types, NBEA is essential for neuromuscular transmission and correlated to autism. LYST and FAN form the final subclass of BEACH proteins. FAN is exceptional in being much smaller than the others, and LYST is well known because mutations in this protein causes Chediak-Higashi syndrome. In summary, the eight BEACH proteins are correlated to a varied set of diseases and studies of their cellular functions so far suggests they have little in common, although some BEACH proteins have been poorly studied. The BEACH domain is highly conserved through the protein family, but the function of the domain is not known.

For ALFY, a region of the protein containing the PH-like and BEACH domains has been shown to interact with the ubiquitin-binding protein p62. p62 associates with misfolded and mutant aggregating proteins to aid in their controlled aggregation to form ubiquitinated p62 bodies, which can be targeted for degradation in the acidic interior of the lysosome. Lysosomal degradation in this case starts with de novo formation of a double-membrane structure that surrounds p62 bodies, sequestering them from the rest of the cell and eventually fusing with a lysosome where they are exposed to degrading hydrolases. This process is called macroautophagy and ALFY is linked to this process by its interaction with p62, but also by interacting with other components of the autophagic machinery through its WD40 and FYVE domains. Through this project we have found that the PH-BEACH domains of several BEACH proteins co-localize and interact directly with p62. The results indicate that BEACH proteins of all subfamilies interact with p62 through a groove formed between the PH-like and BEACH domains where residues from both domains seem to contribute to the interaction. Furthermore, autophagy assays were performed to study a possible role for the BEACH proteins in autophagy. Knockdown of the proteins seems to not influence the rate of starvation-induced autophagy, but might influence the turnover of p62 under conditions of basal selective autophagy. Another screen for involvement in autophagy was performed by investigating localization of endogenous BEACH proteins in cell culture upon autophagy-promoting stressors. The results showed that puromycin-induced aggregation of misfolded proteins causes a clear recruitment of several of the BEACH proteins to the p62 bodies, indicating that similar to ALFY, other BEACH proteins may play a role as scaffolding proteins involved in selective autophagy.

1. Introduction

1.1 AUTOPHAGY

Autophagy is a catabolic mechanism of the cell that allows recycling of organelles and macromolecules into their constituent building blocks. The word autophagy means ‘self-eating’ (from greek *auto phagin*) and the process involves hydrolysis of the cells own biomolecules in the acidic interior of the lysosome. There are three different basic types of autophagy. Microautophagy involves invagination of the lysosomal membrane to isolate and degrade cytoplasmic content. Chaperone-mediated autophagy is a direct import of cytosolic proteins into the lumen of the lysosome and relies upon a chaperone complex that selects for the targeted proteins, allows their unfolding and further by interacting with the lysosomal membrane protein Lamp2a, translocation into the lumen of the lysosome. The third type of autophagy, macroautophagy, is the one that is most studied and is illustrated in Figure 1. Macroautophagy starts with the formation and expansion of a small double-membrane structure called the phagophore. As it fuses around a substrate, isolating it from the rest of the cell, it becomes an autophagosome. The outer memebrane of the autophagosome can fuse with endocytic compartments, forming amphisomes or it can directly fuse with a lysosome, forming an autolysosome. In the autolysosome, the lysosomal hydrolases gain access to the inner membrane vesicle of the autophagosome, degrading it and anything contained in its lumen. The products of this degradation are relased to the cytosol by permeases in the lysosomal membrane. This thesis focuses only on macroautophagy and it will hereafter be referred to simply as autophagy.

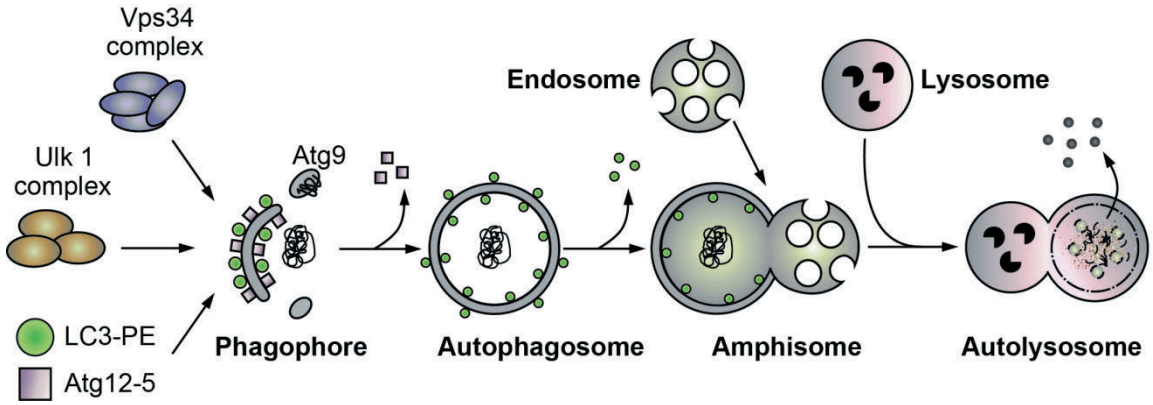

Figure 1: Autophagy in mammalian cells. Autophagosome formation is initiated by the nucleation of a phagophore membrane, which elongates and thereby sequesters parts of the cytoplasm into a double membrane autophagosome vesicle. Nucleation requires the Ulk1 and Vps34 complexes as well as the transmembrane protein Atg9. The two ubiquitin-like proteins Atg12 and LC3 and their conjugation systems are required for expansion of the phagophore. Atg12 is conjugated to Atg5 whereas LC3 is conjugated to the lipid phosphatidylethanolamine (PE) and therefore remains bound throughout the pathway. The autophagosomes mature by fusion with endocytic compartments to form amphisomes and finally lysosomes where the contained material is degraded.

An understanding of the molecular machinery involved in autophagy started with the identification of the autophagy-related (ATG) genes in yeasts (reviewed in [1]) as a set of proteins essential to survive nitrogen deprivation. Homologous Atg proteins have later been found in all eukaryotes and their importance demonstrated by knock-out studies. It has been shown that autophagy is important for cellular homeostasis and differentiation and at the organismal level for normal development and functioning [2]. Knock-out of central ATG genes in mice showed that during early development, autophagy is essential for survival of the neonatal starvation period [3] when amino acid supply through the placenta is lost. Similarly, autophagy allows other organisms to survive physiological phenomena that involve cellular starvation such as fruit body formation in slime mold, dauer formation in nematodes and sporulation in yeast [2]. Because knockout of key autophagy proteins leads to neonatal death, tissue-specific knockout of ATG genes have provided important information about the role of autophagy in vivo. Brain-specific knockout causes accumulation of damaged mitochondria and protein aggregates leading to neuronal death [4, 5]. Similarly, in liver tissue, loss of autophagy causes accumulation of protein aggregates and cell death [6]. These and other studies have shown that autophagy is involved in quality control of cellular components, including organelles. By such quality control, autophagy contributes to cellular homeostasis by degrading damaging or unneeded components like mitochondria [7], peroxisomes [8], ribosomes [9] and intracellular pathogens [10, 11] as well as protein complexes such as midbody remnants [12] and protein aggregates [13].

1.1.1 Core autophagic machinery

The observation that loss of autophagy has such dramatic and similar consequences in distantly related organisms highlights the fact that many proteins involved in regulation and execution of the process are conserved throughout eukaryotic evolution. Human orthologues of most yeast ATG genes have been identified, but in many cases these ATG orthologues were first discovered in other contexts and later linked to autophagy and the original naming is then most often preserved. In this discussion, human gene and protein names are used. Although there is a large variety in the inducing signals and substrates of autophagy, all known autophagosome formation requires four multi-subunit complexes, called the core autophagic machinery, as indicated in Figure 1; 1) The ULK1 (Unc51-like kinase, also called Atg1) complex, including Atg13, FIP200 (Focal adhesion kinase family interacting protein of 200kD) and Atg101. 2) The class III phosphatidylinositol 3 kinase (PI3K) complex I containing the catalytic subunit Vps34 and regulatory subunits 150/Vps15, Beclin 1 and Atg14L. 3) The ubiquitin-like molecules Atg12 and Atg8/LC3 (microtubule-associated protein 1, Light Chain 3) and their conjugation systems; the E1-like enzyme Atg7, E2-like conjugation enzymes Atg10 and Atg3, respectively, as well as the modifying protease Atg4, required for conjugation of LC3 to phosphatidylethanolamine (PE) and Atg5, the target of Atg12-conjugation. 4) The transmembrane protein mAtg9 and its associated membrane-cycling machinery.

The process of autophagy can be divided into three events; nucleation, expansion of the autophagosome membrane and autophagosome maturation. A tight regulation of nucleation is essential, and the mammalian Target Of Rapamycin Complex 1 (mTORC1) has been found to be a master negative regulator of this step. Its activation by amino acids and several growth stimulatory signals causes hyperphosphorylation of the ULK1 complex and thereby inhibition of

autophagy [14]. One of the complexes regulating nucleation is the class III PI3K/Vps34 complex I, which phosphorylate the lipid phosphatidylinositol to create phosphatidylinositol 3-phosphate PI(3)P. PI(3)P is otherwise commonly found on endosomes where it acts as a signaling lipid, involved in recruiting proteins containing FYVE (Fab1 YOTB Vac1 EEA1) domains [15]. Expansion involves growth of the double-membrane structure around the cargo to become degraded. The two ubiquitin-like conjugation systems are essential for this step. The Atg5-Atg12 complex interacts with membrane-bound Atg16L to form a high molecular weight complex which further allows conjugation of LC3 to PE [16], creating autophagosome-specific LC3-PE (also called LC3-II). The final event of autophagosome formation is maturation which involves transport of the autophagosome along microtubules and fusion to endocytic or lysosomal compartments.

1.1.2 Autophagy in health and disease

In addition to the requirement for autophagy during development and nutrient deprivation, autophagy is also upregulated during various cellular stressors, including infection, oxidative stress and accumulation of protein aggregates (reviewed in [17]). The aggregation of proteins into cytoplasmic complexes called inclusion bodies is a pathological feature of diseases known as proteinopathies, many of which are neurodegenereative diseases [18, 19]. In some cases, these diseases are linked to specific mutant proteins such as polyglutamine-extension in the huntingtin protein causing Huntington's disease and point mutations in α-synuclein and tau that cause dominant forms of Parkinson's disease and frontotemporal dementia, respectively. These mutations make the proteins more prone to aggregation and increasingly toxic for the cell [20]. The correlation between tendency for aggregation and toxicity seems to suggest that the inclusion bodies might themselves be toxic, but this is contradicted by several lines of evidence. Comparing different brain regions in individuals with these diseases showed that there is no clear correlation between amount of aggregates and cell death [21, 22]. Furthermore, studies on mutant huntingtin in cell cultures showed that cell death can be predicted by the amount of soluble mutant huntingtin and that formation of inclusion bodies is in fact protective [23]. Mutant huntingtin, α-synuclein and tau are all degraded by autophagy [13, 24] and studies of various other aggregation prone proteins have shown that the tendency to aggregate correlates to their dependence upon autophagy for degradation. This suggests that autophagy serves as a mechanism for the cell to degrade any aggregated proteins, but the role of autophagy in the mentioned diseases remains unclear.

Conditional knock-out of the core autophagic proteins Atg5 or Atg7 in mice brain or liver leads to accumulation of protein aggregates of non-mutant proteins in neurons and hepatocytes [5, 6], suggesting that autophagy serves a quality control function for any aggregating proteins in the cell. Misfolded proteins targeted for degradation are generally 'tagged' by ligation to several moieties of the small protein ubiquitin, which serves as a signal for their degradation in the proteasome [25] or by autophagy [26]. A set of proteins called autophagy receptors are essential for recognition and targeting of ubiquitinated proteins for autophagic degradation. The autophagy receptor p62 (also called SQSTM1, Sequestosome 1) localizes to protein aggregates of various types and has been used as a diagnostic marker of neurodegenerative diseases [27, 28]. Studies have shown that p62 is in fact involved in the formation of these ubiquitinated protein aggregates [29], most likely through homo-polymerization by its PB1 (Phox and Bem1) domain. Reduction

of p62 protein levels significantly increases cell death induced by mutant huntingtin expression [29], supporting that ubiquitinated huntingtin inclusions are neuroprotective and that p62 has a role in the formation of such inclusions. Interestingly, knock-down of p62 in mice with conditional knockout of Atg7 in the liver prevented aggregate formation and decreased the liver-pathology seen in autophagy deficient mice, while the neurodegeneration was not affected by the loss of p62 [30]. This suggests that accumulation of p62 caused by a decreased rate of autophagy can itself cause pathology in certain tissues but not in others. Because p62 is a substrate of autophagy and its levels are correlated to autophagic activity in the cell, this highlights the need to understand autophagy in a cell-type specific context.

Autophagy is a major catabolic pathway in the cell so it is not surprising that it is involved in regulation of cell growth, and as an extension of this, cancer. The first link between autophagy and cancer was the observation that the core autophagic protein Beclin 1 is monoallelically deleted in a large portion of breast, ovarian and prostate cancers [31, 32], suggesting that components of the core autophagic machinery can function as tumor suppressors. The autophagy inhibitor mTORC1 is an important positive regulator of cell growth in a diverse set of organisms [33]. Many tumor suppressor genes that are involved in upstream inhibition of mTORC1 signaling, such as PTEN (Phosphatase and tensin homolog), TSC1 and TSC2 (Tuberous sclerosis protein 1/2) stimulate autophagy while oncogenes activating the mTORC1 pathway, such as class I PI3K and Akt, inhibit autophagy [17]. The central tumor suppressor p53 is also a positive regulator of autophagy in DNA-damaged cells [34]. Interestingly, many anticancer therapies induce accumulation of autophagosomes in affected cells [35] and this was initially thought to be a distinct type of cell death, autophagic (or type II) cell death. However, recent studies have shown that preventing autophagy through silencing of core autophagic genes accellerates cell death rather than inhibiting it [35], suggesting that autophagy is induced as a cell survival mechanism rather than contributing to cell death. Taken together, for therapeutic exploitation of autophagy in treatment of mature tumors, it seems that inhibiting autophagy in tumors in combination with other tumor damaging treatment is the most logical treatment. This is in contrast to preventing development of cancer in premalignant cells, where it seems that autophagy serves as a tumor suppressor pathway regulating cell growth that must be overcome on the path to malignancy. In this case, increased autophagic activity seems beneficial to the cells to prevent development of malignancy.

The emerging role of autophagy as a housekeeper of the cell makes an interesting connection to cellular aging where oxidative damage to proteins, DNA and organelles accumulates to cause a gradual decline in various cellular functions [36, 37]. Autophagy is known to be important for degradation of damaged peroxisomes and mitochondria, organelles whose normal function is important to avoid oxidative damage to the cell [38]. In *C.elegans,* several genetic manipulations have been described that increase lifespan, and among them is a loss-of-function mutations in the insulin-like tyrosine kinase receptor daf-2 [39]. This mutation has been shown to increase the rate of autophagy and gene silencing of the nematode homologue of the core autophagic protein Beclin 1 blocks the life-extension effect of daf-2 [39]. An established method for life extension that seems to be common for all complex organisms is caloric restriction, involving restricting food intake to 40% below normal consumption. Interestingly, inhibition of autophagy prevents the anti-aging benefits of caloric restriction [40, 41]. Aging generally correlates with a decline in autophagic activity while incidence of neurodegenerative diseases dramatically increase with age.

In *D.melanogaster*, the expression levels of many autophagy-related genes is reduced upon aging and this correlates with accumulation of ubiquitinated proteins in cells [42]. Mutations in the fly Atg8 orthologue results in reduced lifespan, accumulation of ubiuiqinated proteins and sensitivity to oxidative stress while overexpression of the Atg8 orthologue has the opposite effect of increasing lifespan [42]. These correlationions suggest that mutations or altered expression of autophagy-related genes can contribute to aging, but the causal relationship is still unclear. Another exciting development related to autophagy in health and disease was a recent publication by He et al [43] showing that autophagy is important for normal muscle metabolism. They demonstrated that mice with dysfunctional regulation of the core autophagic complex containing Beclin 1 is not able to induce changes in the muscle that are associated with beneficial effects of exercise. Furthermore, these mice have metabolic symptoms including elevated levels of blood glucose and insulin and decreased exercise capacity and endurance. The involvement of autophagy in regulation of metabolic homeostasis suggests that modulation of autophagy is a possible therapeutic approach to treat diseases like type-2 diabetes and metabolic syndrome.

1.1.3 Selective autophagy

In recent years, a role for autophagy in selective degradation of targeted cytoplasmic components has been emerging. Such cytoplasmic quality control allows cells to respond to stress or other demands to selectively degrade target components. Triggers can include damaged or excess organelles or proteins, cytoplasmic remodeling or differentiation. During selective autophagy, bulk cytoplasm is excluded from the autophagosome as the phagophore expands closely around the cargo. Cargo-specific names have been given to distinguish the different types of selective autophagy and known targets for selective autophagy so far include mitochondria [7] (mitophagy), lipid droplets [44] (lipophagy), peroxisomes [8] (pexophagy), endoplasmatic reticulum, ER [45] (reticulophagy or erphagy) and parts of the nucleus [46] (nucleophagy). In addition to degradation of organelles, autophagy is known to degrade other components of the cell like ribosomes [9] (ribophagy), protein aggregates [13] (aggrephagy), glycogen particles [47] (glycophagy) and also intracellular pathogens [10, 11] (xenophagy).

Although a wide variety of different cargo have been identified, there is still much to learn about the signals and molecular machinery involved in the different types of selective autophagy. Moreover, little is known about the ligands on the cargo that is recognized by autophagy receptors. Ubiquitin is one such ligand and ubiquitination of cargo is associated with various selective autophagic processes such as mitophagy, aggrephagy and xenophagy. Autophagy receptors are defined as proteins that can interact with an Atg8/LC3-family member such as LC3 and cargo containing a ligand that targets it for degradation (Figure 2). The best known human autophagy receptor is p62, containing an Ubiquitin-associated (UBA) domain, giving it affinity for ubiquitin and polyubiquitin [48], a LC3-interacting region (LIR) giving it affinity for LC3 [49] and a PB1 domain allowing homo- and hetero-polymerization [50]. p62 is shown to be involved in many autophagic processes such as degradation of bacteria [51], mitochondria [52], peroxisomes [53], midbody remnants [12] and protein aggregates [29].There are also other known mammalian autophagy receptors such as the closely related NBR1 (Neighbor of BRCA1 gene protein 1) which is also implicated in degradation of midbody remnants [54]. NDP52 (Nuclear domain 10 protein 52) [55] and optineurin [56] are both receptors involved in degradation of

intracellular pathogens while Nix (NIP3-like protein x) [57] link mitochondria and Stbd1 (Starch-binding domain containing protein 1) [58] glycogen particles to the autophagic machinery.

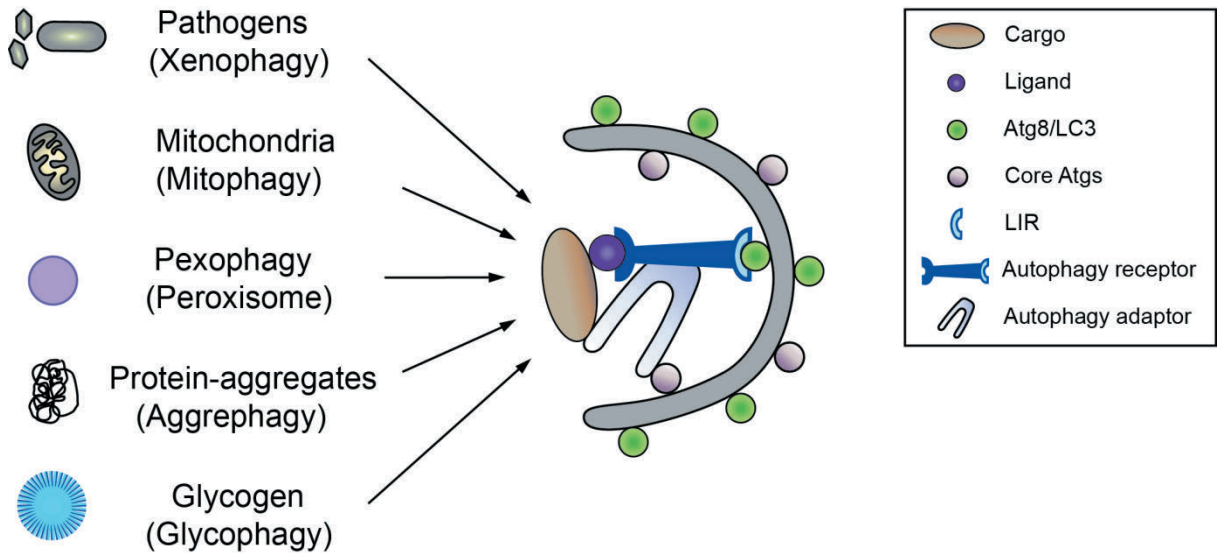

Figure 2: Cargoes of selective autophagy and the associated autophagic protein machinery. Cargo is selected for autophagic degradation by interaction between a ligand on the cargo and an autophagy receptor. The autophagy receptor further interacts with an Atg8/LC3 family member through a LIR. Receptors also interact with autophagy adaptors that act as molecular scaffolds, bringing into proximity the components of the autophagic machinery necessary for the process.

Selective autophagy was first described in yeast, as the cytoplasm-to-vacuole-targeting (Cvt) pathway. Whereas autophagic pathways are normally catabolic, the yeast Cvt pathway is in fact biosynthetic because it delivers resident hydrolases to the yeast equivalent of the lysosome, the vacuole [59]. The hydolases that are known to be delivered by this pathway, Alpha mannosidase 1 (Ams1) and Aminopeptidase I (ApeI) [60, 61] are synthesized as proenzymes where a N-terminal propeptide allows them to oligomerize and further assemble into higher order structures [62]. These complexes are recognized first by the receptor protein Atg19 which further recruits the adaptor protein Atg11 [63, 64]. Atg11 serves as a molecular scaffold, bringing the ApeI complex into proximity with core Atg proteins allowing formation of autophagosome-like Cvt-vesicles. Atg11 is also important for mitophagy [65, 66] and pexophagy [67] in yeast, demonstrating that this autophagic adaptor protein is involved in several forms of selective autophagy. Increased expression of Atg11 stimulates formation of Cvt vesicles [68], suggesting that it serves an important regulatory and rate-limiting role in formation of Cvt vesicles.

In mammalian cells, there is only one recognized autophagic adaptor protein, the large scaffolding protein Autophagy-Linked FYVE domain containing protein (ALFY). ALFY contains a series of conserved domains in its C-terminal end while nothing is known about the rest of the protein. In the C-terminal is a PH-like (Pleckstrin Homology-like) and BEACH (Beige and Chediak-Higashi) domain, followed by a WD40 domain and a FYVE domain. The PH-like and BEACH domains (hereafter called PH-BEACH domain when referenced together) have been shown to have a strong interaction to each other and most likely function as a unit [69] to mediate an interaction with the autophagy receptor p62 [70]. The WD40 domain interacts with Atg5 [71] while the FYVE domain binds PI(3)P [72]. Binding several components involved in selective autophagy

gives ALFY properties of an autophagic adaptor protein, bringing into proximity proteins important for formation of the autophagic membrane around the autophagy receptor-cargo complex (Figure 3). Under normal conditions, ALFY is mostly localized to the nuclear envelope and undergoes continous nucleocytoplasmic shuttling [72]. p62 is also cycling between the nucleus and cytoplasm and can recruit ALFY to ubiquitinated cytoplasmic protein aggregates formed upon cellular stress to initiate their autophagic degradation [70]. Overexpression of ALFY or its C-terminal region have been shown to decrease the number of protein inclusions in primary neuronal and *Drosophila* models of Huntingtons disease [71], indicating that increased ALFY levels can protect the cells against the damaging effects of mutant proteins.

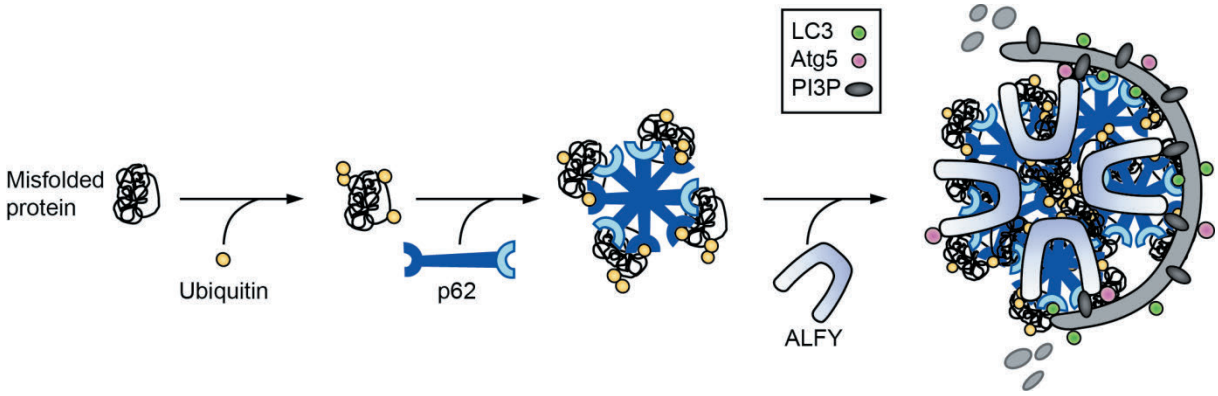

Figure 3: Selective autophagy of protein aggregates. Misfolded proteins are ubiquitinated and recognized by p62, which by homo-polymerization allows a controlled assembly of micro-aggregates, also called p62 bodies. ALFY further assembles p62 bodies into larger aggregates and by interaction with LC3, Atg5 and PI(3)P recruits the autophagic machinery to initiate degradation of the aggregates.

1.1.4 The many roles of p62

One role of p62 is to associate with ubiquitinated cargo and link it to the autophagic machinery, but p62 is also involved in a variety of other cellular processes. By interacting with various other proteins (Figure 4), p62 has been shown to be a major signaling hub that is important in regulation of many essential cellular processes, including oxidative stress signaling and cancer (reviewed in [73]). In addition to being a substrate and cargo selector of autophagy, it also has a regulatory role in the mTORC1 signaling pathway that is a major regulator of cell growth and autophagic activity [74].

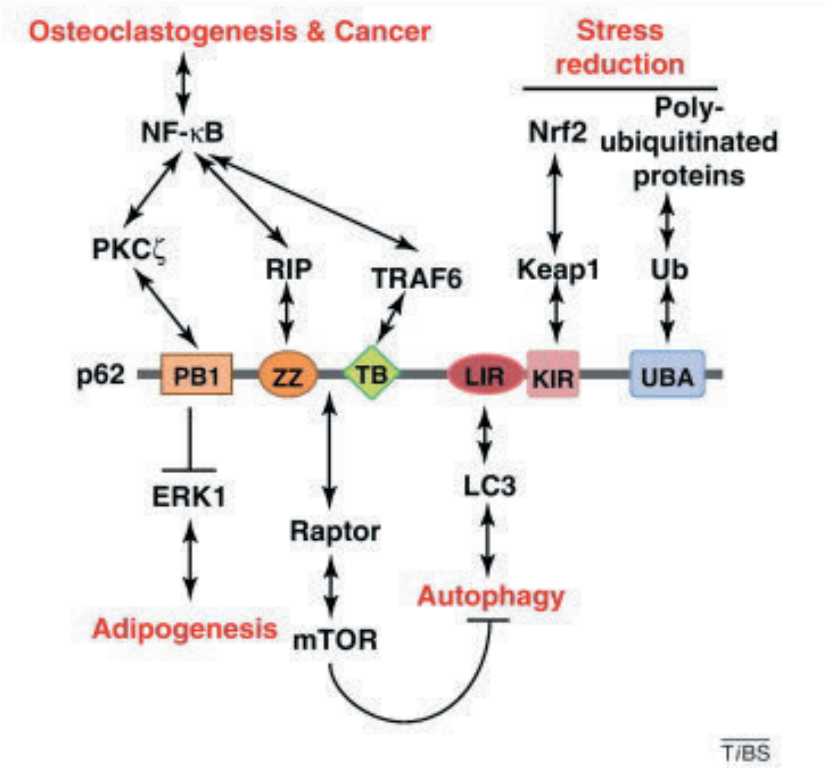

Figure 4: Interacting partners of p62 and involvement in cell processes. Interactions of three domains contribute to NF-κB signaling; the PB1 domain through PKCζ, the ZZ zinc finger domain through receptor interacting protein (RIP) and the TRAF6 binding (TB) domain through TRAF6. The PB1 domain is also involved in regulation of adipogenesis through extracellular signal-regulated kinase 1 (ERK1). A region between the ZZ and TB domains interacts with Raptor to negatively regulate autophagy. The Keap1 interacting region (KIR) interacts with Keap1 to regulate transcription of Nrf2 targets while the UBA domain interacts with polyubiquitin. Figure adopted from Moscat et al [75].

Analysis of p62-deficient mice showed that these mice develop several symptoms reminescent of human metabolic syndrome such as mature-onset obesity and insulin resistance [76]. Through its PB1 domain, p62 can homopolymerize or interact with various other proteins (Figure 4) who also contain PB1 domains such as ERK1 [76], atypical PKCs (Protein kinase C proteins) [77] or the autophagy receptor NBR1 [50]. The interaction with and inhibition of ERK1 suppresses adipogenesis and studies have shown that the dysregulation of ERK1 is the cause of the obesity and type 2 diabetes seen in p62-deficient mice [76]. A specific mutation in p62 is causative of Paget's disease of bone [78], a genetic disease associated with enhanced osteoclastogenic activity. Similarly, mice lacking p62 have a defect in osteoclastogenesis [79]. As mentioned previously, knockdown of p62 in addition to Atg proteins attenuated the pathology related to loss of

autophagy in liver tissue, but not in neurons [30]. This suggests that p62 itself is a cause of pathology in the liver and it has been shown that this is due to an effect of p62 stabilizing the transcription factor Nrf2 (Nuclear factor-like 2) [80] by interacting with Keap1 (Kelch-like ECH-associated protein 1) (Figure 4). Nrf2 target genes include various antioxidant and detoxification enzymes. Liver-specific knockdown of autophagy was recently also shown to induce formation of liver tumors [81, 82]. There are still unknown details around how Nrf2 contributes to liver pathology, but it is possible that it can contribute to tumorigenesis through ROS (reactive oxygen species) detoxification. ROS is involved in initiation of apoptosis and upregulated detoxification can thereby contribute to tumor cell surival. Furthermore, p62 interacts with TRAF6 (TNF receptor associated factor 6) [83] (Figure 4) to activate the NF-κB (Nuclear factor κB) pathway and another consequence of p62 accumulation is chronic inflammation, a common contributor to tumorigenesis.

A recent study discovered a role for p62 in regulation of autophagic activity in response to amino acid availability upstream of mTORC1 [74]. It was shown that this effect is through an interaction between p62 and Raptor, a component of mTORC1 to activate the complex and thereby inhibit autophagy [74] (Figure 4). Because p62 is itself a target of autophagy this creates a feed foward loop through which high or low levels of p62 can sustained. A possible consequence of this mechanism is that cells that reach a critical level of stress through abnormally high or low p62 levels might not be able to recover and are irreversibly destined to undergo cell death. During tumorigenesis, there will be times when the tumor cells are exposed to such situations, typically of lasting low nutrient availability and the p62-mTORC1-autophagy axis might serve as a tumor suppressor pathway in this case.

1.2 BEACH PROTEINS

As illustrated in Figure 5, there are eight human proteins containing a BEACH domain (hereafter called BEACH proteins), but ALFY is the only one shown to have a role in autophagy. The family shares a common C-terminal domain architecture where the PH-BEACH domains are followed by several WD40 repeats that presumably form a seven bladed β-propeller as is common in WD40 domains [84]. The BEACH domain is highly conserved throughout the human protein family (Figure 5, higher and more yellow bars inside the protein box indicate sequence conservation) and it is also well conserved to BEACH proteins in other species. Yeasts have one BEACH protein, *Caenorhabditis elegans* has two and *Drosophila melanogaster* has four. The slime mold *Dictyostelium discoideum* has six BEACH proteins and these proteins have been thoroughly studied [85, 86], but as Figure 6 shows, these proteins are not closely related to the human BEACH proteins. The zebrafish *Dario rerio* looks like an attractive model organism for studying BEACH proteins and their involvement in disease as it contains a closely related ortholog for each human BEACH protein.

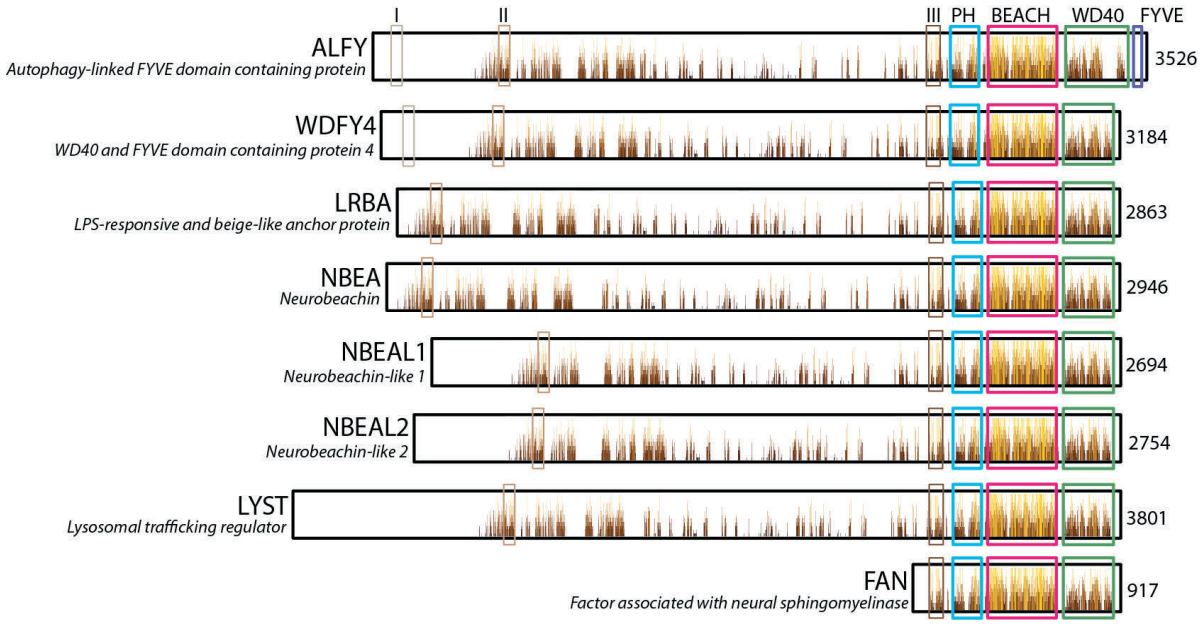

Figure 5: Domain structure and degree of sequence conservation of human BEACH proteins. Inside each protein box, bars indicate the degree of sequence conservation, higher and more yellow bars indicate higher degree of conservation. The graphical output of sequence conservation is from a Jalview [87] illustration of a sequence alignment of the proteins. Grey, light brown and dark brown boxes indicate regions of sequence homology to other, unrelated proteins that were identified by a BLAST search of ALFY, but has not been explored experimentally. Residues 247-351 (of ALFY) in grey [I] is similar to part of 'TBC1 domain family member 30', residues 842-923 in light brown [II] is similar to 'origin recognition complex subunit 2' and residues 2281-2397 in dark brown [III] is similar to 'BCL2 associated transcription factor 1'. Blue boxes indicate PH domains, red BEACH domains, green WD40 domains and purple FYVE domains.

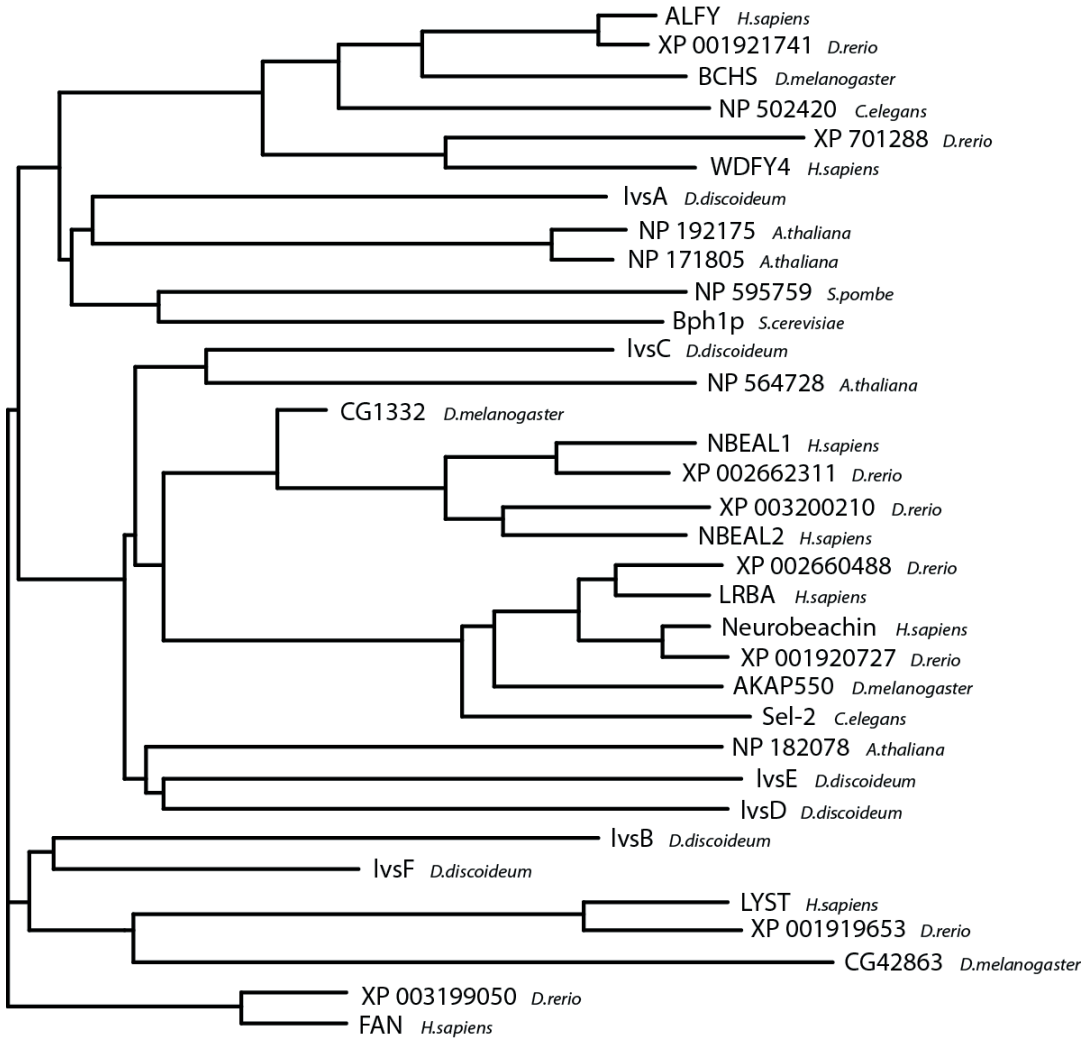

Figure 6: Phylogeny of BEACH proteins in various species. *Homo sapiens*, *Arabidopsis thaliana*, *Caenorhabditis elegans*, *Danio rerio*, *Dictyostelium discoideum*, *Drosophila melanogaster*, *Saccharomyces cerevisiae* and *Schizosaccharomyces pombe* were searched for proteins containing BEACH domains. This resulted in 34 unique and confirmed proteins which were aligned by Clustal Omega [88] and arranged phylogenetically.

1.2.1 Cell biology of BEACH proteins and involvement in disease

The BEACH domain (BEige And CHs) is named from the human Chediak-Higashi syndrome (CHS) and the homologous mouse disease beige. These diseases are caused by mutations in the first BEACH protein identfied, the human protein initially named CHS1 and later commonly called Lysosomal trafficking regulator (LYST) [89]. CHS is a recessive disorder, appearing with loss-of-function mutations in both LYST alleles. The hallmark of the disease is giant cytoplasmic granules around the nucleus which have many characteristics of lysosomes. Ectopic expression of deletion constructs containing only the PH-BEACH-WD40 domains of LYST generates a dominant negative phenotype similar to that of CHS with enlarged lysosomal compartments [90]. The disease involves immunodeficiency due to impaired sorting of Major histocompatability complex (MHC) class II molecules to late endosomes [91], bleeding due to a deficiency of platelet dense bodies [92] and albinism due to abnormal melanosomes [93]. Because platelet dense bodies, lysosomes and melanosomes are all functionally connected to the trans-golgi network

(TGN), it has been proposed that LYST is needed for normal vesicle trafficking between the TGN and late endosomes [94]. A recent study aimed at explaining the altered lysosome size seen in LYST-deficient cells concluded that reduced lysosome fission is the cause of the abnormal lysosomes seen in CHS cells [95]. While human LYST localizes to cytoplasmic puncta and not lysosomes, the related *D.discoideum* BEACH protein Large volume sphere B (LvsB) is seen at lysosomes and LvsB-null cells also have enlarged vesicles [96, 97]. Interestingly, LvsB-null cells show inappropriate fusion between various endolysosomal compartments [97], indicating that LvsB might be involved in establishing or differentiating vesicle identity in the endolysosomal system.

Human Factor associated with neural sphingomyelinase (FAN) is different from the other BEACH proteins in being significantly smaller, consisting of little more than the PH-BEACH-WD40 domains. FAN is shown to interact with three different plasma membrane receptors through its WD40 domain to regulate neutral sphingomyelinase activity and thereby production of the lipid second messenger ceramide. By constitutively binding to receptors it mediates Tumor necrosis factor (TNF)-signaling (responding to cytokines binding to the p55 TNF receptor) [98], Cell differentiation factor 40 (CD40)-signaling (responding to CD40L) [99] and Δ9-tetrahydrocannabinol signaling (cannabinoid type 1 receptor) [100]. Studies of FAN-deficient cell lines have shown that both TNF- [101] and CD40-induced [99] apoptosis are impaired. FAN-deficient mice show a marked delay of recovery after cutanous barrier disruption [102] which indicates that FAN is involved in promoting TNF-induced cell motility and thereby wound healing. Signaling through FAN also has downstream effects on the lysosome, influencing lysosomal permeability [103] and lysosome size [104]. Studies have shown that all these domains are important for normal functioning of the protein [69] and that ectopic expression of only the WD40 domain of FAN causes a dominant negative effect [98]. The PH-like domain of FAN has been proposed to interact with PI(4,5)P2 [105], but another study claims it does not bind phosphoinositides [106].

ALFY (also called WD repeat and FYVE domain containing protein 3, WDFY3) is the only BEACH protein that is linked to autophagy. ALFY is also the only human BEACH protein that has a FYVE domain, a zinc finger-containing domain that specifically interacts with PI(3)P [15], a signaling lipid that is commonly found on endosomes and autophagosomal membranes. While FYVE domain containing proteins typically localize to endosomes, ALFY does not [72]. ALFY is recruited to autophagic membranes by contribution of several of its conserved domains, its FYVE domain interacts with with PI(3)P [72], formed by the class III PI3K-complex 1 on the autophagosomal membrane, and its WD40 domain interacts with Atg5 [71], a component of the core autophagic machinery. Upon treatment of cell cultures with the amino acid analog puromycin, protein aggregates of ubiquitinated unfolded proteins are formed and ALFY is recruited by p62 from the nucleus to these aggregates to presumably facilitate their autophagic degradation [70]. Depletion of ALFY in cell cultures expressing mutant Huntingtin (polyQ) was found to prevent efficient recruitment of both Atg5 and LC3, but not p62, to the protein inclusions [71]. Furthermore, as discussed, overexpression of ALFY has been shown to be neuroprotective in both cell culture and Drosophila models of polyglutamine toxicity. To summarize, what is known about ALFY suggests it is required for formation of autophagic membranes around protein aggregates that are targeted for autophagic degradation.

WD-40 and FYVE domain containing protein 4 (WDFY4) is closely related to ALFY, but despite of its name, it does not contain a complete FYVE domain. It is primarily expressed in immune tissue and the only published data about it is a genome-wide association study correlating a mutation (R1816Q) to systemic lupus erythematosus [107]. In *D. melanogaster*, there is only one orthologue to the ALFY-WDFY4 pair, called blue cheese (bchs). Flies missing this protein have a neurodegenerative phenotype characterized by accumulation of ubiquitin-positive aggregates in neurons and reduced life span [108]. Overexpression of full length bchs or just the C-terminal has been shown to be neuroprotective and increase lifespan in a fly model of polyglutamine toxicity [71]. While bchs is more closely related to ALFY than WDFY4 (Figure 6), the latter protein has not been investigated for a role in degradation of ubiqutinated proteins so it remains unknown if it could be involved in such processes. No human diseases have been linked to mutations in ALFY, but based on results from depletion of ALFY and loss of bchs, it seems likely that mutations or downregulation of ALFY could contribute to neurodegeneration in humans.

The only yeast BEACH protein is called BEACH protein homolog 1 (BPH1). While this protein is not closely related to any one of the human BEACH proteins, it belongs to the subfamily containing ALFY and WDFY4 (Figure 6). BPH1 was initially identified in a screen for genes that are important for growth of *S.cerevisiae* on various synthetic media, in this case media with pH of 4.1-4.3 buffered by potassium acetate [109]. Further studies by Shiflett et al [110] showed that the deletion strain has a cell wall defect and a secretion defect. They were not able to pinpoint the exact cellular origin of the phenotype, but their data suggests a defect in trafficking from the Golgi. The *D.discoideum* BEACH protein LvsA also belongs to the subfamily of ALFY and BPH1. Null mutants of this protein have a defect in cytokinesis [111] and osmoregulation [112]. The protein is, as is common for the BEACH proteins, not associated with membranes under normal conditions, but upon hyperosmotic stress, it associates with the contractile vacuole as the vacuole reaches its maximum diameter, induces emtyping of the vacuole by an unknown mechanism and remains attached throughout the emptying process [112].

Neurobeachin (NBEA) is predominantly expressed in neurons where it is essential for evoked transmission at neuromuscular junctions. This is demonstrated by NBEA knockout mice which die immediately after birth from breathing paralysis [113]. This BEACH protein is unique among the human proteins in containing a motif that binds type II regulatory subunits of protein kinase A, making it an A-Kinase Anchor Protein (AKAP), a family of scaffolding proteins known to be important in establishing cell microdomains [114]. NBEA mainly localizes to the TGN where it initially was suggested to function similarly to vesicle-coat proteins in sorting cargo [115]. More recently, the neurological defect associated with NBEA was elucidated in a publication demonstrating that both homozygous and heterozygous loss of NBEA result in accumulation of actin and the actin-bundling synaptopodin in the Golgi, resulting in reduced formation of dendritic spines [116]. Such spines are normally highly dynamic structures containing the postsynaptic signalling machinery and are dependent upon actin remodeling to function in processes such as learning and memory [117]. NBEA is also of clinical interest because it spans a common fragile site where heterozygous disruptions have in several instances been linked to non-familial autism [118, 119].

Lipopolysaccharide-responsive and beige-like anchor protein (LRBA) was initially discovered as being upregulated in response to bacterial lipopolysaccharide stimulation in B cells and macrophages, but it is ubiquitously expressed [120]. It has been found to be upregulated in several different cancers and knockdown of LRBA significantly sensitizes cancer cells to apoptosis [121]. Ectopic expression of the C-terminal domains of LRBA was shown to have a dominant-negative effect on cancer cells, similar to that of LRBA knockdown and expression of this construct also influences the phosphorylation state of the epidermal growth factor receptor (EGFR) [121]. EGF is a common mitogen and signaling from EGFR is deregulated in many cancers. Thus, a possible explanation for the influence of LRBA on cancer cells is that it is regulating recycling or degradation of EGFR from endosomal compartments. As Figure 6 shows, the related human BEACH proteins NBEA and LRBA have a single orthologue in *C.elegans* and *D.melanogaster*. These proteins, similarly to NBEA are both designated as AKAPs, but what is known about their functions is reminiscent of LRBA. SEL-2, the single *C.elegans* orthologue of the is important for normal localization and trafficking of plasma membrane receptors such as EGFR in polarized epithelial cells [122]. In *D.melanogaster*, loss of the single orthologue AKAP550 (also called Rugose) causes an eye phenotype that has been shown to be a consequence of abnormally activated apoptosis in certain cells of the eye during development [123]. In these cells, EGFR signaling supports cell survival and presumably loss of AKAP550 disturbs EGFR signaling directly through the signaling pathway or indirectly by influencing trafficking of the receptor.

Neurobeachin-like 1 (NBEAL1) is one of the more recently discovered BEACH proteins. Not much is known about this protein, but one publication shows that NBEAL1 is upregulated at the transcriptional level in gliomas [124]. Neurobeachin-like 2 (NBEAL2) is closely related to NBEAL1 and was recently reported to be causative for grey platelet syndrome. This disease involves a bleeding disorder caused by lack of α-granules in platelets which are synthesized in megakaryocytes. Megakaryocytes missing both alleles of NBEAL2 fail to pack their endogenously synthesized secretory proteins into developing α-granules [125-127]. Interestingly, NBEA has been shown to be a negative regulator of granule synthesis and its knockdown results in abnormal granule morphology [128]. One common symptom of Chediak-Higashi syndrome is a bleeding condition caused by deficiency of platelet δ-granules [129], suggesting that LYST is also involved in granule synthesis. The process of producing mature and functional protein granules thus seems to be one system where several BEACH proteins are involved. Another common characteristic of several BEACH proteins that might be related to their role in granule synthesis is an inducible association with vesicle systems.

Table 1: Summary of what is known about the human BEACH proteins.

Protein	Proposed function	Involvement in disease
ALFY	Autophagic adaptor protein linking ubiquitinated protein aggregates to the core autophagic machinery.	Neurodegeneration in fly models and cell culture.
WDFY4	Unknown.	Systemic lupus erythematosus.
LRBA	Regulation of plasma membrane receptors such as EGFR.	Various cancers.
NBEA	Sorting or targeting of proteins from the Golgi.	Autism.
NBEAL1	Unknown.	Glioma.
NBEAL2	Sorting endogenous proteins into granules.	Grey platelet syndrome.
LYST	Vesicle trafficking from the TGN.	Chediak-Higashi syndrome.
FAN	Scaffolding signaling receptors to effectors.	Unknown.

1.2.2 Conserved domains and structural details

In 2002, the crystal structure of a BEACH domain was first reported, that of human NBEA and it was shown to have a novel fold [69]. The investigators also found that a weakly conserved region upstream of the BEACH domain folds into a separate domain containing a seven-stranded β-sandwich similar to the Plecstrin Homology (PH) superfold that is found in PH domains [130]. These PH-like domains are weakly conserved on the sequence level within the protein family while the BEACH domain is highly conserved (Figure 7). As discussed, the PH-like and BEACH domains have a common surface of several ionic contacts, giving them a high affinity for each other [69]. In FAN, it has been demonstrated that mutations disturbing the close contact between the domains attenuates downstream effects of the protein [105], suggesting the two domains function as a unit.

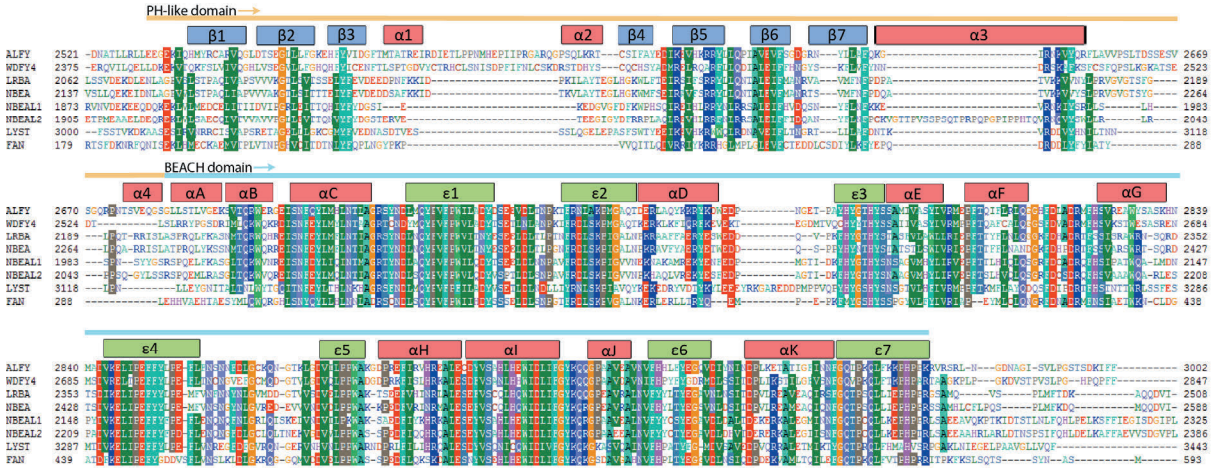

Figure 7: Sequence alignment of human BEACH proteins with domains and secondary structures indiciated. Orange bar above the sequences indicates the PH-like domain and the blue bar the BEACH domain. Annotations of secondary structures is adopted from Jogl et al [69] and is repeated in the following figures showing the PH-like and BEACH domains.

Looking at the BEACH domain from any angle, it can be said to contain three layers, two layers of α-helices flanking a central layer containing partially extended peptide segments making up the hydrophobic core of the domain. These partially extended peptide segments buried in the core of the BEACH domain do not assume regular secondary structures with main-chain hydrogen bonding as within α-helices or β-sheets and were, for ease of discussion, named ε1-7 by Jogl et al [69] whereas the helices flanking the core were named αA-K. Structural elements of the PH domain were named α1-4 and β1-7. This classification scheme was adopted in the sequence alignment of the human BEACH domain containing proteins in Figure 7 and indicated in Figures 8 and 9, showing the secondary structures of the domains. Normally, main-chain hydrogen bonding donors and acceptors interact with other main-chain atoms, as is seen within α-helices and β-sheets, but in the BEACH domain, main-chain amides and carbonyls often hydrogen bond to conserved side-chains of nearby residues [69]. This might be part of the explanation as to why the domain is highly conserved in sequence, supported by the observation that many of the highly conserved sequence elements are in such ε-segments (Figure 7) that are found in the interior of the domain.

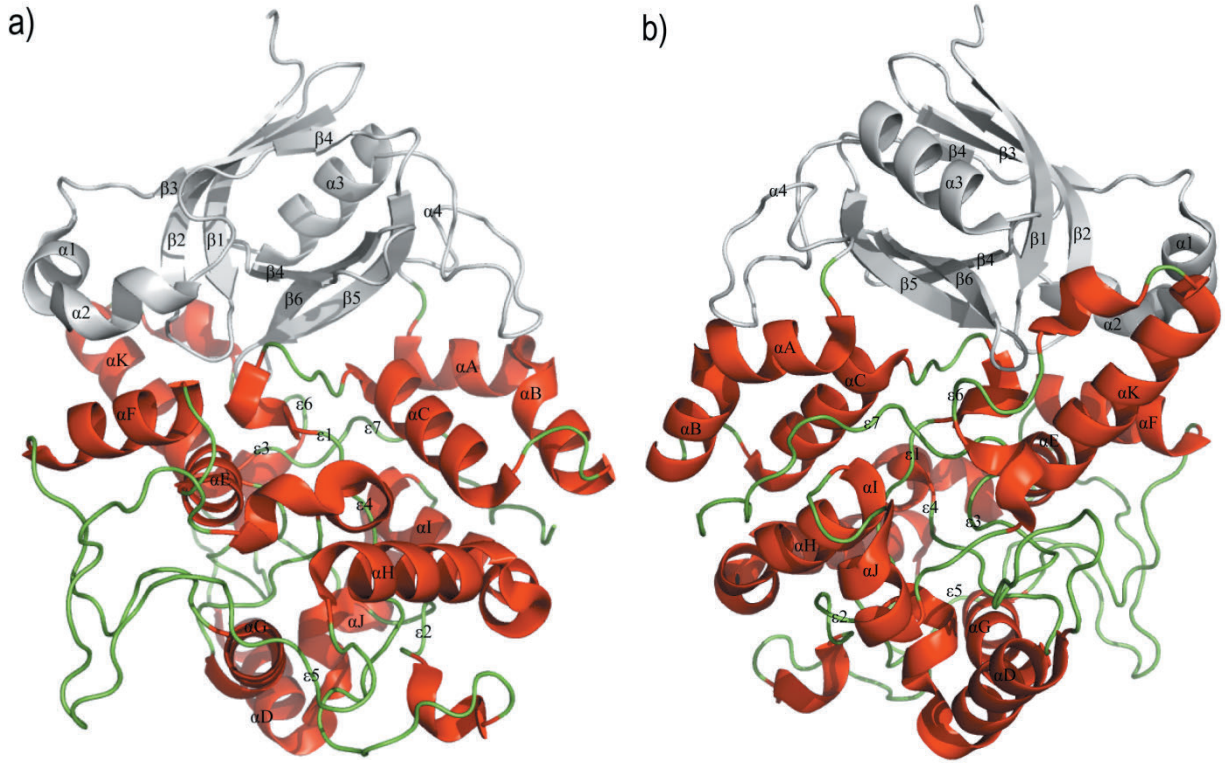

Figure 8: The BEACH domain of LRBA with annotations indicated as in Figure 7. α-helices are in red, loop structures are in green and the PH-like domain in grey. a) The BEACH domain from the direction looking straight into the main groove that is formed between the PH-like and BEACH domains. b) The BEACH domain rotated 180 degrees around the vertical axis.

The β-sandwich core of PH-like domains seen closely associated with BEACH domains is structurally homologous to other PH domains, but only weakly conserved at the amino acid level, 6-12% for structurally equivalent residues [69]. PH domains are characterized by containing a PH superfold of two perpendicular anti-parallel β-sheets (Figure 9, β1-3 and β4-6) followed by an amphiphatic helix (Figure 9, α3). Loops connecting the β-sheets differ greatly in length and sequence, being the source of PH domains binding specificity [130]. PH domains are known to have many different roles, including phospholipid binding, phosphotyrosine binding and protein-protein interactions [130]. The interaction to phospholipids has been mapped to normally be mediated by the loop connecting β1 and β2 of the PH domain. In the PH-like domains of Neurobeachin and LRBA, a helix, α2 is blocking one side of this loop while the other side is blocked by the BEACH domain (Figures 8 and 9). As is seen in Figure 7, the α2 helix seems to be conserved throughout most of the human BEACH proteins except for FAN. Interestingly, the PH-like domain of FAN has been proposed to interact with PI(4,5)P2 [105] while no interaction to phosphoinositides has been observed in the PH-like domains of other BEACH proteins. This could mean that the PH-like domains found together with most of the human BEACH domains have adopted a different role, such as mediating protein-protein interactions.

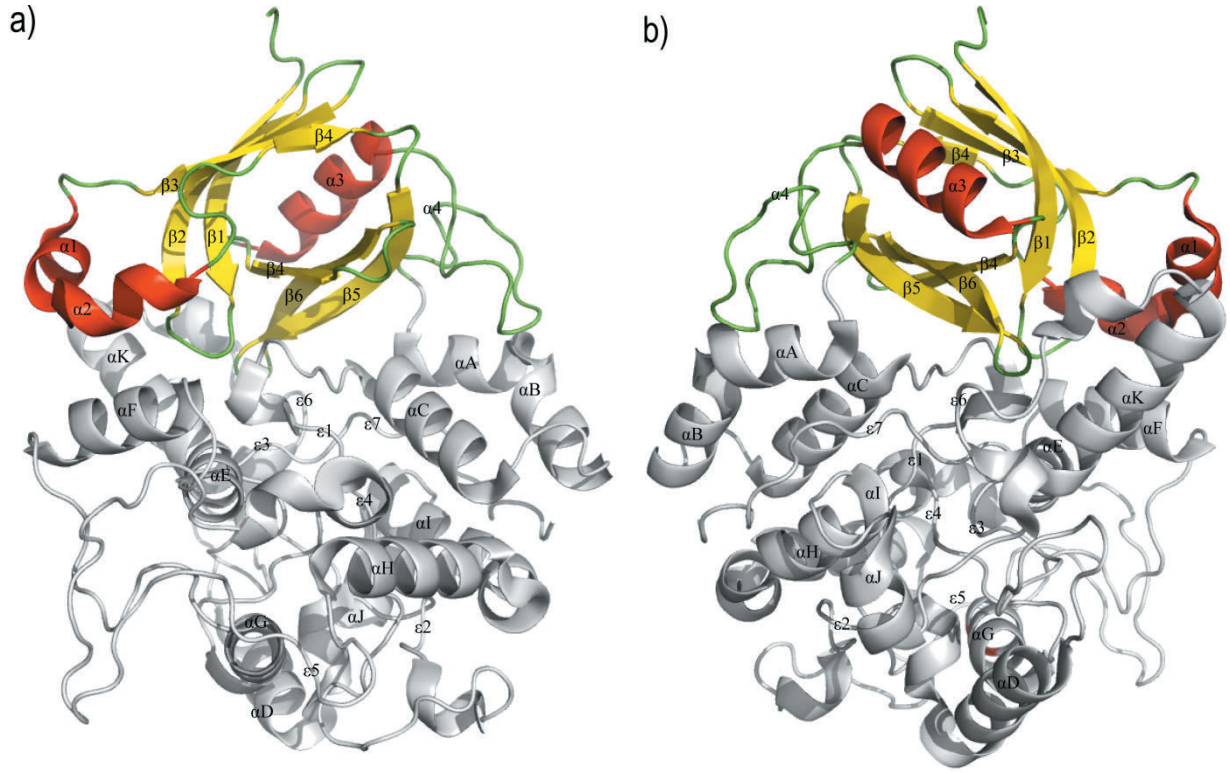

Figure 9: The PH-like domain of LRBA with annotations indicated as in Figure 7. α-helices are in red, β-sheets in yellow, loop structures are in green and the BEACH domain in grey. a) the PH-like domain from the direction looking straight into the main groove that is formed between the PH-like and BEACH domains. b) the PH-like domain rotated 180 degrees around the vertical axis.

While none of the WD40 domains of BEACH proteins have been crystallized, they presumably form the seven-bladed β-propeller structure that is characteristic of WD40 domains. These domains are found in a wide variety of proteins involved in many cellular contexts, but the typical role of the domain is to mediate protein-protein interactions [131]. The large top and bottom surfaces exposed on the β-propeller has been proposed to be well suited as platforms to mediate interactions with several proteins simultanously [131]. The β-sheets that make up the β-propeller in WD40 domains are formed from WD40 repeat sequences, but sequence analysis recognizes variable amounts of WD40 repeats in the BEACH proteins. It is possible that sequences around the WD40 repeats are able to form β-sheets to complete a functional β-propeller, but it might also be that the β-propeller is only completed upon interaction with another protein which donates additional propeller-blades. It will be interesting to get information about the detailed structure of the WD40 domain of a BEACH protein and eventually structural information about how the PH-BEACH-WD40 domains are positioned relative to each other and also relative to the rest of these large proteins.

2. Aims of the project

The observation that the PH-BEACH domain is highly conserved and was found to be responsible for interaction between ALFY and p62, made us curious to investigate if other BEACH proteins also could interact with p62. The assays used in the publication showing this interaction did not go further than showing that the C-terminal domains of ALFY is pulled down by p62 and that the PH-BEACH domain is probably responsible for this [70]. These assays do not exclude that this interaction is indirect so one goal of this project was to establish if this interaction is direct and to map the interaction in as much detail as possible. Furthermore, we investigated the PH-BEACH domain of several human BEACH proteins for an interaction to p62. Because p62 is a well known autophagy receptor protein, any BEACH protein interacting with it could thereby be involved in autophagy. therefore set up two separate screens to investigate BEACH proteins for involvement in various forms of autophagy.

To address these aims, we have used expression of GFP-tagged recombinant proteins in mammalian cells for immunoflouresence analysis of co-localization with endogenous p62 and LC3, as well as in vitro interaction assays using GST- and MBP-tags to investigate if this interaction is direct and to narrow down the regions involved. Autophagic assays were performed to quantify if the rate of autophagosome formation was altered upon knockdown of BEACH proteins. Finally, cells were treated with various cell media or drugs to induce autophagy and the localization of endogenous BEACH proteins and p62 was investigated by confocal immunoflourescence microscopy.

3. Materials and methods

3.1 WORKING WITH DNA

Because most of the proteins studied in this project have not previously been studied in our goup, the starting point of the project was to order cDNA sequences corresponding to the C-terminal part of the different BEACH proteins (ordered from OriGene). Because these proteins are so large, cDNA corresponding to the full-length protein sequences are not commercially available. Sequences corresponding to the C-terminal of ALFY and WDFY4 were already available in the lab. The goal was to obtain cDNA clones that contained sequence starting N-terminal to the PH domain and ending at the C-terminal. Such cDNAs were ordered for LRBA, LYST, NBEA and NBEAL2. For NBEAL1, the only available cDNA did not include the full PH-like domain. Moreover, subcloning of NBEA was successfully completed only during the last months of the project and NBEA was subsequently excluded from some of the assays performed in this project.

Table 2: DNA vectors used in this project. B/M indicates if the vector is suited for bacterial or mammalian expression

Name	Antibiotic resistance, B/M	Use in this project
pEntr-1A	Kanamycin, B	Subcloning entry vector for the Gateway system.
pEntr-2B	Kanamycin, B	Subcloning entry vector for the Gateway system.
pEntr-3C	Kanamycin, B	Subcloning entry vector for the Gateway system.
pDest-15	Ampicillin, B	Destination vector. GST-tag N-terminally of att-sites.
pDest-TH1	Ampicillin, B	Destination vector. MBP-tag N-terminally of att-sites.
pDest-53	Ampicillin, M	Destination vector. GFP-tag N-terminally of att-sites.
pDest-EGFP	Ampicillin, M	Destination vector. EGFP-tag N-terminally of att-sites.
pEGFP-C1	Kanamycin, M	EGFP in vector for mammalian expression

3.1.1 Polymerase chain reaction

Polymerase chain reaction (PCR) is a method that allows production of relatively large amounts of a target DNA fragment, starting from a DNA template and primers that anneal to sequences flanking the target sequence. To allow further subcloning of the amplified DNA fragment, the primers can be designed to contain restriction sites on their 5' ends. Template DNA, primers, a heat-stable DNA polymerase, dNTPs, and an appropriate buffer for optimal functioning of the DNA polymerase are mixed and subjected to the thermal cycling protocol. Three different temperature levels are chosen; 1) Denaturation at 95 °C to allow DNA strand separation, 2) Annealing at 55-65 °C to allow primers to anneal to the template (temperature depends on the melting temperature [Tm] of the primers), 3) Extension 68-72 °C to allow DNA synthesis (temperature depends on DNA polymerase optimum). The process of PCR is summarized in Figure 10.

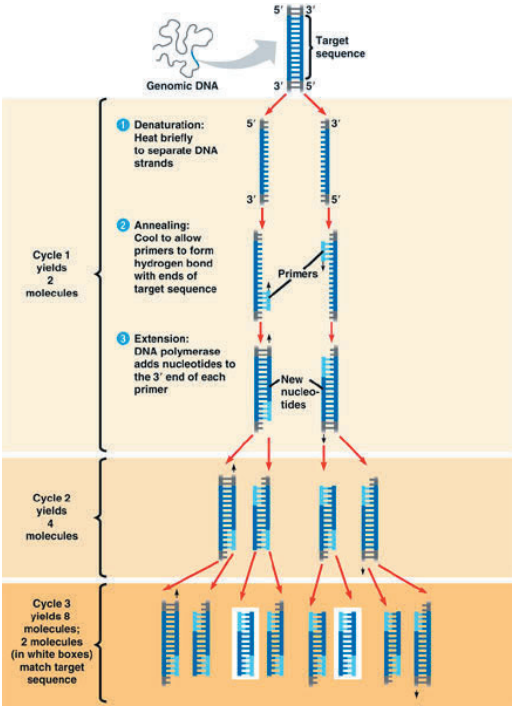

Figure 10: Overview of the mehchanism of PCR. Figure adopted from Copernicus project [132].

During this work, techniques called hot-start and touchdown PCR were applied. Hot-start PCR involves adding the DNA polymerase after the sample was heated to 95 °C to prevent unspecific products that can be formed at lower temperatures because of unspecific primer binding. Touchdown PCR involves gradually lowering the annealing temperature for each cycle that passes, giving less unspecific annealing of primers to the template and thereby less unspecific products. As a polymerase, PfuTurbo DNA polymerase (Agilent) was.

PCR protocol:

1. Mix in PCR strips; 10-20 ng template plasmid DNA, 1.5 µl of each 10 µM primer, 1 µl dNTPs, 5 µl 10x polymerase buffer and dilute to 50 µl with dH_2O.
2. Set up the thermal cycler (BioRad S1000) with the program below and start.
3. When the temperature of the sample has reached 95 °C, pause the machine and add 1 µl of the polymerase to each reaction mixture.

PCR program:

1. Pre-PCR hold 95°C – 3:00
2. 95°C – 0:45
3. [Tm] °C – 0:30
4. 68 °C – 2:30

   Cycle 0-12 – Decreasing [Tm]°C 0.5 °C per cycle
5. 95 °C – 0:45
6. ([Tm] °C - 6 °C) – 0:30
7. 68 °C – 2:30

   Cycle 13-45 – Constant at ([Tm]°C - 6 °C)
8. Post-PCR hold 72 °C – 7:00
9. 4 °C - ∞

3.1.2 Primer design for subcloning

For cloning and expression purposes where amplified segments of DNA were to be subcloned into various DNA vectors, PCR primers were designed to contain restriction sites on the 5'-end. For this application, the same restriction site must be present in the multiple cloning site of the target vector. Restriction sites were also chosen based on compatibility for double digestion and buffer activity. Sequences of primers were chosen to flank the whole domain that was to be amplified and include as little as possible of surrounding sequence. The amount of annealing nucleotides decides the Tm of the primer-template complex, and primers were designed with the aim of having a Tm around 65^{o}C. To the 5'-end of each primer was inserted an ATAT sequence to ensure proper restriction cutting efficiency of the PCR products. Two sets of primers were made for NBEA subcloning and only after many attempts with the second primers was subcloning successful, most likely because the bacterial clone we received with the NBEA construct did not contain only one clone, but a major population of other cDNA as well.

Table 3: Primers designed for amplification and subcloning of PH-like and BEACH domains.

Name	Sequence (written from 5' to 3')	Restriction site	Tm(^{o}C)
ALFY_PH_fwd	ATATGTCGACCGCCTGTTAGAGGAAGGAG	SalI	60
ALFY_PH_rev	ATATGCGGCCGCTAATCCGTTAGAGATGGCACTAC	NotI	66
ALFY_BEA_fwd	ATATGTCGACAGTGTGGAGCAGGGATCTG	SalI	60
ALFY_BEA_rev	ATATGCGGCCGCTATCCTCGCTTTGGTGGATGAGG	NotI	70
WDFY4_PH_fwd	ATATGTCGACGAACTGTGTCGGGAAAGACAAG	SalI	66
WDFY4_PH_rev	ATATTCTAGAGGCTGGGTTGGAAAGAGCAG	XbaI	64
WDFY4_BEA_fwd	ATATGTCGACCCTCAGTCTAAGGAGATACC	SalI	60
WDFY4_BEA_rev	ATATTCTAGATCCTGGCTGGGTGAGGTTTG	XbaI	64
LRBA_PH_fwd	ATATGTCGACGGTCCTGTTAGCCTGAGC	SalI	58
LRBA_PH_rev	ATATTCTAGACAACGCCAACACGAGGTAG	XbaI	60
LRBA_BEA_fwd	ATATGTCGACTTAGCTAGTCCACGTCAGC	SalI	58
LRBA_BEA_rev	ATATTCTAGAATCTGGGAGGATGGGGCTC	XbaI	60
LYST_PH_fwd	ATATGTCGACAGTGAATCTATAAGAGTGAATCG	SalI	62
LYST_PH_rev	ATATGCGGCCGCTAGAGTATATTGTGGTATACATCATC	NotI	64
LYST_BEA_fwd	ATATGTCGACCCTAATCTTCTGGAATATGG	SalI	56
LYST_BEA_rev	ATATGCGGCCGCTATCTGCTCACATGGGCCATG	NotI	56
NBEA_PH_fwd	ATATGTCGACAGGCCCAGTGGTTCTCAGC	SalI	62
NBEA_PH_rev	ATATTCTAGACCCGAGGCAAGCTATAGAC	XbaI	60
NBEA_BEA_fwd	ATATGTCGACTCATTGGCCACTCCTCGAC	SalI	60
NBEA_BEA_rev	ATATTCTAGAACCGAGGCGGATGTGGCTC	XbaI	62
NBEA_PH_fwd2	ATATGAATTCTGACAACCTTGCAGGCCCAG	EcoRI	64
NBEA_PH_rev2	ATATGCGGCCGCTATACTCCAACCCGAGGCAAGC	NotI	64
NBEA_BEA_fwd2	ATATGAATTCACCAGCTATGGTCTGCCACAAG	EcoRI	68
NBEA_BEA_rev2	ATATGCGGCCGCTAACACAGGTGCATGGCAGAG	NotI	64
NBEAL1_BEA_fwd	ATATGTCGACAAGCAGATCACCACAGGAG	SalI	58
NBEAL1_BEA_rev	ATATTCTAGAATCTTGGAGGGTGTGGTTCC	XbaI	58
NBEAL2_PH_fwd	ATATGTCGACCGTGAGAAGCTGGTGCTG	SalI	58
NBEAL2_PH_rev	ATATTCTAGAATAGGCGCAGGAGCCACG	XbaI	60
NBEAL2_BEA_fwd	ATATGTCGACTACCTAAGCAGCCGCTCC	SalI	58
NBEAL2_BEA_rev	ATATTCTAGAACCGAGTTGGATGTGGCTC	XbaI	58

3.1.3 Restriction enzyme digestion

Restriction endonucleases are enzymes of bacterial origin that cut double- or single-stranded DNA at specific sequences called restriction sites. All restriction enzymes used in this project are from New England BioLabs and all of them except for EcoRI were added small amounts of Bovine serum albumin (BSA) for optimal enzymatic activity.

Protocol:

1. Add in an eppendorf tube; 0.2 – 1.5 µg DNA, 2 µl 10x BSA, 2 µl of appropriate 10x NEB buffer, 1 µl restriction enzyme and dilute to 20 µl with dH_2O.
2. Incubate at 37 ^oC for 2 hrs.

3.1.4 Gel electrophoresis and DNA purification

Gel electrophoresis is a method to separate DNA fragments of different lengths. Applying a current to an agarose gel containing DNA will cause the DNA to migrate towards the anode side of the gel due to the negative charges in the backbone of the DNA. The speed of migration depends only on the length of a linear DNA fragment and because of this, agarose gel electrophoresis can be used to analyze DNA content of a sample or to separate DNA strands of different lengths. In this project, 'Ultrapure Agarose' (Invitrogen) and TAE buffer were mixed along with 'SYBR safe' (Invitrogen) to make the agarose gel. Samples were added a '6x DNA loading buffer' (Fermentas) and loaded along with a '1kb DNA ladder' (Fermentas).

After separation of DNA fragments, the SYBR safe staining allows DNA in the gel to be visualized by a 'Safe Imager blue light transilluminator' (Invitrogen). It is then possible to cut pieces of the gel to isolate DNA of certain lengths. This is useful for isolating the appropriate fragments from restriction digested PCR products and vectors. To further isolate pure DNA from the extracted block of agarose, a 'NucleoSpin Extract II' (Machery-Nagel) kit was used.

Protocol:

1. Put 0.8 g agarose in 100 ml TAE buffer. Boil in microwave at a high setting for 2 min.
2. Cool agarose to a temperature where it can be touched and add SYBR safe staining. Pour the mixture into the chamber and put a comb in. Let it solidify for 15 min.
3. Add samples along with ladder and run at 100V for 30-60 min.
4. Put the gel on the Safe Imager. If DNA is to be isolated from the gel, cut chosen bands from the gel using a scalpel.
5. Cut agarose pieces can be cleaned up using an appropriate kit.

Table 4: TAE buffer

Component	Final concentration
EDTA	1 mM
Tris-HCl ph 8.0	40 mM
Acetic acid	20 mM
dH_2O	

3.1.5 Nucleic acid quantification

In this project, a Thermo Scientific NanoDrop 2000c spectrophotometer was used to quantify nucleic acids. This method allows a quick quantification of nucleic acids using a very small volume. The quantification is performed by measuring absorbance of the sample at 230 nm, 260 nm and 280 nm. The instrument generates a output for DNA and RNA concentration using absorbance at 260 nm with Beer-Lamberts equation that defines a direct correlation between absorbance and sample concentration. Measurements of A230 and A280 are in this case used to measure purity of the sample. The A260/280 ratio is the main measure of purity and a pure DNA sample will have a ratio of ~1.8 while a pure RNA sample will have ~2.0. Lower values indicate contamination of proteins or various other compounds. The A260/A230 ratio is expected to be in the 1.8-2.2 range, and will be lower with increasing contamination of ethanol, EDTA (ethylenediaminetetraacetic acid) or carbohydrates.

Protocol:

1. Add 1.5 µl of the solution that the nucleic acids are diluted in and click ‘blank’.
2. Use a tissue to remove any liquid left on the pad. Add 1.5 µl of the sample and click ‘sample’. The software gives an output of the concentration in ng/µl.

3.1.6 Ligation

Ligation is a method for attaching free ends of DNA to each other. The enzyme DNA ligase catalyzes an ATP-dependent formation of a phosphodiester bond between a free 5’ and 3’ end of DNA. Ligation is most specific and efficient in ligating double-stranded DNA with “sticky end” overhangs that anneal to each other, as is the case if the ends that are to be ligated are cut with the same restriction endonuclease that creates an overhang. In this work, a T4 DNA ligase (New England Biolabs) was used. In a ligation reaction, it is important to have a correct molar relationship between vector and the insert fragment. A 1:6 molar relationship between vector and insert is optimal, and the amount of insert to add is found by the calculation:
Insert(ng) = 6 × (insert(bp) / vector(bp)) × vector (ng).

Protocol:

1. Put in eppindorf tube; 10 ng vector and insert in a 1:6 molar relationship. Add dH_2O to 8.5 µl, 1 µl 10x ligase buffer (NEB) and 0.5 µl T4 DNA ligase (NEB).
2. Incubate in room temperature for 1 hr or at 16 ^{o}C overnight.

3.1.7 Gateway cloning system

The Gateway cloning system is commercially developed by Invitrogen and exploits the site-specific recombination system of the bacteriophage lambda. The recombination enzymes can exchange an insert DNA sequence between two vectors with high fidelity if both vectors contain a sequence flanked by sequence elements called att-sites. When subcloning with the Gateway system, the process commonly starts with inserting a DNA sequence into a pENTR vector (also called an entry vector), containing a kanamycin resistance gene, by traditional restriction enzyme digestion and ligation.

When the sequence has been confirmed to be inserted correctly in the entry vector by DNA sequencing, a recombination reaction (LR reaction) can be set up between the entry vector and a pDEST vector (also called a destination vector), containing an ampicillin resistance gene, by mixing appropriate amounts of each vector and adding the Invitrogen LR clonase mix. This causes a recombination between the attL sites in the entry vector and attR sites in the destination vector, exchanging the insert DNA sequence from the entry vector with a toxic ccdB gene in the destination vector. The toxic gene and the fact that entry and destination vectors contain different antibiotic resistance genes allows simple and reliable selection for the destination vector which has gone through a recombination event. The process of LR recombination is summarized in Figure 11.

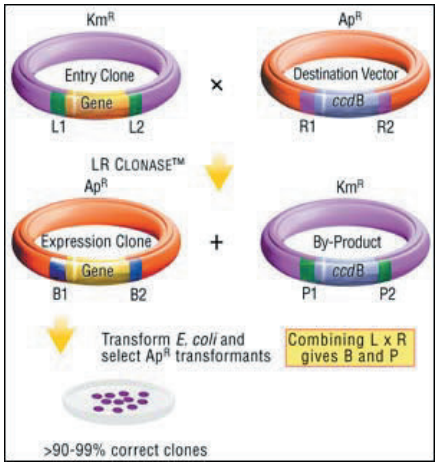

Figure 11: The Invitrogen Gateway cloning LR reaction. Figure adopted from Bioresearch online [133].

The TE buffer added to the reaction mixture contains EDTA which is a polyprotic acid that functions as a chelator of divalent metal ions. Such ions are common co-factors of many nucleases so EDTA is commonly added to solutions containing nucleic acids to protect them from degradation. Tris-HCl (tris(hydroxymethyl)aminomethane, pH adjusted by HCl) is a common buffer, here used to create slightly alkaline conditions that keep DNA deprotonated and soluble in solution.

Protocol:

1. Mix ~100 ng entry vector and ~150 ng destination vector, add TE buffer to 9 µl and 1 µl Gateway LR clonase enzyme. Mix and spin briefly then incubate at room temperature for 3 h or overnight.
2. Add 1 µl proteinase K and incubate at 37 °C for 10 min.

Table 5: TE buffer

Component	Final concentration
EDTA	1 mM
Tris-HCl ph 8.0	10 mM
dH_2O	

3.1.8 Site-directed mutagenesis

Through site-directed mutagenesis, a mutation can be introduced into a DNA sequence by primer design and PCR. The primer is designed to contain a mutation in the middle of a longer stretch of annealing nucleotides. By thermal cycling, the primer is extended to create full copies of the template plasmid containing the introduced mutation.

Because template DNA is isolated from bacteria, after the thermal cycling, the template (nonmutated) DNA can be selectively degraded by a specific restriction endonuclease (DpnI) that recognize methylated sequences that are found in bacterial plasmids but not in the PCR-synthesized DNA. The Quickchange process is summarized in Figure 12. For whole-plasmid synthesis it is important to use a non-displacing DNA polymerase such as the Pfu polymerase so that the polymerase extends the primers only until the plasmid is fully synthesized. For this project, primer design was aided by the Agilent QuickChange Primer Design online tool [134].

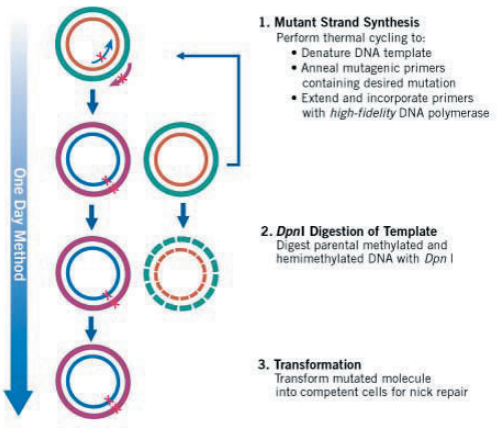

Figure 12: Quickchange site-directed mutagenesis. Figure adopted from Agilent quickchange kit product website [135].

Protocol:

1. Mix in PCR strips; 10-20 ng template, 1,5 µl of each primer (10 µM), 1 µl dNTPs, 5 µl 10x Pfu buffer and dH_2O to 49 µl.
2. Add samples to a thermal cycler set with the program below. Start the program and when the samples are heated to 95 °C , add 1 µl Pfu ultra polymerase to each sample.
3. After the program is finished, move content to eppendorf tubes and add 1 µl DpnI to each sample. Incubate at 37 °C for 2 hrs. Products can now be transformed into bacteria.

Thermal cycling program:

1. 95 °C – 1 min
2. 55 °C – 1 min
3. 68 °C – 6 min

Cycle 0-18

4. 4 °C - ∞

Table 6: Primers designed for site-directed mutagenesis of selected residues of ALFY

Name	Sequence (written from 5' to 3')	Tm °C
E2630A_F2632A	GCAGCCTATTGCTGTGGCAGTTGCCTCTGGAGATGGACGGA	78.7
E2630A_F2632A_antisense	TCCGTCCATCTCCAGAGGCAACTGCCACAGCAATAGGCTGC	78.7
M2710A_T2714A	TGAAATCAGCAACTTCCAATATTTGGCGCATTTGAACGCTTTGGCTGGCAGATCA	79.4
M2710A_T2714A_antisense	TGATCTGCCAGCCAAAGCGTTCAAATGCGCCAAATATTGGAAGTTGCTGATTTCA	79.4
Q2814A_D2819A	CAGATATTCTTAAGGCTAGCGGGTGGCCACTTTGCCCTGGCTGACCG	79.7
Q2814A_D2819A_antisense	CGGTCAGCCAGGGCAAAGTGGCCACCCGCTAGCCTTAAGAATATCTG	79.7
R2895A_E2899A	AGAATTCATCAGAGTCCATGCTGAGGCTTTGGCGTGTGATTACGTGAGTGC	78.7
R2895A_E2899A_antisense	GCACTCACGTAATCACACGCCAAAGCCTCAGCATGGACTCTGATGAATTCT	78.7

3.1.9 DNA Sequencing

When subcloning it is important to sequence entry vectors to confirm that they contain the correct sequences and that the reading frame is preserved. In this project, a DNA sequencing service at UiO IMBV was used. The sequencing lab has two ABI 3730 high-throughput capillary electrophoresis machines sequencing based on the Sanger method. This method is based on the random incorporation of fluorescently labeled ddNTPs along with normal dNTPs in a thermal cycling setup with a DNA polymerase. Incorporation of ddNTPs causes chain termination, resulting in chains of various lengths which end with a ddNTP that is fluorescently labeled according to the nucleotide that was inserted last. The chains are then separated by a capillary electrophoresis system and the sequence is read by analyzing the fluorescent tag on the ddNTPs as they pass through the electrophoresis system in order of length.

Protocol:

1. Add to PCR strips; ~200 ng DNA, 2 µl of 5 µM primer and mqH_2O to 10 µl.
2. Deliver samples to IMBV sequencing facility with appropriate sample information.

3.2 WORKING WITH BACTERIA

E.Coli is the bacterial workhorse of molecular biology, allowing for reliable production and maintenance of introduced DNA fragments and protein production. Sterile technique is essential when working with bacteria and equipment and reagents should be sterile filtered or autoclaved before use. For all work with *E.Coli*, liquid broth (LB), super optimal broth (SOB) or super optimal broth with catabolite repression (SOC) was used. Two strains of *E.coli* was used in this project, ‘DH5α’ and ‘BL21 Star’. DH5α is a strain that is primarliy used for subcloning as it is highly competent for transformation and relatively quickly produces large amounts of introduced plasmid DNA. BL21 star (DE3) are designed to produce proteins coded from introduced plasmids in an inducible T7 promoter-based expression system.

Table 7: Bacterial growth media

Reagent	Concentration LB	Concentration SOB	Concentration SOC
Peptone from caseine (VWR)	10 g/L	20 g/L	20 g/L
Yeast extract granulated (VWR)	5 g/L	5 g/L	5 g/L
NaCl	10 g/L	0.5 g/L	0.5 g/L
KCl		0.19 g/L	0.19 g/L
$MgCl_2$		0.95 g/L	0.95 g/L
$MgSO_4$		1.20 g/L	1.20 g/L
D-Glucose			3.60 g/L

Making bacterial growth medium:

1. Mix bactotryptone, yeast extract, NaCl and KCl (for SOB and SOC) according to Table 7 and autoclave flasks. After cooling, the LB is ready for use.
2. For SOC and SOB, add by sterile filtering through a 0.2 µm filter $MgCl_2$ and $MgSO_4$. For SOC, also add glucose by sterile filtering.

3.2.1 LB agar plates

LB agar plates are used for growing bacteria on a surface, typically to analyze how well a bacteria grows on a certain media with or without antibiotics or to isolate single clone colonies of transformed bacteria.

Making LB plates:

1. Mix components of LB medium according to Table 7 and add 15 g/L agarose then autoclave.
2. After autoclaving, cool to ~55 ^{o}C and add appropriate antibiotics; 50 µg/ml ampicillin or 25 µg/ml kanamycin.
3. Pour on to plates enough to cover the surface and let it cool before storage at 4 ^{o}C.

3.2.2 Making competent cells

Competent cells are bacterial cells that are highly susceptible to uptake of exogenous DNA. After growing cells in SOB medium, the media is removed and cells are resuspended in $CaCl_2$ before freezing them. This makes them competent because the divalent cations makes added plasmid DNA attach to the bacterial cell walls. The added glycerol ensures that the cells survive freezing. As competent cells contain no antibiotic resistance genes, and thus are grown in media without antibiotics, sterile technique through the process is especially important to prevent contamination by other bacteria.

Protocol:

1. Make an overnight culture in 5 ml SOB medium without antibiotic from a clone of the competent cells.
2. The morning after, innoculate 250 ml SOB with the 5 ml culture. Incubate in shaker at 37 ^{o}C until A_{600}=0.4 then centrifuge cultures 10 min at 4 ^{o}C, 5000 rpm.
3. Drain media thoroughly and resuspend by gently adding 50 ml cold 100 mM $MgCl_2$. Centrifuge 10 min at 4 ^{o}C, 5000 rpm.
4. Again pour off the supernatant and resuspend in 12.5 ml cold 85 mM $CaCl_2$ with 15% glycerol.
5. Immediately aliquot 310 µl into eppendorf tubes that are kept in metal blocks on dry ice. Freeze at -80 ^{o}C as quickly as possible.

3.2.3 Transformation of competent E.coli

To highly competent *E.Coli*, exogenous DNA can be introduced into the cells simply by mixing DNA with the cells, followed by a temperature change protocol called heat shocking. The plasmid will adhere to the competent cells as described above and the 37 °C heat shock will open pores that are naturally found in competent cells, allowing the plasmid to enter the cells. Subsequent cooling allows the cells to seal with the introduced plasmid inside. The amount of plasmid DNA that should optimally be added to the cells varies according to the vector that is used.

Protocol:

1. Thaw competent cells on ice. In a 14 ml Falcon tube add 30 µl dH_2O and plasmid DNA. For DH5α transformation, add 200-1000 ng plasmid DNA while for BL21 Star, add 10-50 ng plasmid DNA.
2. Add 100 µl competent cells and mix carefully by pipetting. Incubate 30 min on ice.
3. Heatshock at 37 °C for 2 min then quickly cool on ice.
4. Add 500 µl SOC medium and incubate at 37 °C in shaker for 45 min.
5. Plate 250 µl on LB plates with appropriate antibiotics and incubate at 37 °C overnight.

3.2.4 Liquid clone culture

After a single colony from a plate has been isolated, it can be further grown in a liquid LB culture to allow the single clone of bacteria to proliferate. Appropriate antibiotics is added to the LB liquid culture to select for bacteria containing a certain vector.

Protocol:

1. Put 5 ml LB media in a 14 ml Falcon tube. Add antibiotics to 50 µg/ml for ampicillin or 100 µg/ml for kanamycin.
2. Pick an average-sized colony (from an LB-plate) or scrape off a bit of frozen clone culture (from freeze stock) and transfer the bacteria to the clone culture.
3. Incubate at 37 °C in shaker overnight.

3.2.5 Bacterial freeze stock

Before starting the isolation of plasmid DNA from a clone culture, a freeze stock should be made so that more plasmid DNA can easily be made without having to re-transform when it is needed. Cultured *E.coli* in LB is added glycerol to a final concentration of 25% so that the bacteria survive the freezing process. If the freeze stock is kept at -80 °C, it remains viable for years.

Protocol:

1. Add 500 µl of the clone culture to a pre-cooled cryo-tube with 500 µl 50% glycerol in dH_2O. Freeze at -80 °C immediately.

3.2.6 Miniprep

Miniprep is a method for relatively small-scale isolation of plasmid DNA from bacteria. The method is based on an NaOH and SDS (sodium dodecyl sulfate) lysis of bacteria with following precipitation of proteins, genomic DNA and membranes. The supernatant containing plasmid DNA is then added to a DNA-binding column and washed before eluting the DNA. The commercial miniprep kit Machery-Nagel NucleoSpin was used in this project.

Protocol:

1. Centrifuge the culture at 11000 g for 30 sec. Pour off LB media and resuspend in Buffer A1 with added RNase A, then add A2 and A3 from the miniprep kit. Centrifuge at 11000 g for 5 min.
2. Add supernatant to the DNA-binding column and wash using buffer A4 with ethanol before eluting in a slightly alkaline AE buffer (5 mM Tris/HCl, pH 8.5).

3.2.7 Production of recombinant proteins in E.coli

Production of recombinant proteins in *E.Coli* starts with transformation of an appropriate bacteria expression vector into an *E.Coli* strain that is suitable for protein production, such as BL21 Star (DE3). This *E.coli* strain has a T7 polymerase that is inducible by adding isopropyl-1-thio-β-D-galactopyranoside (IPTG) to the culture. Vectors used for recombinant bacterial expression in this strain will contain a T7 promoter sequence upstream of the protein that is to be produced. BL21 Star (DE3) is also engineered in other ways to increase protein yield, among other things it contains a mutation in an endogenous RNase gene that normally contributes significantly to degradation of mRNA.

Protocol:

1. Grow a 5 ml liquid clone culture (section 3.2.4) with antibiotics in a 37 ^{o}C shaking incubator overnight.
2. The next morning, use the clone culture to innoculate 95 ml of LB with antibiotics. Grow at 37 ^{o}C with shaking until OD_{600}=0.5-0.7 then reduce temperature to 25 ^{o}C with shaking and incuce expression of the recombinant proteins by adding IPTG to a concentration of 0.5 mM. Further grow for at least 5 hrs or alternatively overnight at 20 ^{o}C.
3. Transfer cultures to ice and after cooling, centrifuge at 5000 rpm at 4 ^{o}C for 10 min.
4. Drain LB media and resuspend bacteria in 4 ml bacterial lysis buffer and incubate 20 min on ice.
5. Add 400 µl 10% Triton X-100 in dH_2O and freeze at -80 ^{o}C for at least 1 hr.

Table 8: Bacterial lysis buffer

Component	Final concentration
Tris HCl pH 7.4	20 mM
NaCl	200 mM
EDTA	1 mM
DTT, added fresh	1 mM
Protease inhibitor (EDTA-free, Roche), added fresh	1 x (from tablet)
dH_2O	

3.3 WORKING WITH PROTEINS

3.3.1 Purification of recombinant proteins produced in bacteria

Recombinant protein expression in bacteria allows for expression of a protein or protein domain with a tag attached that can be easily isolated from a bacterial lysate. Tags used for this purpose during this project include GST (glutathione S-transferase) and MBP (maltose binding protein) that both are found directly upstream of the inserted sequence in the destination vectors used for bacterial expression (Table 2). GST binds strongly to glutathion and MBP to maltose. This is exploited by using agarose beads with glutathion (GE Healthcare, Glutathion sepharose high perforance) or maltose (NEB, Amylose-agarose resin) attached. Adding bacterial lysate to these beads and several cycles of washing gives a simple method to isolate purified recombinant protein.

Protocol:

1. Wash 300 µl beads 3 times in 1 ml PBS and 2 times in PBS-T (0.1% tween). Then, equilibrate beads in bacterial lysis buffer by washing once and resuspending to make a 50% solution of beads in this buffer.
2. Thaw bacterial lysate (produced according to section 3.2.7) and sonicate with high amplitude using a program of 15 sec on and 45 sec off in 6 cycles.
3. Centrifuge at 4 ^{o}C, 10000 rpm, for 10 min. Transfer supernatant to a new falcon tube and add 150 µl of the prepared beads solution. Incubate on a rotating wheel at 4 ^{o}C for 1-2 hrs.
4. Centrifuge at 4 ^{o}C, 1000 g for 3 min. Remove supernatant but keep ~1 ml in the tube and transfer the remaining volume to an eppendorf tube.
5. Wash beads 6 times in PBS-T by adding 1 ml PBS-T, centrifuging and removing most of the liquid, then again adding PBS-T.
6. Beads with bound proteins can be stored as a 50% solution in PBS-T with protease inhibitors added, (EDTA-free, Roche) 1 x from tablet.

3.3.2 Elution of recombinant protein from beads

For storage and various other applications of purified protein, it is useful to be able to elute the recombinant protein from the beads. For glutathion and maltose beads this is performed by adding an appropriate concentration of glutathion (Sigma, reduced L-glutathion) or maltose (Sigma, D-maltosemonohydrate) that will compete with the bead-bound glutathion and maltose for binding to the recombinant tags. This frees the recombinant proteins from the beads and by using a simple Biorad polyprepylene column to retard the beads while allowing the liquid to pass, the purified recombinant proteins can be isolated in the eluate.

Protocol:

1. Add solution with beads to a polyprepylene column. Add 5 ml of bacterial lysis buffer (Table 8) and let it flow through.
2. Prepare bacterial lysis buffer with 20 mM glutathion or 10 mM maltose. For glutathion, the pH needs to be adjusted to ~8.
3. Add 350 µl elution buffer twice, letting it flow through after each addition. Collect flowthrough and split the collected ~700 µl into several aliquots and freeze at -80 ^{o}C.

3.3.3 SDS-PAGE and single-protein quantification

SDS-PAGE allows separation of proteins based on their electrophoretic mobility. Samples are added sodium dodecyl sulfate (SDS, from Sigma), dithiothreitol (DTT, from Sigma) and heated before applying to a gel. DTT acts as a reducing agent, ensuring that disulfide bonds are reduced for complete denaturing by heating. SDS is a detergent that will coat hydrophobic surfaces exposed in denatured proteins with a negative charge. The negative charge allows the proteins to be separated in an electrophoretic setup by applying a electronic potential over the gel. The charge of the SDS-coated peptide is dependent only on the mass of the polypeptide chain, giving a linear relationship between electrophoretic mobility and peptide chain length. For visualization of the proteins in the gel, the gel can be stained by various methods. In this project, SimplyBlue (Invitrogen) was used. To decide the concentration of a single protein in a sample, the same gel can be added BSA in known amounts, allowing for quantification by comparing sample band intensity with the BSA bands.

Protocol:

1. Add 1:10 of the sample volume of DTT and 1:3 of 4x SDS sample buffer to the sample. Incubate samples at 95 ^{o}C for 5 min, then cool down and centrifuge briefly.
2. Prepare a gel and proper running buffer in a gel running chamber, then add samples along with a protein standard.
3. Apply a current and let the gel run until there is sufficient separation of the proteins that are to be analyzed. The separation can be followed by looking at the protein standard.
4. Rinse the gel with three 5 minute washes with water, then stain in SimplyBlue (Invitrogen) for 1 hr. For simple applications, a quick destain in water is sufficient, but it can be extended to overnight for clearer results.
5. Visualize the gel by a system such as the Odyssey Infrared Imaging System (LI-COR). The software in this system allows easy quantification of protein bands by comparing the relative intensity of a single protein band in a sample to the intensity of a band from a solution that was added with a known amount of BSA.

Table 9: 4x SDS sample buffer

Component	Final concentration
Tris HCl pH 6.8	200 mM
SDS	8%
Glycerol	40%
Bromphenol blue	0.2%
dH_2O	

Table 10: 1x SDS-PAGE gel running buffer, Criteron (BioRad) gels

Component	Final concentration
Tris	0.3%
Glycine	1.4%
SDS	0.1%
dH_2O	

3.3.4 Protein transfer (blotting)

Protein transfer allows transfer of proteins separated by SDS-PAGE on to a membrane where the protein content of the gel can be further analyzed by immunodetection. After separating proteins based on size in a gel according to section 3.3.3, the gel is applied to a system where a current moves proteins out of the gel and on to a membrane while keeping the protein arranged relative to each other as they were separated in the gel. Different types of membranes and techniques for transfer are available, but for this project PVDF membranes (Millipore, Immobilon 0.45 µm) were used in a wet-blot tank transfer system (BioRad). Before use, PVDF membranes need to be activated in 100% methanol for a few seconds before equilibrating in transfer buffer. Methanol is also added to the transfer buffer for optimal transfer efficiency. Larger proteins are transferred more efficiently with lower methanol concentrations and opposite for smaller proteins.

Protocol:

1. Equilibrate the finished SDS-PAGE gel briefly in transfer buffer. Activate a PVDF membrane in 100% methanol for a few seconds and then equilibrate in transfer buffer.
2. In a chamber containing transfer buffer, assemble the gel and membrane on top of each other with pieces of cardboard and sponges on each side. Carefully remove any bubbles that might have accumulated between the layers.
3. Put the setup in a wet-blot transfer chamber containing transfer buffer and apply a current.

Table 11: 1x Transfer buffer

Component	Final concentration
Tris	0.3%
Glycine	2.4%
SDS	0.1%
Methanol	10-15%
dH_2O	

Table 12: Ponceau S

Component	Final concentration
Ponceau S	0.1%
Acetic acid	5%
dH_2O	

3.3.5 Membrane immunodetection and visualization

The goal of protein transfer on to a membrane is to be able to detect specific proteins by immunoblotting. This technique involves applying a specific primary antibody to the membrane, followed by a secondary antibody binding primary antibodies from a specific species. Secondary antibodies are conjugated to a tag to allow their visualization by methods such as chemiluminescence or infrared illumination. Milk and/or BSA proteins are added to the membrane before and with the antibodies to reduce background binding of antibodies to the membrane and nonspecific epitopes.

Visualization of antibodies on the membrane can be done by several methods. During this project, both chemiluminescence and illumination by infra-red wavelengths were used to detect secondary antibody conjugates. Secondary antibodies conjguated to the enzyme horseradish perodixase (HRP) can be used to detect proteins on a membrane when a substrate for the enzyme is added to the membrane. In this project, ECL Prime (Amersham) was used as a substrate. The reagents contained in this kit are processed by HRP and light is thereby emitted, allowing it to be detected by a camera, in this case a Syngene G:Box (VWR). Another membrane visualization method used in this project is based on secondary antibodies conjugated to molecules that absorb infra-red radiation at 680nm or 800nm. Illumination of the membrane in an Odyssey Imager (Li-Cor) visualizes the secondary antibodies in this case.

Protocol:

1. After transfer to membrane, equilibrate the membrane in PBS.
2. Add ~20 ml of Ponceau S and incubate for 5 min.
3. Wash carefully with dH_2O enough to remove much of the background staining while the protein bands are still visible then scan the membrane in a normal tabletop scanner (here a HP Scanjet G4050).
4. Destain of Ponceau S by incubating in 0.1M NaOH for 30 sec, equilibrate the pH in PBS, then in PBS-T (0.1% tween).
5. Incubate membrane in 7.5% non-fat milk powder in PBS-T for 1 hr on tipping platform.
6. Wash membrane in PBS-T, first 2x quickly then 3x for 5 min on tipping platform.
7. Put membrane in 5 ml PBS-T containing primary antibody and 5% BSA in a 50 ml tube. Incubate on a rolling platform at 4 ^{o}C overnight.
8. Wash membrane, first 2x quickly then 3x for 5 min on tipping platform.
9. Incubate membrane in 15 ml PBS-T with secondary antibody and 5% milk on a tipping platform for 45 min.
10. Wash membrane, first 2x quickly then 3x for 5 min on tipping platform.
11. Expose signal according to the type of secondary antibody used. For chemiluminescence, add a small amount of substrate (ECL Prime) to the membrane, incubate 5 min then expose under a camera (Syngene G:Box) for several minutes. For infra-red sensitive secondary antibody conjugates, take a picture of the membrane at an appropriate wavelength using the Odyssey Imager.

Table 13: Primary and secondary antibodies used for immunodetection in western blotting.

Antigen, conjugate	Raised in (species)	Source of antibody, cat.no	Dilution used
p62	Mouse	T. Johansen	1:1000
LC3	Rabbit	Cell signaling, 2775s	1:1000
β-actin	Mouse	Sigma, ac-15	1:20000
Ulk1	Rabbit	Santa Cruz, sc-33182	1:1000
GST	Mouse	Abcam, ab92	1:10000
MBP	Mouse	NEB, e8032s	1:10000
GFP	Rabbit	T. Johansen	1:1000
ALFY	Rabbit	In house	1:200
WDFY4	Rabbit	Protein Tech, 17558-1-AP	1:500
LRBA	Mouse	Abcam, ab22067-100	1:200
LYST	Mouse	Sigma, SAB1401075	1:200
NBEA	Guinea pig	Synaptic Systems, 194004	1:500
NBEAL1	Goat	Santa Cruz, sc-168716	1:200
anti-mouse, HRP	Goat	Jackson, 115-035-003	1:6000
anti-rabbit, HRP	Goat	Jackson, 111-035-144	1:5000
anti-goat, HRP	Rabbit	Rockland, 705-035-147	1:5000
anti-guinea pig, HRP	Donkey	Jackson, 706-035-148	1:5000
anti-mouse, IRDye 800	Goat	Licor, 926-32210	1:15000
anti-rabbit, IRDye 800	Goat	Licor, 926-32213	1:15000
anti-goat, IRDye 800	Goat	Licor, 926-32214	1:15000
anti-guinea pig, IRDye 800	Goat	Licor, 926-32411	1:15000

3.3.6 Membrane band quantification

Quantification of bands from a western blot experiment is useful to illustrate several replicates of an experiment and/or create a more visual representation of a set of results. Quantification of bands on membranes visualized by chemiluminesence was performed by ImageJ. For membranes visualized by the Odyssey system, the attached software has its own quantification tool where all that is needed is to mark the band of interest with a rectangle to get a value for the intensity of the band relative to the background.

Protocol ImageJ quantification:

1. Use the rectangle tool to mark the first band of interest. Use ‘Analyze’ - ‘Gels’ - ’Select next lane’ and select all bands of interest.
2. Click ‘Analyze’ - ‘Gels’ - ’Plot lanes’ to get a two-dimensional representation of the intensity of the selected bands.
3. Use the line tool to draw a line on the bottom of each peak, creating a closed of area of the band intensity above background intensity.
4. Select all peaks in the two-dimensional representation using the wand tool. Numerical values for area under the peaks will appear in a separate window.

3.3.7 Co-immunoprecipitation (co-IP)

Immunoprecipitation takes advantage of the affinity and specificity of an antibody to isolate a target protein from a solution with many proteins such as a cell lysate. The antibody is commonly attached to beads to pull it out of solution by centrifugation. Mild washing of the beads is then applied in several steps to remove proteins that are not specifically binding to the antibody or the associated protein complex. The goal of the assay is to wash away all proteins in the lysate except for the ones binding to the antibody and any interacting proteins. After washing, the protein content left associated with the beads is analyzed by western blotting. In the co-IP performed in this project, an anti-GFP antibody raised in rabbit was added to cell lysate from GFP-construct transfected cells and recombinant protein A (Thermo scientific) on agarose beads was added to be able to isolate the antibody and any binding protein from the lysate. The recombinant protein A has a high affinity for rabbit (and other species) IgG.

Protocol:

1. Cells (transfected or not) are washed 2x in cold PBS. After last wash, drain the plate on the side a few seconds to remove as much as possible of the PBS.
2. Add cold HeLa lysis buffer (200 µl for 6cm dish, 400 µl for 10cm dish) and leave on a horizontal shaker at 4 ^{o}C for 20 min.
3. Scrape content of dishes into eppindorf tubes. Centrifuge at 4 ^{o}C for 15 min at 250 g then transfer supernatant to new tubes.
4. Add 10 µl protein A beads (equilibrated in HeLa lysis buffer) to each sample as preclearance. Incubate on rotating wheel at 4 ^{o}C for 30 min then centrifuge at 4 ^{o}C for 10 min at 250 g. Transfer supernatant to new tubes.
5. Add precipitating antibody to each tube and incubate on rotating wheel at 4 ^{o}C overnight.
6. The next day, add 20 µl protein A beads (equilibrated in HeLa lysis buffer) and incubate on rotating wheel at 4 ^{o}C for 1 hr.
7. Wash the beads 6x with HeLa lysis buffer. Remove liquid after last wash, add SDS loading buffer with DTT and apply to SDS-PAGE. Results are further analyzed by western blotting.

Table 14: HeLa lysis buffer

Component	Final concentration
NaCl	150 mM
Tris HCl pH 7.5	10 mM
EDTA	0.5 mM
NP-40	0.5%
Phosphatase inhibitors (add fresh)	1x
Protease inhibotors (add fresh)	1x
dH_2O	

3.3.8 GFP-trap immunoprecipitation

Another variant of immunoprecipitation that can be used when immunoprecipitating GFP-tagged recombinant proteins is the GFP-trap (Chromotek) system. In this system, a GFP antibody is already covalently attached to beads and is therefore only applicable for isolating recombinant GFP-tagged proteins from cell lysate. An advantage of the GFP-trap system is that the GFP-antibody used is raised in camel, which have antibody proteins of significantly smaller molecular weights than most other species, meaning less contaminating proteins in the immunoprecipitation results.

Protocol:

1. Transfected cells are washed 2x in cold PBS. After last wash, drain the plate on the side a few seconds to remove as much as possible of the PBS.
2. Add cold HeLa lysis buffer (200 µl for 6cm dish, 400 µl for 10cm dish) and leave on side-to-side shaker at 4 ^{o}C for 20 min.
3. Scrape content of dishes into eppindorf tubes. Centrifuge at 4 ^{o}C for 15 min at 250 g then transfer supernatant to new tubes.
4. Add 15 µl GFP-trap beads (equilibrated in HeLa lysis buffer) and incubate on rotating wheel at 4 ^{o}C for minimum 2 hrs or overnight.
5. Wash the beads 6x with HeLa lysis buffer. Remove liquid after last wash, add SDS loading buffer with DTT and apply to SDS-PAGE. Results are further analyzed by western blotting.

3.3.9 Pulldown assays with purified recombinant protein on beads

Pulldown assays can be used to analyze protein interactions because proteins attached to beads can easily be centrifuged out of solution, bringing any interacting proteins with it. Cycles of adding a washing buffer and centrifuging the beads will remove proteins that do no specifically interact with the bead-bound protein from solution while interacting proteins will not be removed to the same degree. Several different types of pulldown assays were used during this project.

In vitro translation is one type of pulldown assay where a protein or domain of interest is synthesized with radioactive amino acids to allow highly specific and sensitive detection of the synthesized protein. In this project, a 'TnT Coupled Recticulocyte Lysate' (Promega) system was used with radioactive ^{35}S methionine (Promega). The reaction mixture is added a TnT RNA polymerase (Promega) that has a high rate of mRNA synthesis from suitable plasmids such as pDEST53. The synthesized mRNA is translated by ribosomes of the reticulocyte lysate, generating proteins with radioactive isotopes. RNasin is added to the reaction as a ribonuclease inhibitor to get an increased yield of mRNA and thereby protein from the system. Another method to analyze protein interactions by pulldown is to add a total cell lysate to the beads and detecting proteins that are specifically pulled down with the protein or domain on the beads by western blotting. If the purpose is to study direct protein interactions, both in vitro translation and cell lysate pulldown has a weakness in containing other proteins that might bridge an interaction to the protein on the beads. A way to prove a direct interaction between two proteins is by adding another purified recombinant protein to the one on the beads and performing the pulldowns.

Protocol in vitro translation pulldown:

1. Set up one in vitro translation mix for each unique translation. For each translation that is to be applied to N pulldowns, add N+1 of the following: (N+1) × 12.5 µl reticulocyte lysate, (N+1) × 1 µl TNT buffer, (N+1) × 0.5 µl TNT polymerase, (N+1) × 0.5 µl amino acids –met, (N+1) × 0.5 µl Rnasin, (N+1) × 1 µl ^{35}S.
2. Last, add (N+1) × 9 µl of 100 ng/µl plasmid DNA to each unique translation. Incubate at 30 ^{o}C for 90 min.
3. Add each unique translation to 15 µl empty beads for pre-clearance of proteins binding to the beads. Incubate on a rotating wheel in 4 ^{o}C for 30 min.
4. Divide the preclearance supernatant into the set amount of pulldown reactions and take an input sample. Add to pulldown tubes with sample beads and incubate on a rotating wheel in 4 ^{o}C for 60 min.
5. Wash beads 6x with 1 ml NETN buffer.
6. Remove all liquid after last wash, add SDS-loading buffer with DDT, boil and run on SDS-PAGE. After visualization of all protein content of the gel, the gel is dried on a piece of carboard in a vacuum drier (SDG 2000 Slab Gel Drier, Thermo Savant) at 75 ^{o}C for 3 hrs. The dried gel is then incubated with a radioactivity-sensitive phosphor screen (GE healthcare) for minimum 24 hrs before radioactive bands can be detected on the screen by a Typhoon IR phosphor screen imager.

Protocol total cell lysate pulldown:

1. Grow mammalian cells in several 10 cm plates and lyse them in HeLa lysis buffer. Scrape cells into eppendorf tubes and centrifuge at 4 ^{o}C, 250 g for 15 min. Transfer supernatant to new tubes and quantify the protein content by the BCA method (section 3.4.11).
2. Equilibrate beads with recombinant protein in NETN buffer and add appropriate amount of cell lysate. Add NETN buffer to 300 µl. Incubate at 4 ^{o}C on rotating wheel for 2 hrs.
3. Wash beads 6x with 1 ml NETN buffer.
4. Remove all liquid after last wash, add SDS-loading buffer with DDT, boil and run on SDS-PAGE. Protein content in the gel is analyzed by western blotting (section 3.3.4, 3.3.5).

Protocol pulldown of two recombinant proteins:

1. Both recombinant proteins are produced in *E.coli* BL21 (section 3.2.7) and bound to beads (section 3.3.1). One of the protein is then eluted from the beads (section 3.3.2).
2. Equilibrate beads in NETN buffer and add a decided amount of the other recombinant protein. Add NETN buffer to 300 µl and incubate at 4 ^{o}C on rotating wheel for 2 hrs.
3. Wash beads 6x with 1 ml NETN buffer.
4. Remove all liquid after last wash, add SDS-loading buffer with DDT, boil and run on SDS-PAGE. Protein content in the gel is analyzed by western blotting (section 3.3.4, 3.3.5).

Table 15: NETN buffer

Component	Final concentration
Tris HCl pH 8.0	20 mM
NaCl	200 mM
EDTA	6 mM
EGTA	6 mM
NP-40	0.5%
dH_2O	

3.4 MAMMALIAN CELL CULTURE

In mammalian cell culture, immortalized cell lines are cultured to grow under controlled conditions. All cell lines used in this thesis are adherent and grow optimally on a plastic surface in an incubator with 37 ^{o}C, close to 100% humidity and 4-10% CO_2. Strict sterile technique is required when working with cell culture to avoid infection.

The main cell medium used was Dulbeccos Modified Eagle Medium (DMEM, Lonza) with 4.5 g/L glucose and L-glutamine. For normal culturing conditions, this medium was supplemented with 10% fetal bovine serum (FBS) for growth factors and 1% penicillin+streptomycin (P/S) for antibiotics. As a transfection medium, DMEM without serum or antibiotics was used. Autophagy-assays where cells are starved was performed using Earles Balanced Salt Solution (EBSS, Invitrogen), a medium lacking serum and amino acids. The mammalian cell lines used in this project include HeLa from cervical cancer, HEK from embryonic kidney and U2OS from osteosarcoma. All cell lines were obtained from ATCC.

3.4.1 Freezing and thawing cells

Mammalian cells can be stored indefinitely in a tank of liquid nitrogen if they are frozen in a specific medium. The cryoprotective substance dimethyl sulphoxide (DMSO) is important in this medium as it prevents crystallization of water that would normally kill the cells. The cells are frozen in a specialized container that assures that the temperature drops gradually at 1c/min. DMSO is toxic to the cells so they need to be kept on ice and frozen quickly after adding the freezing media. When thawing cells, the cells should as quickly as possible be diluted into a large amount of media to minimize the toxicity of DMSO.

Freezing cells protocol:

1. Grow the cells that are to be frozen in large amounts until near confluency. One T175 flask yields five cryo-tubes with 1 ml each.
2. Trypsinize cells and add DMEM medium with 10% FBS and 1% P/S. Move to a 50 ml tube and centrifuge at 4 ^{o}C, 10 min, 1000 rpm.
3. Prepare 5 ml freezing medium per T175 flask. Mix DMEM, 20% serum and 5% DMSO. Keep it on ice. Prepare cryo-vials and put them on ice.
4. Remove supernatant from the centrifuged cell suspension and add the freezing medium. Distribute 1 ml to each cryo-vial.
5. Put cryo-vials in slow-cooling container and freeze at -80 ^{o}C. Move to nitrogen tank the next day.

Thawing cells protocol:

1. Keep cells on dry ice as they are moved from the liquid nitrogen container.
2. Have the tube in the 37 ^{o}C bath at short intervals until the cells are thawed just enough to be sucked into a pipette.
3. For cultivation of a T75 flask, put the cells in 15 ml DMEM. Split at least once before using the cells for experiments.

3.4.2 Subculturing and seeding cells

The cell lines used in this work are immortalized and have a set of genetic changes that may make them susceptible to accumulate additional genetic aberrations. Because of this they should only be grown for a certain number of generations before a fresh stock of cells that have gone through fewer generations are thawed. To keep a homogenous population of adherent cells, they should be split before they reach a degree of confluency of ~80%. Splitting them involves taking an amount of the originating culture and diluting it in an appropriate volume before re-introducing it into a new culturing flask. For all cell lines used in this project, splitting twice a week to a 1:10 ratio was appropriate. When splitting or seeding adherent cells for experiments, a solution of trypsin with EDTA is used to detach the cells from the surface they stick to. Trypsin is a serine protease which disrupts the extracellular matrix that the cells use to attach to the surface while EDTA acts as a chelator, sequestering calcium ions that has a dual role in keeping the cells attached and inhibiting trypsin activity.

Protocol:

1. Remove media then wash once with trypsin/EDTA solution.
2. Add trypsin/EDTA (3 ml for T75 flask) and put in incubator for 3 minutes.
3. When most of the cells are confirmed to be detached, add 10ml DMEM with 10% FBS and 1% P/S.
4. For splitting, add part of the cell suspension together with fresh media in a new flask. For seeding for experiments, first count cells (section 3.4.3), then distribute appropriate amount of cells into dishes or wells.

3.4.3 Counting cells

When setting up experiments, it is important to be able to determine the amount of viable cells that are found in suspension after trypsination. This can be done by the ‘Countess automated cell counter‘ (Invitrogen) system in which trypan blue is added to a small amount of cell suspension. Because dead cells are stained by trypan blue while live cells are impermeable to the staining, image analysis of the suspension can determine the amount of live and dead cells.

Protocol:

1. 5 µl of cell suspension is mixed with 5 µl of trypan blue and this mixture is added to one of the chambers on the ‘Countess cell counting slide’.
2. The slide is inserted into the cell counter and the amount of viable cells is determined.

3.4.4 Poly-D-lysine coating

Certain cell lines such as HEK attach poorly to the plastic surfaces in the containers that the cells are commonly grown. To help with the attachment, the surface can be coated with a synthetic extracellular matrix such as poly-d-lysine (Millipore).

Protocol:

1. Add 1.5 ml of a solution containing 33 µg/ml poly-d-lysine to each well of a 6-well plate. Leave for one hour at room temperature.
2. Wash 3x in autoclaved PBS and carefully remove all PBS after last wash.
3. Add cell media first and then the cell suspension.

3.4.5 Plasmid transient transfection

To study how a protein or protein domain influences a cell or where in the cell it localizes, its corresponding cDNA in an appropriate vector can be transfected into a cell transiently. According to the analysis being performed, the protein can have a tag attached. For this project, the 'FuGENE 6 Transfection reagent' (Roche) was used to transfect cells in a 24-well plate 24 hours before the cells were fixed and prepared for confocal microscopy analysis.

Protocol:

1. In an eppindorf tube add 20 µl DMEM and 0.6 µl FuGENE 6 reagent. Flick the tubes carefully and incubate 5 min at room temperature.
2. Add 0.2 µg of the DNA that is to be transfected. Flick the tubes and incubate 15 min at room temperature.
3. Add the mixture to the cells dropwise and ensure an even distribution of the mixture.

3.4.6 Drug treatment

In this project, several drugs were used to treat cells in a short time-period before fixation for microscopy or lysis for biochemical analysis. Puromycin (Sigma) is an amino acid analogue that causes premature chain termination at the ribosome, causing formation of protein aggregates. The drug Bafilomycin A1 (Baf A1, AH diagnostics) can be used in autophagy assays to measure autophagic flux. Because it inhibits the proton pump (H+-ATPase) of endosomal and lysosomal compartments, it inhibits lysosomal degradation and thereby causes accumulation of autophagic cargo. Another drug used in this project is the mitochondral uncoupler CCCP (Sigma) which disrupts the membrane potential over mitochondrial membranes that is important for its function and thereby induces degradation of mitchondria by autophagy. Puromycin and CCCP was used only for analysis by immunoflouresence while Baf A1 was used both for immunoflouresence and biochemical analysis of cell lysates.

Protocol:

1. Remove the existing medium and replace with DMEM with 10% FBS and 1% P/S that is added 10 µg/ml puromycin, 30 µM CCCP or 100 nM Baf A1. Leave for 2 hrs.
2. For immunoflouresence samples, proceed with PFA fixation or methanol fixation (section 3.4.8) or for biochemical analysis of lysate, lyse cells (section 3.4.10).

3.4.7 Starvation assay

The most common way of inducing non-specific autophagy is simply by starving the cells. This is done by growing cells in Earles Balanced Salt Solution (EBSS) without serum or amino acids for a short period of time. Combining EBSS starvation with Baf1 A1 allows quantification of autophagic flux when comparing a sample with only starvation to one with starvation and Baf A1 treatment.

Protocol:

1. Remove existing media and wash once with EBSS. Add EBSS and leave for 2 hrs in incubator.
2. For immunoflouresence samples, proceed with PFA fixation or methanol fixation (section 3.4.8) or for biochemical analysis of lysate, lyse cells (section 3.4.10).

3.4.8 Immunoflourescence and microscopy

Immunoflourescence was used in this project to analyze the localization of endogenous and transfected proteins. Endogenous proteins can be detected by first incubating the cells in a solution with a primary antibody recognizing the protein of interest, followed by incubation with a secondary antibody containing a flourochrome that recognizes the primary antibody. A transfected protein is normally detected by a directly conjugated flourochrome tag such as GFP (green flourescent protein) or others. Flourochromes used during this project include GFP with an absorbance maximum at 490 nm and emission maximum at 509 nm, Cy3 with absorbance maximum at 550 nm and emission maximum at 570 nm and Cy5 with absorbance maximum at 649 nm and emission maximum at 670 nm.

Table 16: Primary and secondary antibodies used for immunodetection in microscopy

Antigen, conjugate	Raised in (species)	Source of antibody, cat.no.	Dilution used
ALFY	Rabbit	In house	1:200
WDFY4	Rabbit	Protein tech, 17558-1-AP	1:200
LRBA	Mouse	Abcam, ab22067	1:200
LYST	Mouse	Sigma, SAB1401075	1:200
NBEA	Guinea pig	Synaptic system, 194004	1:200
NBEAL1	Goat	Santa Cruz, sc-168716	1:200
p62	Guinea pig	Progen, GP62-C	1:1500
p62	Mouse	BD biosciences, 610833	1:200
LC3	Rabbit	Cell signaling, 2775s	1:200
Rabbit, CY3	Goat	Jackson, 111-165-144	1:500
Mouse, CY3	Goat	Jackson, 115-165-146	1:500
Guinea pig, CY3	Donkey	Jackson, 706-165-148	1:500
Goat, CY3	Donkey	Jackson, 711-165-151	1:500
Guinea pig, CY5	Donkey	Jackson, 706-175-148	1:500
Mouse, CY5	Goat	Jackson, 715-175-150	1:500

In flourescence microscopy, a laser illuminates the sample at a specific wavelength and the flourochromes that absorb this wavelength will further emit light at a longer wavelength. The emitted light can then be detected in the microscope and show the localization of the flourochrome. A confocal microscope passes light emitted from the sample through a pinhole

aperture which rejects out-of-focus light. This allows a confocal microscope to analyze a sample in slices, minimizing background and increasing the resolution.

For analysis by microscopy, the cells need to be fixed and permeabilized before incubation with antibodies. In this project, two different methods were used for fixation, either paraformaldehyde (PFA) or methanol. PFA functions as a cross-linking agent, creating a network of linked antigens in the cell by forming intermolecular bridges through free amino groups. After fixing by PFA, NH_4Cl is added to quench any free PFA that could influence added antibodies. Methanol is an organic solvent that will remove lipids and percipitate proteins on the architecture of the cell. After fixation, PFA-treated samples are added saponin in all solutions with antibodies to permeabilize the cells. For methanol fixation, the cells are permeabilized by the methanol. BSA is added in a blocking step and to all antibody solutions to reduce unspecific background binding of the antibody.

PFA fixation protocol:

1. Remove media from well. Wash 2x in cold PBS.
2. Add 200 µl 3% PFA in PBS to each well. Leave 15 min on ice.
3. Wash 2x in PBS. Add 200 µl of 50 mM NH_4Cl to each well and leave 15 min.
4. Wash 2x in PBS. Add blocking solution of 200 µl 1% BSA, 0.05% saponin in PBS to each well. Leave 30 min.
5. Remove blocking solution. Create primary antibody solution in 1% BSA, 0.05% saponin in PBS. Put cover slip on a 25 µl drop of primary antibody solution on parafilm in a humidified container for 1 hr.
6. Wash 3x 5 min in PBS containing 0.05% saponin. Incubate in secondary antibody solution with 1% BSA and 0.05% saponin in PBS for 45 min.
7. Wash 3x 5 min in PBS containing 0.05% saponin.
8. Mount cover slips in 5 µl Mowiol (Prolong Gold, Invitrogen) with 0.5 µg/ml DAPI for staining of DNA.

Methanol fixation protocol:

1. Remove media from well. Wash 2x in cold PBS.
2. Add 200 µl 100% methanol cooled to -20 ^{o}C. Incubate 10 min on ice.
3. Wash 3x in PBS. Add 200 µl blocking solution of 1% BSA in PBS and leave 30 min.
4. Remove blocking solution. Create primary antibody solution in 1% BSA in PBS. Put cover slip on a 25 µl drop of primary antibody solution on parafilm in a humidified container for 1 hr.
5. Wash 3x 5 min in PBS. Incubate in secondary antibody solution with 1% BSA in PBS for 45 min.
6. Wash 3x 5 min in PBS.
7. Mount cover slips in 5 µl Mowiol (Prolong Gold, Invitrogen) with 0.5 µg/ml DAPI for nuclear staining of DNA.

3.4.9 siRNA-mediated knockdown

By siRNA (short-interfering RNA) transfection of mammalian cells, the expression level of certain proteins can be selectively lowered substantially. The technique of using siRNA is called RNA intereference (RNAi) and it exploits a mechanism of the cell that is probably designed to protect against viral infection. A protein machinery of the cell will recognize the transfected RNA, cleave it into smaller pieces and then use this fragment of the transfected siRNA to cleave mRNA that is complementary to it. In this project, ON-TARGET plus SMARTpool siRNA (Dharmacon) were used for all BEACH proteins. SMART-pool siRNA contains four different oligonucleotides against the same target in each pool, decreasing the concentration needed and thereby reducing off-target effects compared to transfecting with a single siRNA.

Protocol:

1. For 72 hour transfection, seed 1×10^5 cells in each well of a 6-well plate.
2. The day after, set up transfections. For each well that is to be transfected, mix 1 ml DMEM with 3.2 µl RNAiMAX Lipofectamine (Invitrogen) and siRNA to create a 40 µM solution. Incubate 20 min.
3. Add 1 ml trasfection mixture to each well and leave for 4 hrs in the incubator.
4. Remove the transfection mixture and add DMEM with 10% FBS and 1% P/S.

3.4.10 Lysate preparation

If the molecular constituents of a cell culture is to be analyzed biochemically, the content of the cells need to be extracted. This is normally achieved by incubating the cells in a lysis buffer containing detergents such as Triton X-100 or NP-40 which disturb cell membranes. A protease inhibitor is commonly added to the lysis buffer to prevent proteases from degrading cellular proteins as they are released during cell lysis.

Protocol:

1. Remove media then wash once in PBS. Leave tilted on ice for 1 min and remove all the PBS.
2. Add Triton lysis buffer, 100 µl for each well of a 6-well plate. Leave on ice 10 min with movement or shaking in intervals.
3. Scrape cells and add lysate to eppendorf tubes. Centrifuge at 4 ^{o}C, 18000 g, 10 min.
4. Add supernatant to new tubes. For biochemical analysis, proceed with protein quantification (section 3.4.11) and further with SDS-PAGE (section 3.3.3) and western blotting (section 3.3.4, 3.3.5).

Table 17: Triton lysis buffer

Component	Final concentration
NaCl	50 mM
Tris HCl ph 7.5	10 mM
EDTA	5 mM
Triton X-100	1%
Protease inhibitor (EDTA-free, Roche), added fresh	1x (from tablet)
dH_2O	

3.4.11 Lysate protein quantification

After lysate preparation, it is useful to be able to quantify the concentration of proteins in samples that are to be compared. For biochemical analysis of lysates, the amout of each lysate loaded to a SDS-PAGE needs to be comparable and this can be ensured by adjusting loading volume or diluting more concentrated lysates to correlate to the least concentrated ones. In this project, a BCA protein assay (VWR) was used to quantify the protein content of lysates. The BCA assay is based on a two-step reaction where first the biuret reaction between proteins and Cu^{2+} creates Cu^{+}. In the second reaction, bicinchoninic acid (BCA) reacts with the reduced copper and creates a puple-colored complex that absorbs at 562 nm with a linear relationship between protein concentration and absorbance. Absorbance was measured by a Flourstar OPTIMA plate reader (BMG labtech).

Protocol:

1. Pipette 5 µl of each sample in duplicate into a clear 96-well plate. Also add 5 µl in duplicate of a blank containing only lysis buffer and 5 µl in duplicate of a prepared set of standard-curve samples of known concentrations of BSA.
2. Mix BCA solution A+B, making 200 µl per well by adding solution B to solution A in a 1:50 relationship. Add 200 µl to each well and incubate at 37 ^{o}C for at least 30 min, maximum 2 hrs.
3. Measure absorbance of the wells at 560 nm using a plate reader.

3.4.12 RNA isolation

RNA isolation is an important prerequisite for analysis of the RNA content of cells. The preparation of lysates for biochemical analysis described above does not conserve the RNA content of the cell so a separate and identically treated cells needs to be cultured to be able to isolate RNA for further analysis. This procedure is sensitive to RNase contamination and special care needs to be taken to ensure sterile technique and use of only RNase-free equipment and buffers. In this project, a RNeasy plus kit (Quiagen) was used. The protocol starts with use of a lysis buffer with β-mercaptoethanol. The β-mercaptoethanol is added to disable the ribonucleases in the cells from degrading the RNA during the isolation procedure. The lysate is centrifuged through a QIAshredder column which fragments the DNA before adding to a gDNA-binding column which allows removal of the DNA from the sample.

Protocol:

1. Lyse cells in 350 µl β-ME-containing RCT lysis buffer. Scrape the cells and add to a QIAshredder column. Centrifuge 14000 rpm, 2 min.
2. Load flow-through to a gDNA binding column. Centrifuge 8500 g, 30 sec.
3. Add 350 µl 70% ethanol to the flow-through and load to a RNA-binding column. Centrifuge 8500 rpm, 15 sec.
4. Empty flowthrough and add 700 µl buffer RN1. Centrifuge 8500 g, 15 sec then put column into a new collection tube.
5. Add 500 µl buffer RPE. Centrifuge 8500 g, 2 min then put column into a new collection tube. Centrifuge again 14000 rpm, 1 min.
6. Put column into a sterile eppindorf collection tube. Add 30 µl RNase-free water and centrifuge at 8500 g, 1 min to elute.

3.4.13 cDNA synthesis and qPCR

For the application of quantifying mRNA through quantitative real-time PCR (qPCR), mRNA is converted to DNA through a reaction involving a reverse transcriptase enzyme with oligo-dT and random hexameric primers. The purpose is to create single-stranded DNA from mRNA of the sample where the amount of ssDNA correlates to the amount of mRNA that was present. In this project, the kit 'iScript DNA synthesis' (BioRad) was used for cDNA synthesis.

Quantitative real-time PCR (qPCR) uses the principle of thermal cycling and a heat-stable polymerase to amplify DNA fragments. A DNA intercalating fluorophore is added to monitor the formation of amplified products. The amount of cycles it takes to reach a certain level of fluorescence (called the Ct (cycle threshold) value) correlates to the amount of starting template cDNA. The primers added to each reaction define which cDNA is quantified. It is important to also analyze the Ct value of a housekeeping gene that should have a constant expression level regardless of how the cell is treated to control for the amount of cDNA added. After analyzing fluorescence from a given amount of cycles, a melt curve analysis of each sample is performed, where the temperature is gradually increased and fluorescence measured simultaneously. The fluorophore used in qPCR detects any and all dsDNA in the sample, so if the melt curve shows only one peak, it confirms that the primers are specific for a single sequence and that there is no contribution to fluorescence by primer dimers. Primer dimers are distinguished from PCR products in the melt curve because it has a significantly lower melting temperature than longer PCR products. In this project, a 'Sso Fast EVA green supermix' (BioRad) was used, containing a DNA polymerase, dNTPs, the fluorescent reporter and appropriate buffers.

cDNA synthesis protocol:

1. Measure the concentration of the isolated RNA using the NanoDrop 2000c (section 3.1.5).
2. Add 0.8 µg RNA for each sample in a PCR-strip. Dilute to 15 µl in total with RNase-free water. Add 4 µl 5x reaction buffer and 1 µl reverse transcriptase enzyme. Also set up a –RT control sample which has all components except the reverse transcriptase.
3. Run the following program in a thermal cycler:
   25c – 5 min
   42c – 30 min
   85c – 5 min
   4c - ∞

qPCR protocol:

1. Dilute cDNA 1:20 in water and add 12.5 µl of the diluted cDNA template to each well.
2. Create a mastermix for each primer set, adding 25 µl EVA green supermix, 5 µl primer (20 µM) and 7.5 µl water. Add 37.5 µl of this mastermix to each well. For each primer, also set up a sample adding the –RT control sample as template and another adding water instead of template.
3. Run the thermal cycling program:
   95 °C – 1 min
   95 °C – 5 sec
   55 °C – 5 sec
   Plate read
   72 °C – 5 sec
   Plate read
   Cycle 1-40
   then
   65 °C -> 95 °C at 0.5 °C increase per 3 sec step with plate read per step

3.5 BIOINFORMATICS

During this work, bioinformatics was used all through the project to design experiments and illustrate concepts. In silico cloning was consistently used during subcloning to choose vectors, restriction endonucleases, primers and check sequencing results. Because the only published phylogenetic analysis of BEACH proteins is outdated [86] (containing only five of the eight currently recognized human BEACH proteins), a thorough phylogenetic analysis was performed. A type of bioinformatic analysis was also used to form hypotheses about where on the BEACH domain surface protein-protein interactions are likely to take place and thereby choose residues to mutate by site-directed mutagenesis.

3.5.1 Identifying BEACH domain containing proteins in various species

For identification of BEACH domain containing proteins in different species, a protein BLAST search [136] was performed starting from the sequence of the BEACH domain of human ALFY, amino acids 2683-2976. The search was limited to species *H.sapiens*, *D.melanogaster*, *D.rerio*, *C.elegans*, *A.thaliana*, *D.discoideum*, *S.cerevisiae* and *S.pombe*, initially resulting in 106 entries containing a BEACH domain. After carefully reviewing the list, eliminating duplicate entries and unconfirmed and low quality entries originating from only one sequencing study, the list was narrowed down to 34 entries.

3.5.2 Multiple sequence alignments

A multiple sequence alignment uses the sequence information from three or more nucleotide or protein sequences to arrange different parts of the sequence relative to each other. This can give information about common parts of genes or proteins and can infer evolutionary relationship. In this project, multiple sequence alignments were used to illustrate homologous sequences in proteins and to make a phylogenetic analysis. The relatively new freely available online algorythm Clustal Omega [88] was used for alignments in this project due to its fast and accurate processing of large data sets. The alignment of human PH-BEACH domains in Figure 7 is taken from the graphical representation of the alignment in BioEdit [137]. The sequence conservation information inside the protein boxes in Figure 5 is the conservation plot displayed when showing an alignment in Jalview [87].

3.5.3 Phylogenetic analysis

Phylogenetic trees give a useful illustration of the evolutionary relationship between proteins. Because multiple sequence analysis and phylogenetic analysis is more accurate the more information is put into them, the sequence alignment that was the basis of the phylogenetic tree shown in Figure 6 was based on the full protein sequence of all the 106 initially found BEACH protein sequences in the NCBI database. Only after the alignment were the duplicate and unconfirmed sequences removed. The phylogenetic tree was constructed using the online EMBL ClustalW2 phylogeny [138] tool using default settings. What is shown in Figure 6 is a replication of the output from that online application made in Adobe Illustrator.

3.5.4 Structural analysis, prediction of interaction sites

For two BEACH proteins, the crystal structure of the PH-BEACH domains has been published. This allowed analysis of the structure to make rational choices about the location of likely interaction sites. There are many freely available web-based servers that make predictions about protein-protein interaction sites, but for this project, an algorithm that analyzes degree of residue conservation is especially well suited. The web-based service that was chosen for this purpose was CONSURF [139]. This service is based only on analysis of evolutionary conservation of amino acids, scoring them according to a substitution matrix and calculating evolutionary rate. The analysis starts with a BLAST-search, finding protein sequences with a chosen degree of sequence conservation, aligning them, organizing them phylogenetically and calculating amino acid conservation according to amino acid properties by the Rate4Site [140] algorithm. For this project, the pdb-entry of LRBA (1t77) was submitted, allowing sequences with 95-65% conservation and aligning them using MUSCLE [141]. All other settings were left as default. LRBA was chosen because the BEACH domain of this protein is the one that is published with the highest resolution. The output of the software is a .pdb file with information about the degree of conservation of each residue stored as a b-value attached to the residue. Using PyMOL [142] with a modified python script [143], a visual representation of the domains with coloration according to degree of conservation was created. This can further be used to analyze the domain to find patches on the surface of the domain that most likely participates in protein-protein interactions. Furthermore, by looking at the peptide chains making up the patches, specific residues can be chosen as targets of site-directed mutagenesis.

3.5.5 Computational structure prediction

There are many freely available online protein structure prediction tools, but they are of varying quality. A quite recently developed method called RaptorX [144] has emerged as one of the most accurate algorithms for structure prediction that are freely available. Similarly to many other services it is based upon homology threading, but it stands out from other algorithms in doing multiple-template threading and alignment quality assessment between iterations. By using several templates in homology threading, a structure can be obtained that integrates information from several sources according to how similar the sequences and structural elements are. During this project, a structure prediction was performed for the WD40 domain of ALFY. ALFY contains five WD40 repeat sequences, but WD40 domains are known to have a common architecture of a seven-bladed β-propeller. The analysis was performed to give an indication of the possibility of ALFY's WD40 domain creating the seven-bladed β-propeller even if it does not contain seven WD40 repeats. Homology threading will always be biased toward creating structures that are similar to the structures that are published so the results of the analysis have to be interpreted with caution.

4. Results

4.1 Characterization of the ALFY – p62 interaction

A collaboration between the group this project was performed in and a group in Tromsø resulted in a 2010 publication by Clausen et al [70] showing that ALFY and p62 interact to facilitate degradation of p62-associated ubiquitinated protein aggregates. Puromycin was used to induce formation of aggregates of misfolded proteins and it was shown by transfecting cells with deletion constructs of ALFY that the PH-BEACH domains is the part of ALFY that is required for its recruitment to the p62-positive aggregates. A construct also including the rest of the C-terminal end of ALFY showed a significant co-localization with p62 on the induced aggregates. Moreover, pulldown assays showed that an in vitro translated C-terminal ALFY construct was pulled down by MBP-p62 and that a deletion construct of p62(Δ170-221) abolished this interaction. A downside of this assay is that the in vitro translated protein used for the pulldown assay is synthesized in a rabbit reticulocyte lysate so it can not be excluded that other proteins in the lysate can contribute to the interaction. Thus, a direct interaction between ALFY and p62 has not been confirmed and one major goal of this project was therefore to obtain more information about the ALFY – p62 interaction.

The PH-like and BEACH domains of ALFY were subcloned separately or together into the pDEST-EGFP (Table 2) vector containg a GFP-tag for transfection into HeLa. Immunoflouresence analysis by confocal microscopy was performed to look for co-localization with endogenous autophagy markers p62 and LC3. LC3 remains bound to an autophagosome throughout the process of autophagy from formation of the phagophore to fusion with the lysosome (Figure 1) so it can be used as a general marker of autophagic vesicles. Investigating proteins for co-localization with LC3 is therefore a common assay to look for involvement in autophagy either at the regulatory level or as a substrate of autophagic degradation. Co-localization with p62 can also indicate an involvement in autophagy or the cargo selection of the process, or alternatively other processes that p62 is implicated in.

While the Clausen et al [70] co-localization experiments induced aggregate formation by treating cells with puromycin, we found that puromycin treatment was not needed to induce significant co-localization between the ALFY constructs and p62 (Figure 13). Whereas the PH-like domain (2528-2663) of ALFY was mainly nuclear and showed little or no co-localization with p62, the BEACH domain (2677-2977) showed co-localization with p62, but not with LC3 (Figure 13). Interestingly, the construct containing both the PH-like and the BEACH domains (2528-2977) seemed to co-localize even more strongly with p62, indicating that both domains together might be contributing to the affinity of specificity of the p62 interaction. p62 and LC3 co-localized extensively in puncta that were negative for GFP-BEACH or GFP-PH-BEACH. The lack of colocalization of the ALFY PH-BEACH domain with LC3 is in line with our previous findings showing that depletion of ALFY prevented recruitment of LC3 to p62-positive protein aggregates [71] and suggests that these domains may be having a dominant negative effect on autophagosome formation around the p62 bodies. This is likely because the ALFY WD40 and FYVE domains, binding to Atg5 and PI(3)P, respectively are required for recruitment of autophagic membranes to the p62-positive structures.

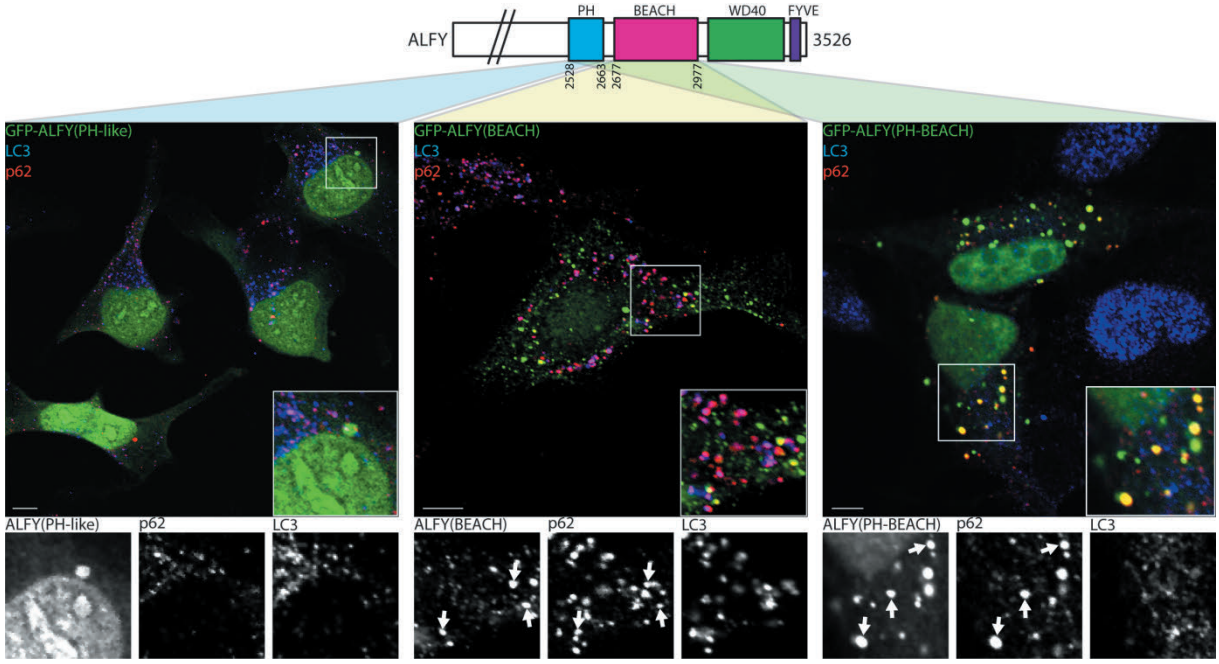

Figure 13: The BEACH domain of ALFY is responsible for its co-localization with p62. HeLa were transfected with plasmids encoding GFP-ALFY(2528-2663, PH-like), -ALFY(2677-2977, BEACH) or –ALFY(2528-2977 PH-BEACH) and stained for endogenous p62 (red) and LC3 (blue). Arrows indicate GFP foci with clearly specific co-localization with p62. Scale bar is 10 µm.

Next, we wanted to get more information about the ALFY-p62 interaction using in vitro pulldown assays. Several different variants of such assays were set up, trying various tags and deletion contstructs of ALFY and p62. Firstly, in vitro translated ALFY deletion constructs were tested against GST- and MBP-tagged p62. In the Clausen et al [70] publication, an in vitro translated construct of myc-ALFY(2586-3526) is significantly pulled down by MBP-p62. We found that in vitro translated GFP-ALFY constructs corresponding to the BEACH domain (2677-2977), the PH-BEACH domains (2528-2977) and the complete C-terminal of ALFY (2528-3526) were pulled down to a low, but similar degree by GST-p62 (Figure 14a). When compared to the 10% input, it is obvious that the observed interaction is significantly weaker than what is previously published [70], but it is noteworthy that the interaction is of a similar strength for the three cases, suggesting that the BEACH domain alone is mediating the interaction. We also tried to replicate the setup that was used by Clausen et al [70], using MBP-p62 on beads (Figure 14b), but did not detect any interaction with this setup.

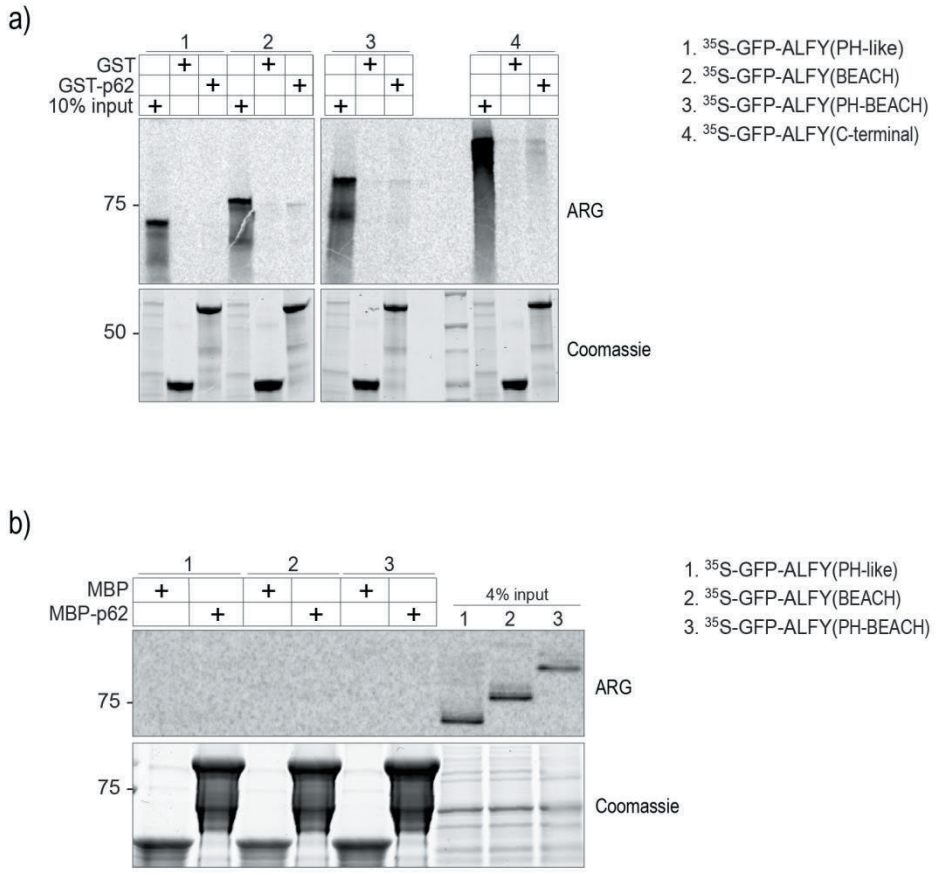

Figure 14: The BEACH domain of ALFY interacts with p62. In vitro translation pulldowns, adding in vitro translated GFP-ALFY constructs to p62 on beads. In vitro translated ^{35}S-GFP-ALFY(2528-2663, PH-like), -ALFY (2677-2977, BEACH), –ALFY (2528-2977, PH-BEACH) and –ALFY (2528-3526, C-terminal) were incubated with a) 2 µg GST or GST-p62 or b) 5 µg MBP or MBP-p62. In both cases, beads were washed 6x in NETN before SDS-PAGE. The gel was stained with coomassie to detect all recombinant proteins, then dried and incubated with a radioactivity-sensitive screen (autoradiography, ARG) to detect the bound in vitro translated proteins.

Another way to investigate protein-protein interactions is to add a mammalian cell lysate to a recombinant protein bound to beads, followed by pulldown and immunodetection of a protein from the lysate. When a HeLa cell lysate was added to recombinant GST-tagged PH-like and/or BEACH domains from ALFY we found that in this case, the PH-like domain alone shows the strongest interaction to p62 (Figure 15). The BEACH domain alone and PH-BEACH domains also pull down p62 to a larger degree than the GST control (Figure 15). Based on the lack of co-localization by immunoflouresence analysis (Figure 13), it seems likely that the PH-like domain is contributing to the affinity and/or specificity of the PH-BEACH domains for p62. Thus, one explanation for the observed results is that the PH-like domain is mediating an interaction to another interaction partner of p62 that is seen in this lysate pulldown assay but not in the immunoflouresence co-localization for unknown reasons. However, it is also possible that the PH-like domain is pulling down p62 in this assay due to unspecific contacts that are exposed when the domain is expressed alone. The PH-like and BEACH domains normally have a relatively large contact surface with ionic contacts giving them a high affinity for each other [106] and this surface could be mediating unspecific contacts in the pulldown assay.

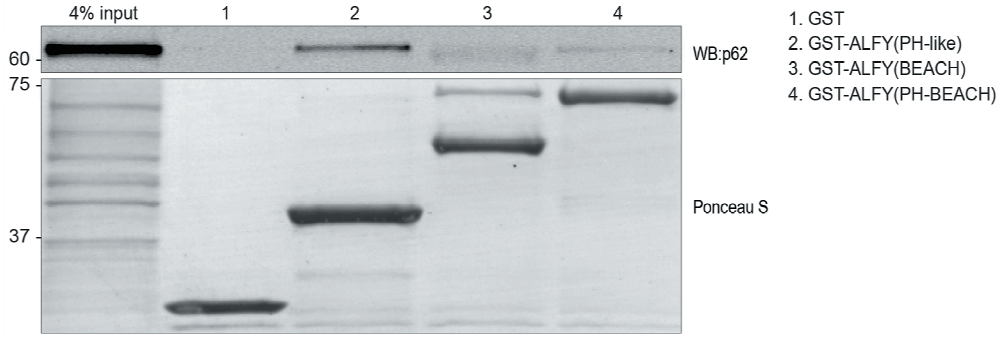

Figure 15: Pulldown of p62 from lysate by GST-tagged ALFY domains. Recombinant GST-ALFY(2528-2663, PH-like), -ALFY (2677-2977, BEACH), –ALFY (2528-2977, PH-BEACH) and GST alone were isolated from bacterial (E.coli BL21) lysates and purified. 200 µg HeLa lysate was added to 2.5 µg GST-domains, samples were incubated for 1hr then washed 6x with NETN before SDS-PAGE and immunoblotting with an anti-p62 antibody. Ponceau S shows the GST proteins.

To investigate if the observed interaction between the PH-BEACH domains of ALFY and p62 is direct, we purified recombinant GST-tagged ALFY domains, eluted them from beads and added them to beads with purified MBP-p62 (Figure 16a). We also performed the assay in reverse, keeping GST-tagged ALFY domains on the beads and adding eluted MBP and MBP-p62 (Figure 16b). The results showed that eluted GST-tagged ALFY BEACH domain (2677-2977) was significantly pulled down with MBP-p62 as compared to MBP alone (Figure 16a). The PH-like domain (2528-2663) and both domains together (2528-2977) were pulled down by MBP alone as well as with MBP-p62. This could be explained by the GST-tagged PH-like domain having an affinity for the MBP-tag in this assay. When the GST-tagged ALFY domains are kept on beads and MBP-p62 is eluted and added to a pulldown, we see a very weak interaction between the BEACH domain (2677-2977) and MBP-p62 that is also seen for the PH-BEACH domains (2528-2977), but not for PH-like alone (Figure 16b). The interactions seen in this assay using only recombinant proteins suggest there is a weak direct interaction between the BEACH domain of ALFY and p62, but although the results are reproducible, the interaction is too weak for any definitive conlusion to be drawn. We would also like to see the same interaction for the PH-like and BEACH domains together as this is the natural state of the protein domains.

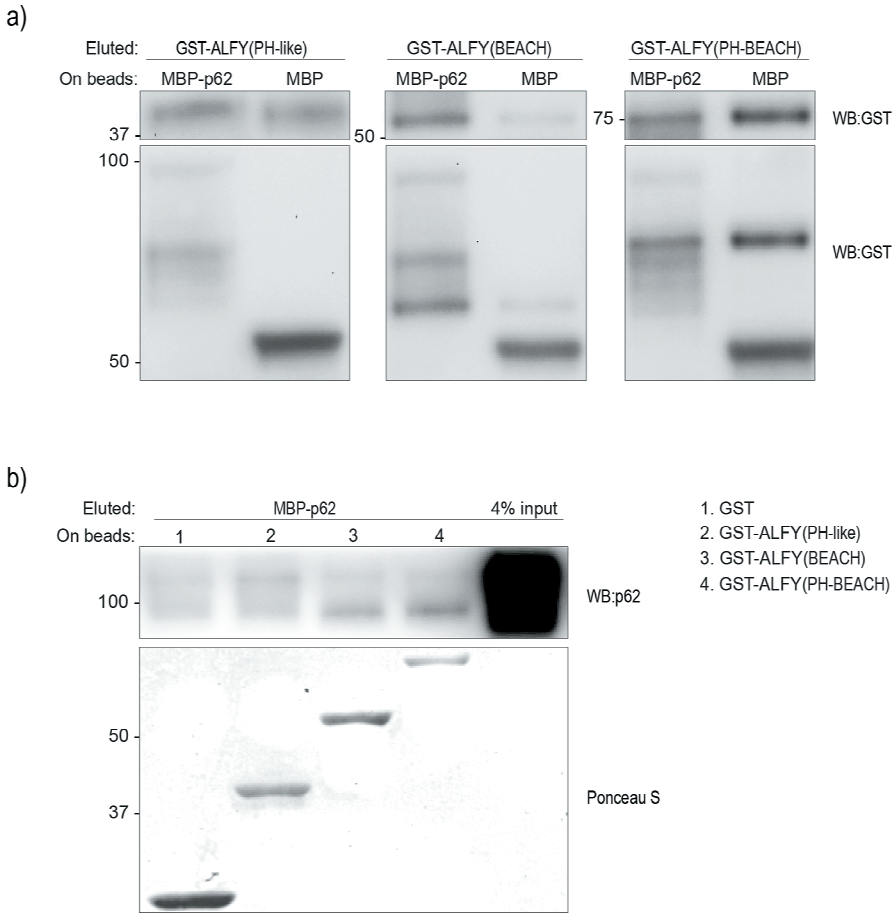

Figure 16: The BEACH domain of ALFY shows a weak direct interaction with p62. Recombinant GST-ALFY (2528-2663, PH-like), -ALFY (2677-2977, BEACH), –ALFY (2528-2977, PH-BEACH), MBP and MBP-p62 were isolated from bacterial (E.coli BL21) lysates and purified. The pulldown assay was performed in two orientations; a) 2 µg MBP and MBP-p62 kept on beads were incubated with 2 µg eluted GST-tagged ALFY domains, incubated for 1hr then washed 6x with NETN and run on SDS-PAGE, before immunoblotting with a

GST antibody. The GST antibody used here also binds to MBP so it was used to demonstrate the loading of MBP and MBP-p62 as well as to detect the ALFY domains. b) 1.5 µg GST-ALFY domains bound to beads were incubated with 2 µg MBP-p62. After 1 hr the beads were washed 6x with NETN and analyzed by SDS-PAGE and immunoblotting with an anti-p62 antibody. Ponceau S staining shows GST proteins. The theoretical molecular weight of MBP-p62 is 92kDa.

4.2 Which part of the PH-BEACH domains is responsible for the interaction with p62?

As shown above, the BEACH domain of ALFY seems to have a weak but specific interaction to p62 while the PH-like domain might be contributing to or modulating this interaction by interacting with other proteins. As nothing is known about which parts of the PH-BEACH domains is responsible for the interaction we set out to investigate this. As we will show later, recombinant PH-like and BEACH domains of many BEACH proteins show similar binding characteristics to p62 as has been shown for ALFY, suggesting that evolutionarily conserved features of the PH-BEACH domains mediate an interaction to p62. We took advantage of this to make a hypothesis about likely protein-protein interaction regions and involved residues on the PH-BEACH domains of ALFY. The online bioinformatics tool Consurf [139] was used to create a .pdb file which contains information about the degree of evolutionary conservation of all residues in the domains. Because the affinity for p62 seems to be conserved throughout BEACH domains, the residues responsible for the interaction should also be conserved. The structure obtained by Consurf contained two obvious concave grooves on the surface of the domains with considerable residue conservation (Figure 17a; main groove and 17c; alternative groove). Four patches with two residues in each patch were selecated for mutagenesis due to their appropriate position in the grooves, high degree of consevation and orientation of the residues towards the surface of the grooves (Figure 17b, d). The Consurf analysis was performed on the PH-BEACH domains of LRBA while the following biochemical experiments (Figure 18) were performed on the PH-BEACH domains of ALFY because the selected residues were absolutely conserved in ALFY (Figure 17f) and the characteristics of the interaction between PH-BEACH domains and p62 is better described for ALFY.

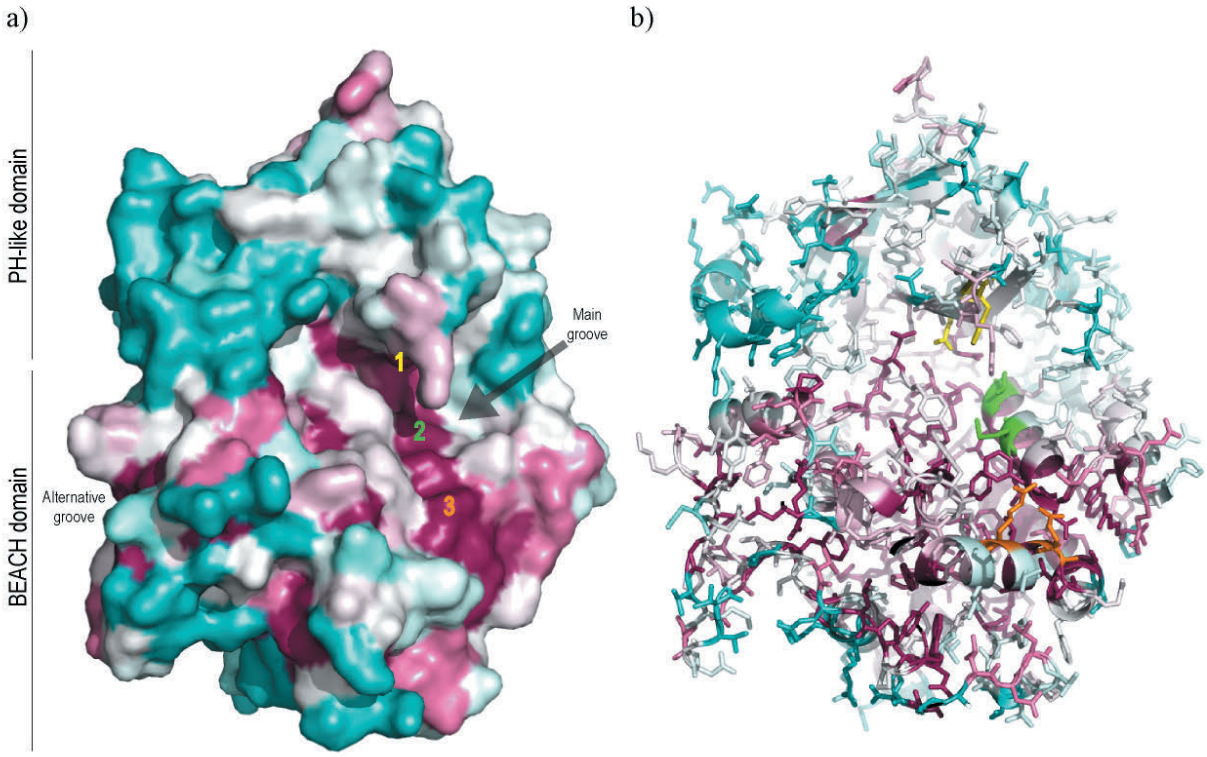

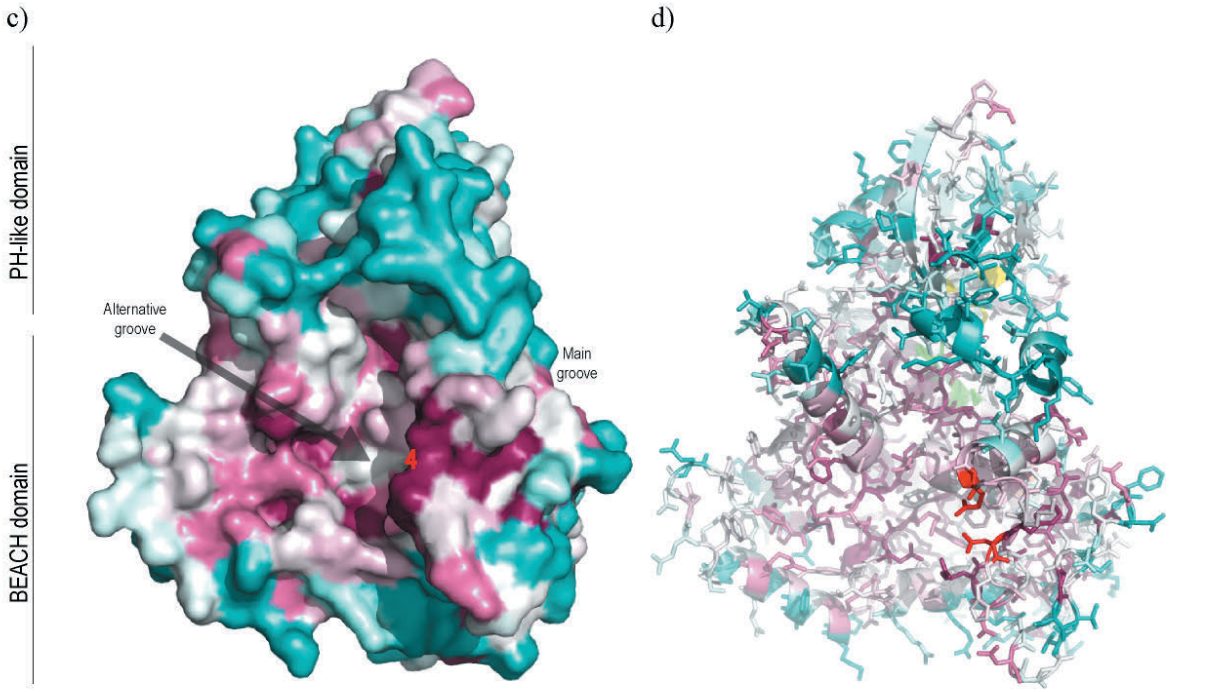

e)

	LRBA	ALFY
1	E2153, F2155	E2630, F2532
2	M2226, T2230	M2710, T2714
3	R2407, E2411	R2895, E2899
4	D2333, R2337	Q2814, D2819

f)

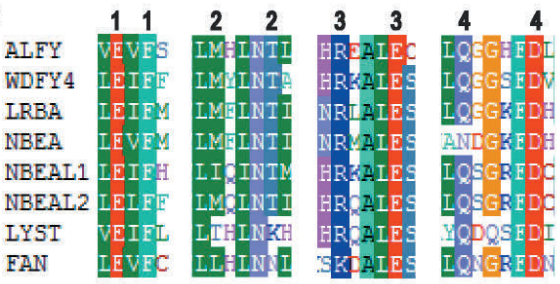

Figure 17: The PH-like and BEACH domains of LRBA contain two conserved grooves with conserved residues that might mediate protein-protein interactions. Figures are from PyMOL of LRBA (PDB id: 1t77 chain A) with coloration of residues according to the degree of evolutionary conservation. Numbers on figure a) and c) indicate patches of conserved residues in LRBA that were selected for site-directed mutagenesis in ALFY. Figure a) shows the most promising protein-protein interaction groove (indicated as main groove), formed by residues of both the PH-like and BEACH domains. From a) to c), the domain is rotated 90 degrees around the vertical axis to demonstrate the second conserved groove, formed by residues of the BEACH domain (indicated as alternative groove). Figures b) and d) are stick representations of the same figures with specific coloration of the residues that were mutated. Coloration according to conservation is made by the Consurf algorythm with a customized python PyMOL coloration script where blue indicates not conserved, white somewhat conserved and red more conserved. In e) is shown the specific residues that are indicated in the figures of LRBA and their corresponding residues in ALFY. f) shows pieces of a sequence alignment of the human BEACH proteins where just the residues that were selected for mutagenesis are extracted and indicated by numbering corresponding to the patches shown in a, c and e.

To investigate if any of the selected residues are important for the ALFY PH-BEACH domains to bind p62, the mutated ALFY domains were expressed as GST-fusion proteins, bound to beads and incubated with a HeLa cell lysate. The residues selected for mutation on basis of the Consurf analysis of LRBA were fully conserved in ALFY and the numbering scheme of the conserved patches from Figure 17 is repeated in the results from the pulldown shown in Figures 18a and b. The hypothesis was that one or several of the selected conserved residues were responsible for mediating an interaction with p62, and therefore one or several of the investigated alanine mutations should reduce p62 binding. The results showed that none of the mutations consistently reduced the binding of p62 to the tested (Figure 18a, b). The mutated residues in the PH-like domain (2528-2663) reduced binding when mutated in the PH-like domain alone in the first replicate of this experiment (Figure 18a), but upon repeating it the binding to p62 was actually increased by the mutation (Figure 18b). The variation seen between these replicates can be interpreted to be because p62 binds to the PH-like domain, when expressed alone, by indirect unspecific contacts between the domain and proteins from the lysate. When the same residues (patch 1) were mutated in the PH-BEACH domain, we were surprised to see that the domains binding to p62 was increased. Similarly, the other mutation of residues deep in the main groove on the PH-BEACH domains (Figure 18, patch 2) also increased the binding of p62 when mutated in the PH-BEACH construct in one of the replicates. Mutations of residues of the outer part of the main groove (Figure 18, patch 3) or the alternative groove (Figure 18, patch 4) did not influence binding to p62. The observed results suggest that the main groove is responsible for binding to p62, but the dynamics of this interaction remains unclear. One possible explanation is that the mutated residues annotated as patch 1 and 2 have a role in keeping the main groove in a closed conformation, and when mutated they open the groove up, allowing increased binding of p62. Taken together, the results suggest that p62 interacts with the PH-BEACH domain of ALFY in the main groove. Furthermore, the positioning of these residues and the fact that the mutations promote p62 binding indicates that the PH-BEACH domains function as a unit to create a dynamic interaction surface that selectively interacts with p62, possibly influenced by other interaction partners or post-translational modifications.

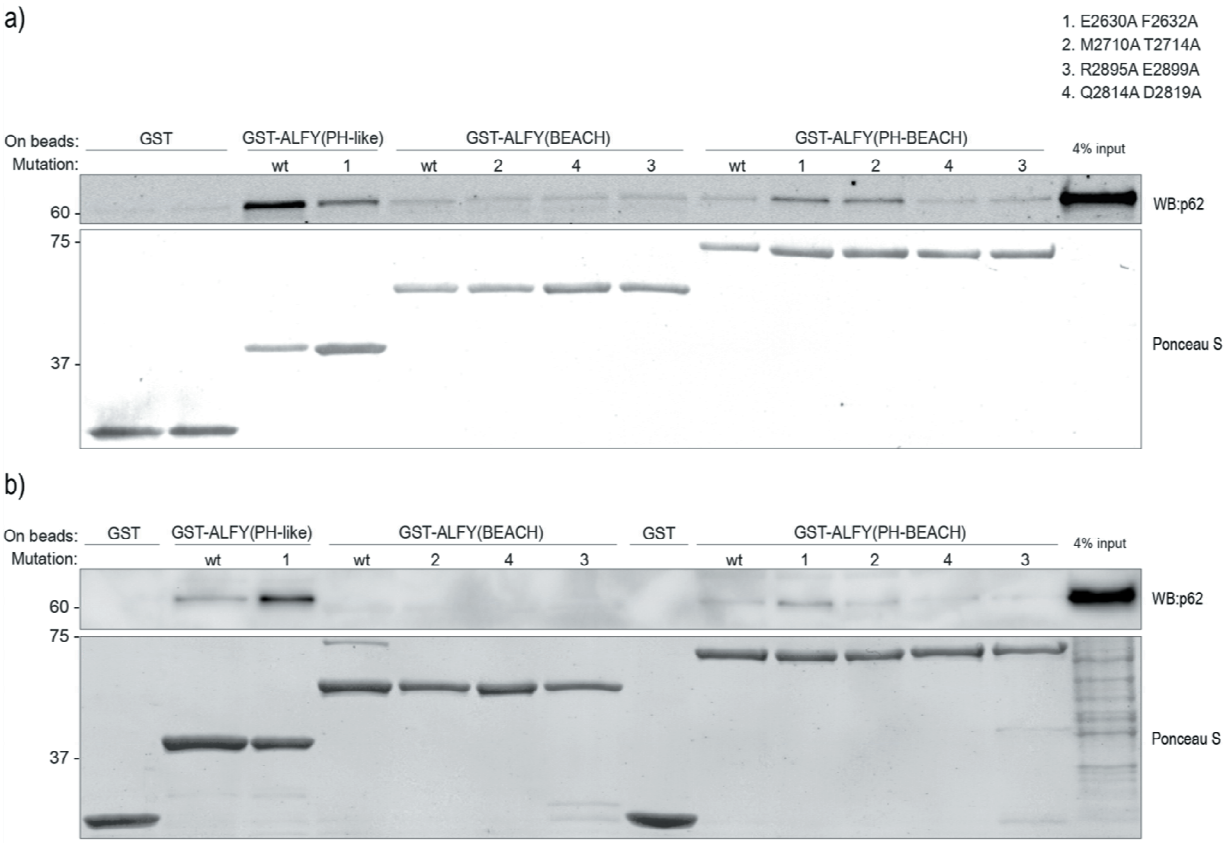

Figure 18: Pulldown of p62 from HeLa lysate using GST-tagged ALFY domains with selected mutations. Recombinant GST-ALFY(2528-2663, PH-like), -ALFY (2677-2977, BEACH), –ALFY (2528-2977, PH and BEACH) with and without mutations were isolated from bacterial (E.coli BL21) lysates and purified. The numbering of the mutations (1-4) corresponds to the numbering of the conserved patches in Figure 17. 150 µg HeLa lysate were added to 2.5 µg of GST-domains in each pulldown and washed six times in NETN before SDS-PAGE and immunoblotting with anti-p62 antibody. Ponceau S shows the GST proteins. a) and b) are replicates of the same experiment with slight adjustments in the amount of GST-proteins added. The differences in sensitivity of the immunoblotting between the replicates is due to the Odyssey system being used for detection in a) while HRP-based chemiluminescence was used in b).

4.3 Do PH-BEACH domains of other BEACH proteins also interact with p62?

There are in total eight human proteins containing a BEACH domain (Figure 5) and so an important part of this project was to investigate if other BEACH proteins can also interact with p62 and thereby possibly be involved in autophagy. FAN was excluded from this investigation because it differs from the other BEACH proteins being significantly smaller and therefore less likely to function as a scaffolding protein. For the other BEACH proteins we obtained cDNA clones containing sequence of their C-terminal and used PCR to amplify the PH-like and BEACH domains, which were then subcloned separately or together into various vectors containing relevant tags. For NBEAL1, the cDNA clone did not include the PH-like domain so only the BEACH domain was investigated for this protein. Subcloning of NBEA was only successfully completed in the last months of the project after trying several primer pairs. Because of this, NBEA was not included in several of the analyses. Immunoflouresence co-localization, co-immunopercipitation and pulldown assays were set up to investigate a possible interaction of the BEACH proteins with p62.

4.3.1 *Co-localization studies*

HeLa cells were transfected with GFP-tagged constructs encoding the PH-like and/or BEACH domains of the various BEACH proteins. Cells were fixed and stained for endogenous p62 and LC3 to determine if the PH-like and BEACH domains of these proteins co-localize with either of these autophagy markers. The PH-like domain (2372-2515) of WDFY4 shows a similar staining as the ALFYs PH-like domain, a diffuse and mostly nuclear staining (Figure 19). The BEACH domain (2525-2821) and PH-BEACH domains (2372-2821) also behave similarly as ALFY in forming cytoplasmic foci that to some degree co-localize with endogenous p62 but rarely with LC3. However, it is noteworthy that there seems to be less recruitment of p62 to the GFP foci formed by constructs containing the BEACH domain of WDFY4 than is the case for ALFY BEACH-containing constructs.

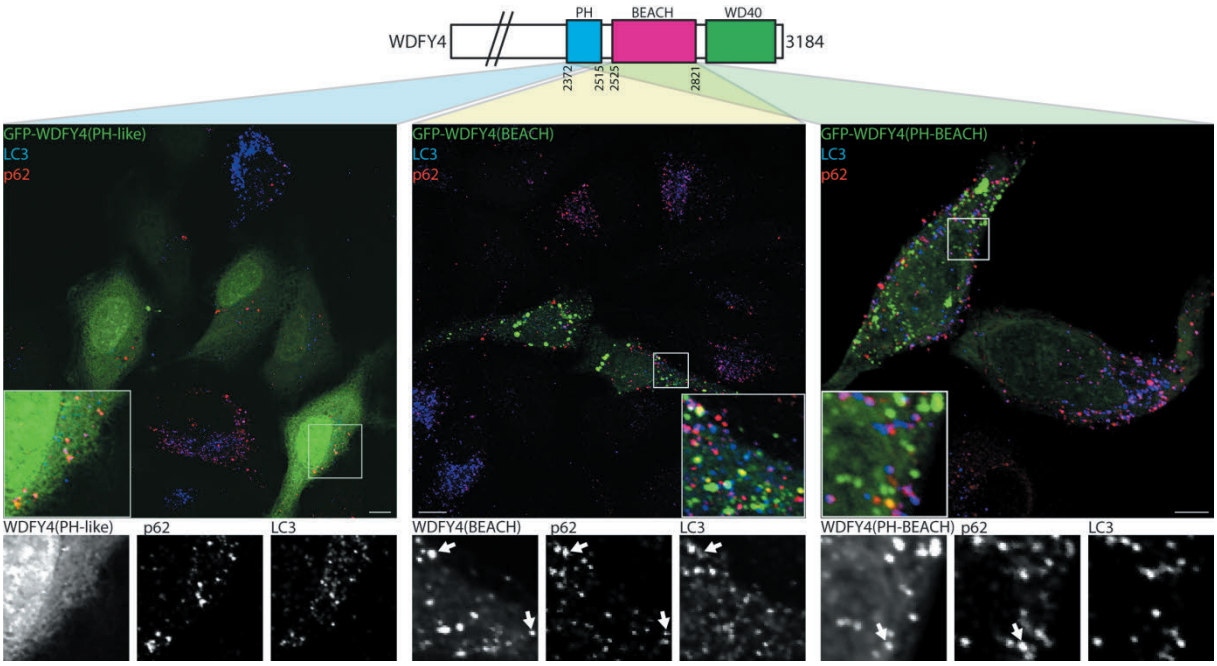

Figure 19: The BEACH and PH-BEACH domains of WDFY4 co-localizes to some degree with p62 and LC3. HeLa were transfected with plasmids encoding GFP-WDFY4(2372-2515, PH-like), -WDFY4(2525-2821, BEACH) or –WDFY4(2372-2821 PH-BEACH) and stained for endogenous p62 (red) and LC3 (blue). Arrows indicate GFP foci with clearly specific co-localization with p62 and/or LC3. Scale bar is 10 µm.

The PH-like domain of LRBA (2076-2185) shows a diffuse staining throughout the cell with some weak foci formation, but no specific co-localization with p62 or LC3 (Figure 20). The BEACH (2199-2489) and PH-BEACH domains (2076-2489) co-localize with p62 and rarely also with LC3. In this case, similarly to what is seen with ALFY, both domains together seem to have a more specific co-localization with p62 than the BEACH domain alone, suggesting that both domains together contribute to the specificity and/or affinity of the interaction in vivo.

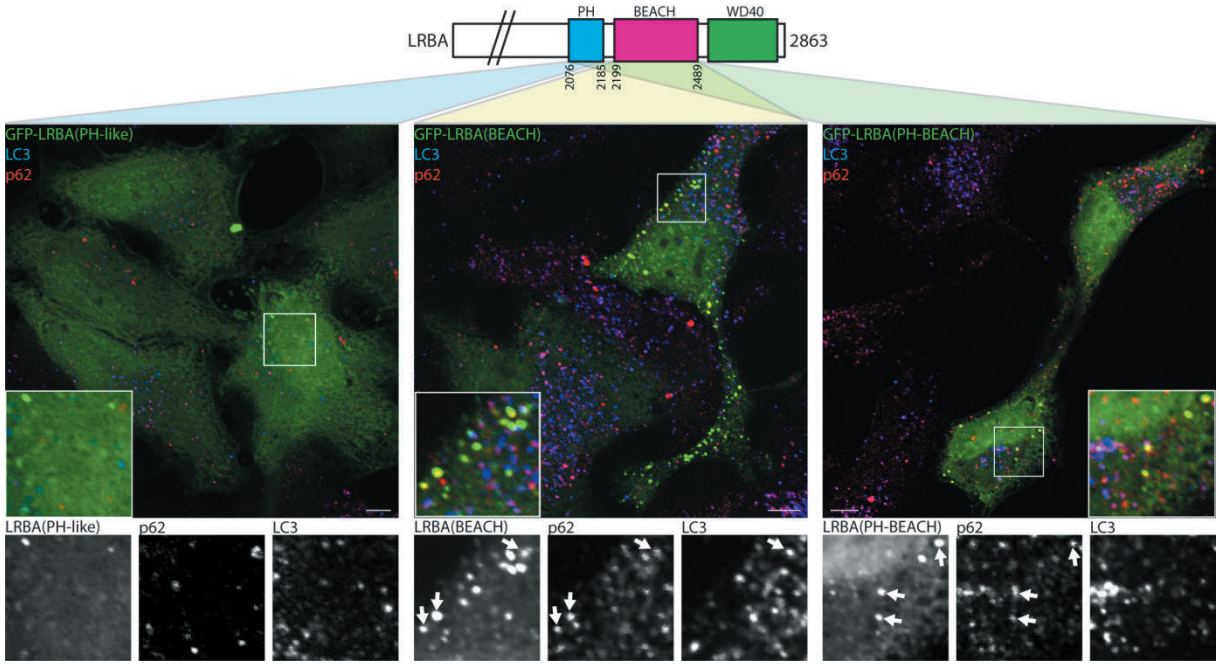

Figure 20: The BEACH and PH-BEACH domains of LRBA co-localize with p62. HeLa were transfected with plasmids encoding GFP-LRBA(2076-2185, PH-like), -LRBA(2199-2489, BEACH) or –LRBA(2076-2489 PH-BEACH) and stained for endogenous p62 (red) and LC3 (blue). Arrows indicate GFP foci with clearly specific co-localization with p62 and/or LC3. Scale bar is 10 µm.

The localization of the GFP-tagged domains of LYST is significantly different than the other BEACH proteins studied in this project. Whereas GFP foci formed by PH-like domains of other BEACH proteins almost never colocalize with p62 and/or LC3, the PH-like domain (3011-3115) of LYST was found to co-localize extensively with both p62 and LC3 (Figure 21). In line with what is seen for other BEACH proteins, the BEACH domain of LYST (3120-3422) shows some co-localization with p62, although less than for the other BEACH proteins. The LYST PH-BEACH domains (3011-3422) however, clearly co-localize with both p62 and LC3. This could indicate that the PH-like domain of LYST is interacting with a protein associated with autophagosomes, but it could also mean that it is targeted for autophagic degradation. When overexpressing proteins for analysis of aggrephagy it is always difficult to differentiate aggregation due to overexpression from specific and relevant co-localization due to regulation or execution of autophagy. However, because the localization of the PH-like domain of LYST consistently co-localizes with LC3 even at relatively lower expression levels and is seen for both the PH-like domain alone and the PH-BEACH domains we think this pattern of co-localization is relevant to the function of the PH-like domain of LYST rather than simply being a consequence of overexpression. These results suggest that the PH-BEACH domains of LYST function to localize the domains to autophagosomes, and that in this case, the PH-like domain is the main contributor. It is also noteworthy that one of the positions where alanine mutations increased binding of p62 in ALFY is not conserved in LYST (Figure 17f, patch 2). This, together with the co-localization results (Figure 21) that also vary significantly from what is seen for the other BEACH proteins suggest that the PH-BEACH domains of LYST have adopted a slightly different role than the other BEACH proteins, although they still seem to be inovlved in the autophagic pathway.

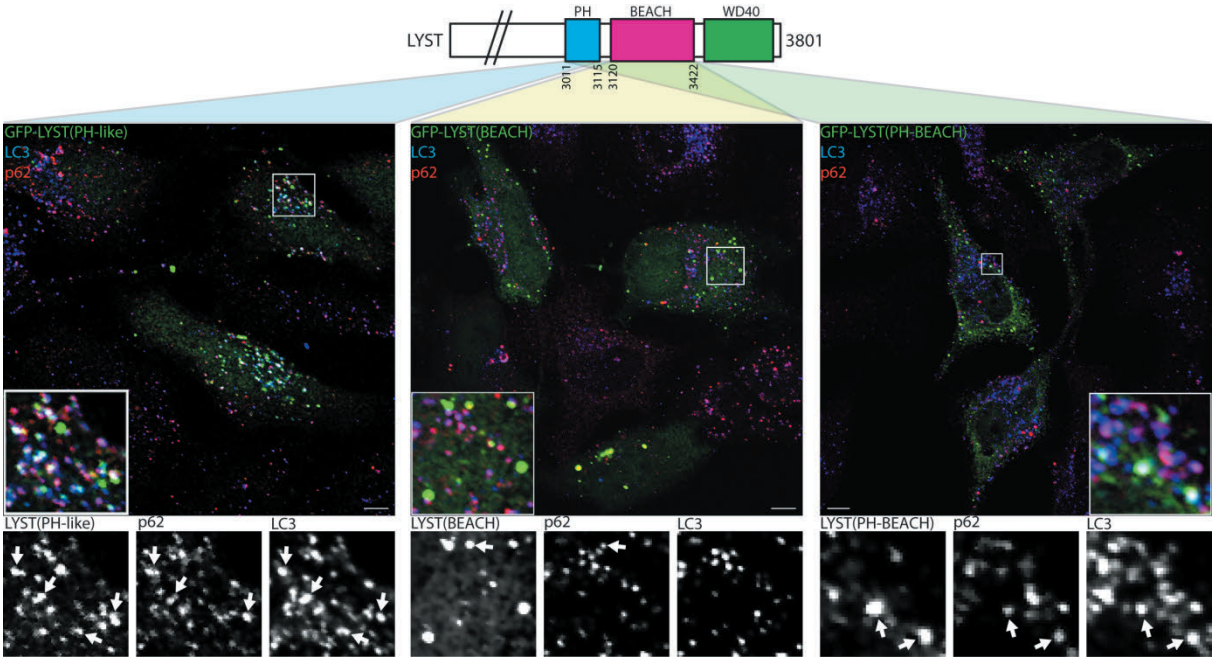

Figure 21: The PH-like and PH-BEACH domains of LYST co-localize with both p62 and LC3. HeLa were transfected with plasmids encoding GFP-LYST(3011-3115, PH-like), -LYST(3120-3422, BEACH) or –LYST(3011-3422 PH-BEACH) and stained for endogenous p62 (red) and LC3 (blue). Arrows indicate GFP foci with clearly specific co-localization with p62 and/or LC3. Scale bar is 10 µm.

For NBEAL1, only the BEACH domain (1991-2284) was available for subcloning. Transfection of this domain with a GFP-tag showed very similar results as transfection of the BEACH domains of ALFY and LRBA. It forms foci at relatively low expression levels and has a clear co-localization with endogenous p62, but not with LC3 (Figure 22).

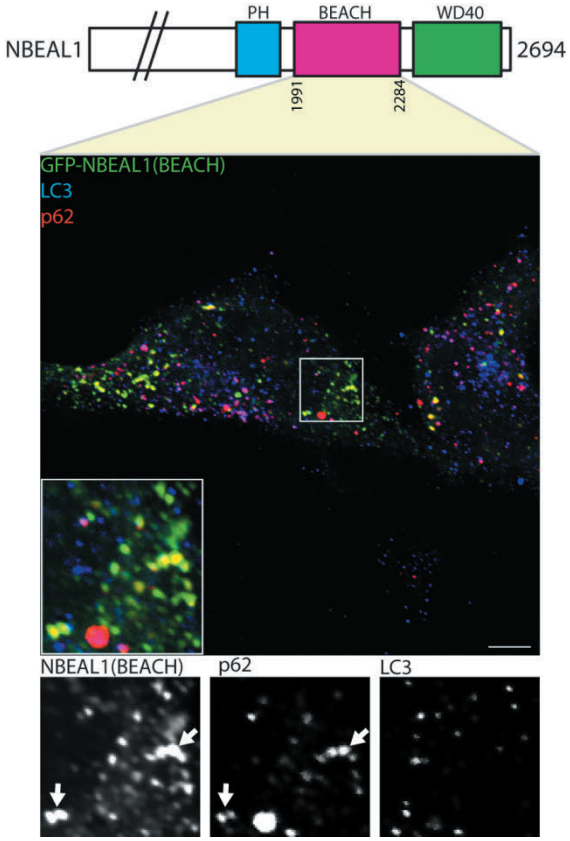

Figure 22: The BEACH domain of NBEAL1 co-localizes with p62. HeLa were transfected with plasmids encoding GFP-NBEAL1(1991-2284, BEACH) and stained for endogenous p62 (red) and LC3 (blue). Arrows indicate GFP foci with clearly specific co-localization with p62. Scale bar is 10 µm.

Transfected GFP-tagged deletion constructs of NBEAL2 shows that the PH-like domain (1917-2042) of this protein alone has a mostly diffuse localization, and also similarly to the PH-like domain of LRBA it is more prone to form foci than the PH-like domains of ALFY and WDFY4 (Figure 23). Similar to LRBA, it also has a significantly less nuclear localization than what is seen for the PH-like domains of ALFY and WDFY4. The BEACH domain (2049-2345) of NBEAL2 specifically co-localizes with p62, whereas the PH-BEACH domains (1917-2345) co-localize with both p62 and LC3.

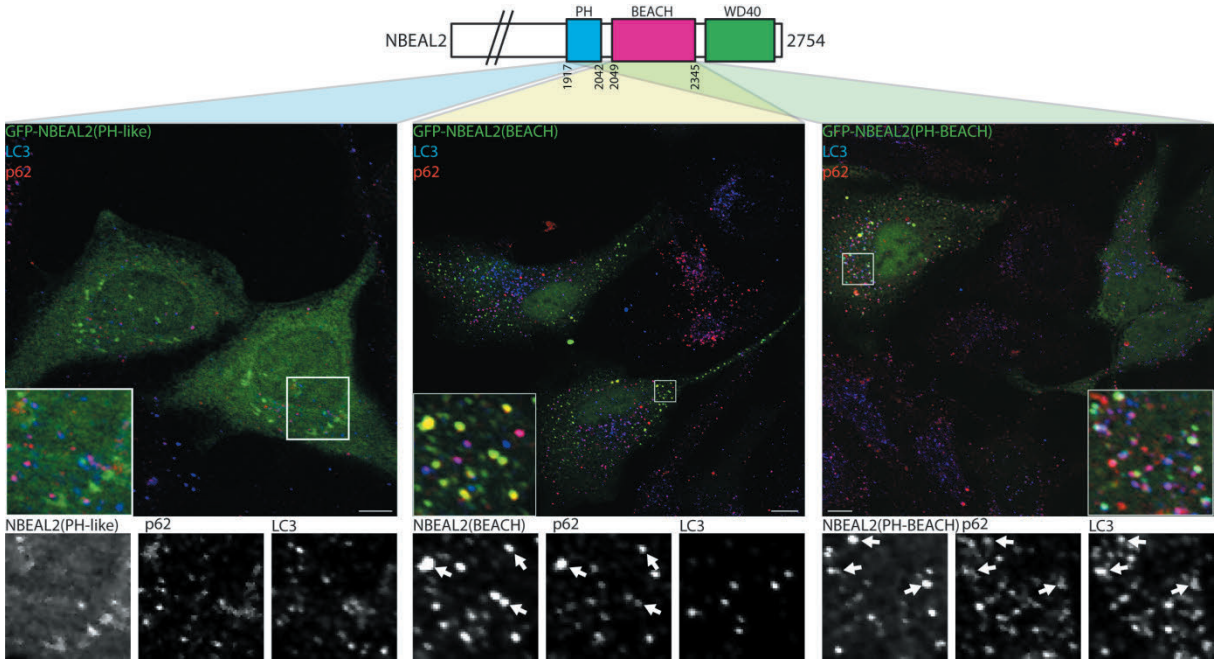

Figure 23: The BEACH and PH-BEACH domains of NBEAL2 co-localize with p62. HeLa were transfected with plasmids encoding GFP-NBEAL2(1917-2042, PH-like), -NBEAL2(2049-2345, BEACH) or –NBEAL2(1917-2345 PH-BEACH) and stained for endogenous p62 (red) and LC3 (blue). Arrows indicate GFP foci with clearly specific co-localization with p62 and/or LC3. Scale bar is 10 µm.

4.3.2 *Co-immunoprecipitation analysis and pulldown assays*

To further investigate an interaction of PH-BEACH domains of BEACH proteins with p62, we set up co-immunoprecipitation (co-IP) experiments where GFP-tagged BEACH protein domains were overexpressed in HeLa cells, followed by GFP immunoprecipitation and p62 immunoblotting. The immunoprecipitation assay was attempted in two slightly different ways, first using an anti-GFP antibody attached to protein A beads (Figure 24a) and then using GFP-trap beads (lama anti-GFP antibody conjugated to beads) (Figure 24b). For the protein A beads co-IP, a construct containing the full C-terminal of ALFY was included as a positive control because this construct has been published to co-IP with p62 [70]. Unfortunately, in both sets of experiments, p62 was pulled down in samples transfected with GFP alone as well as for all the other samples (Figure 24a, b), making it impossible to get any information out of these assays. Although the mentioned published co-IP of ALFY and p62 did not have this problem [70], there are other studies showing that stress from transfection itself can be enough to cause ubiquitination of GFP and thereby co-aggregation with p62 [145]. This seems a likely explanation for the unspecific binding of p62 to GFP observed in our co-IP experiments. Similar experiments should therefore be performed using a smaller tag (e.g. Flag og myc) to avoid this problem. Moreover, transfection of other cell lines or other cell culture conditions might not give such a stress response.

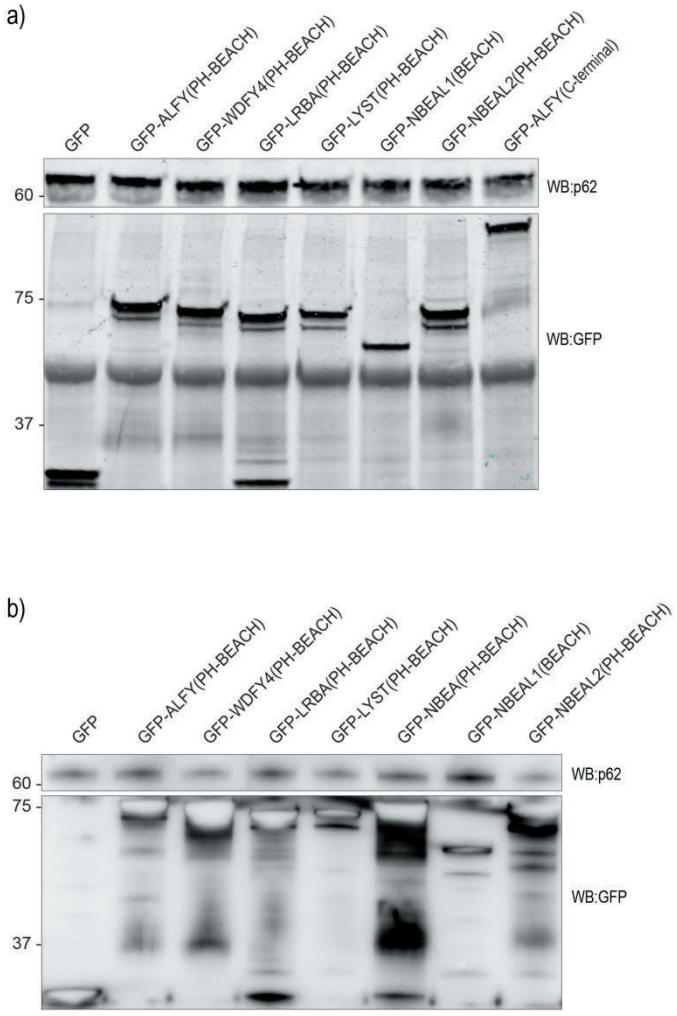

Figure 24: Co-immunoprecipitation of p62 with overexpressed BEACH protein domains. HeLa were transfected with plasmids encoding GFP-ALFY(2528-2977, PH-BEACH), -WDFY4(2372-2821, PH-BEACH), –

LRBA(2076-2489, PH-BEACH), –LYST(3011-3422, PH-BEACH), –NBEA(2148-2570, PH-BEACH), –NBEAL1(1991-2284, BEACH), –NBEAL2(1917-2345, PH-BEACH), –ALFY(2528-3526, C-terminal). a) Co-IP using anti-GFP from lysate of cells transfected with GFP constructs then washing 6x in HeLa lysis buffer. SDS-PAGE then immunoblotting for p62 and GFP. b) Co-IP from cells transfected with GFP constructs using GFP-trap then washing 6x in HeLa lysis buffer. SDS-PAGE then immunoblotting for p62 and GFP.

As an alternative assay to test the various BEACH protein domains for an interaction with p62, GST-tagged PH-like, BEACH and PH-BEACH from the various BEACH proteins were incubated with HeLa cell lysate, followed by GST-pulldown, SDS-PAGE and p62 immunoblotting (Figure 25a). We found that in general, the GST-tagged BEACH and PH-BEACH have a significantly higher affinity for p62 than the GST control (Figure 25c, d). While the PH-like domain of ALFY alone shows a high affinity for p62, most of the PH-like domains of the other BEACH proteins do not pull down p62 much more than the GST control (Figure 25b). Some BEACH domains have a significantly higher affinity for p62 when expressed alone (Figure 25c) as compared to the PH-BEACH domains, but when expressed as PH-BEACH domains, there is a more consistent higher affinity (around 2-fold) for p62 than GST alone (Figure 25d). This further suggests that the PH-like domain somehow modulates the interaction between the BEACH domain and p62. Based on the immunoflouresence results, the LYST PH-like domain would also be expected to pull down p62 in this assay, but this was not the case. This could be explained by the PH-like domain of LYST having affinity for LC3 or another component of autophagic membranes or regulatory complexes rather than p62. Taken together, the variable results for the PH-like and BEACH domains alone compared to PH-BEACH domains together further suggest that the two domains function together to regulate binding to p62 and that binding p62 is a common characteristic of the domains from the different proteins.

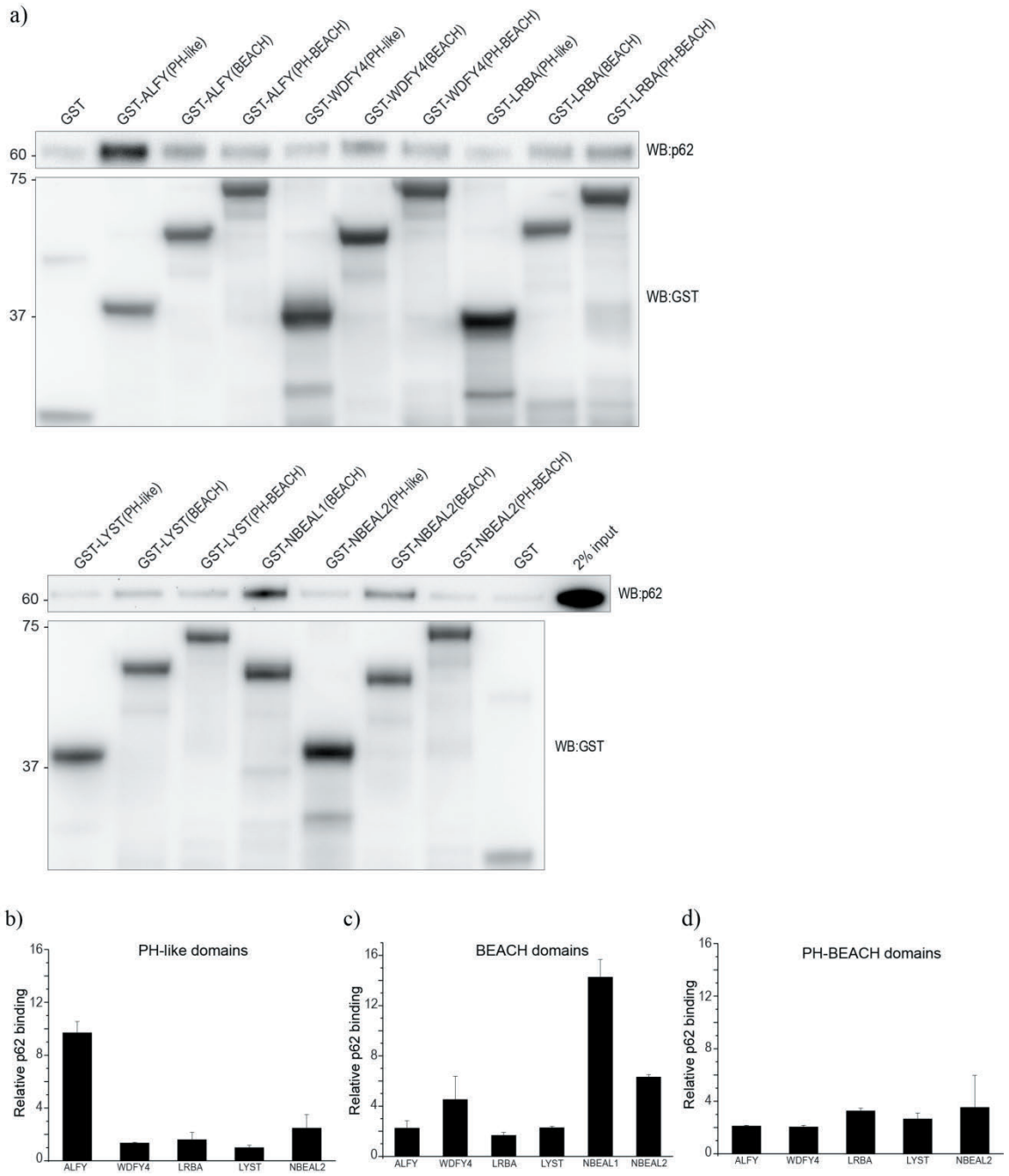

Figure 25: Pulldown of p62 from lysate using GST-tagged PH-like, BEACH and PH-BEACH protein domains. a) GST-ALFY(2528-2663, PH-like), -ALFY(2677-2977, BEACH), –ALFY(2528-2977 PH-BEACH), WDFY4(2372-2515, PH-like), -WDFY4(2525-2821, BEACH), –WDFY4(2372-2821 PH-BEACH), -LRBA(2076-2185, PH-like), -LRBA(2199-2489, BEACH), –LRBA(2076-2489 PH-BEACH), -LYST(3011-3115, PH-like), -LYST(3120-3422, BEACH), –LYST(3011-3422 PH-BEACH), -NBEAL1(1991-2284, BEACH), -NBEAL2(1917-2042, PH-like), -NBEAL2(2049-2345, BEACH) or –NBEAL2(1917-2345 PH-BEACH) were kept on beads (1 µg) and 200 µg HeLa lysate was added. Washed 6x in NETN then run on SDS-PAGE and immunoblotted with anti-p62 and –GST. b, c, d) Quantifications of two representative experiments where in the second replicate (blots not presented), the amount of GST control was increased with no significant increase in p62 binding. The relative p62 binding is calculated from p62 intensity of a sample domain pulldown divided by the p62 band being pulled down by GST alone.

Based on the results of immunoflouresence co-localization analysis and pulldown experiments from cell lysates, it seems that the BEACH domains of several BEACH proteins mediate an interaction to p62. Because we were able to show a direct interaction between the ALFY BEACH domain and p62 (Figure 16), we wanted to confirm that the BEACH domains of other BEACH proteins also have such a direct interaction. This was tested using purified GST-tagged BEACH domains of several BEACH proteins incubated with purified MBP or MBP-p62 bound to beads. Indeed, the BEACH domains of many, but not all the tested BEACH proteins demonstrate a direct interaction with MBP-p62 (Figure 26). The BEACH domains of WDFY4 and LYST have lower affinity for the recombinant MBP-p62 than BEACH domains of the other proteins, in line with the immunoflouresence results above (Figures 13, 19-23) showing that GFP-tagged BEACH domains of WDFY4 and LYST are not able to recruit p62 to GFP foci to the same degree as the other BEACH domains.

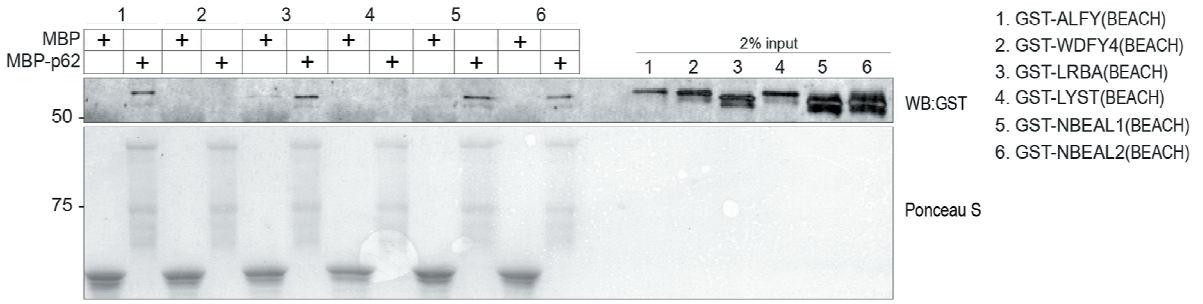

Figure 26: There is a direct interaction between the BEACH domains of several BEACH proteins and p62. Recombinant GST-ALFY(2677-2977, BEACH), -WDFY4(2525-2821, BEACH), -LRBA(2199-2489, BEACH), -LYST(3120-3422, BEACH),), -NBEAL1(1991-2284, BEACH), -NBEAL2(2049-2345, BEACH) were isolated from bacterial (E.coli BL21) lysates, purified and eluted from beads. MBP and MBP-p62 were similarly isolated from bacterial lysates and purified, but kept on the beads for this assay. 1 µg GST-tagged BEACH domains were added to 2 µg MBP or MBP-p62, they were incubated for 1h then washed 6x with NETN buffer. Results were analyzed by SDS-PAGE and immunoblotting with anti-p62. Ponceau S show MBP and MBP-p62.

4.4 What is the functional role of the PH-BEACH to p62 interaction?

4.4.1 *siRNA screen*

The observed co-localization and interaction between BEACH domains of several BEACH proteins and p62 suggests that several of the BEACH proteins are involved in processes where p62 has been implicated. As discussed earlier, p62 is involved in a variety of celluar processes, but this project aimed to investigate if BEACH proteins are involved in autophagy. One way of testing if a protein is involved in regulating autophagic activity is to deplete it by siRNA and investigate if the amounts of LC3 or p62 are influenced by the knockdown. Quantification of lipidated LC3 (LC3-II) levels from a western blot gives a measure of the amount of autophagosome-associated LC3. Bafilomycin A1 (Baf A1) is a specific inhibitor of the vacuolar H^+-ATPase that normally functions to acidify endosomal compartments. Treatment by this drug prevents fusion of autophagosomes and lysosomes, resulting in an accumulation of autophagosomes and thereby increased LC3-II and p62 levels. Comparing LC3-II levels in cells treated with Baf A1 with untreated cells can therefore be used to measure the autophagic flux. p62 is a common autophagic cargo and quantification of p62 levels in control cells and siRNA treated cells can be used to measure if the depleted proteins influence autophagic degradation. To induce autophagy, cells are grown in a starvation media (EBSS) lacking serum and amino acids.

We set up a small screen using two different cell lines for investigating involvement in starvation-induced autophagy for the BEACH proteins. For knockdown in HEK293 (human embryonic kidney), ALFY, LYST. NBEA and NBEAL1 where included while for U2OS (human osteosarcoma), ALFY, WDFY4, LRBA, LYST, NBEAL1 and NBEAL2 were included. Knockdown of target mRNA was confirmed by quantitative real-time PCR (qPCR). The proteins were depleted in cells grown in normal cell media (DMEM), starvation media (EBSS) or EBSS with two hours of Baf A1 treatment. We first set up a knockdown in HEK using 40 nM of the siRNA oligos and qPCR results confirmed that the degree of mRNA knockdown was greater than 75% for all siRNAs used (Figure 27b). This screen also included ULK1, a protein of the core autophagic machinery, as a negative control. Because knockdown of ULK1 is known to inhibit initiation of autophagy [14], we expected in those samples to see an accumulation of p62 that is similar for all three growth conditions (DMEM, EBSS, EBSS+Baf A1) and a lower autophagic flux, seen by a reduced difference between LC3-II of EBSS and EBSS+Baf A1 relative to the siSCR control. The p62 and LC3-II levels in cells with ULK1 knockdown confirmed that autophagic acitivty was severely inhibited (Figure 27c, d). Although depletion of none of the BEACH proteins tested caused an accumulation of p62 to the same degree as ULK1 depletion, depletion of all BEACH proteins caused an accumulation of p62 when cells were grown in DMEM and EBSS as compared to the siSCR control (Figure 27c). The fact that p62 levels are similar in BEACH protein depleted cells incubated in EBSS and EBSS+Baf A1 may indicate that the BEACH proteins are important for recruitment of p62 into autophagosomes or fusion of autophagosomes with lysosomes upon starvation. The most notable candidate for involvement in autophagy from this one experiment is NBEAL1, where knockdown seems to influence autophagic activity, causing reduced degradation of p62 and reduced levels of LC3 under EBSS+Baf A1 conditions and increased levels in DMEM as compared to the siSCR control (Figure 27c, d). These observations suggest that loss of NBEAL1 impairs normal autophagic degradation under both normal and starvation conditions. There are several interesting candidates in these results that suggest an involvement for BEACH proteins in autophagy, but these results

will have to be repeated several times to eliminate possible influence of background variation on the results.

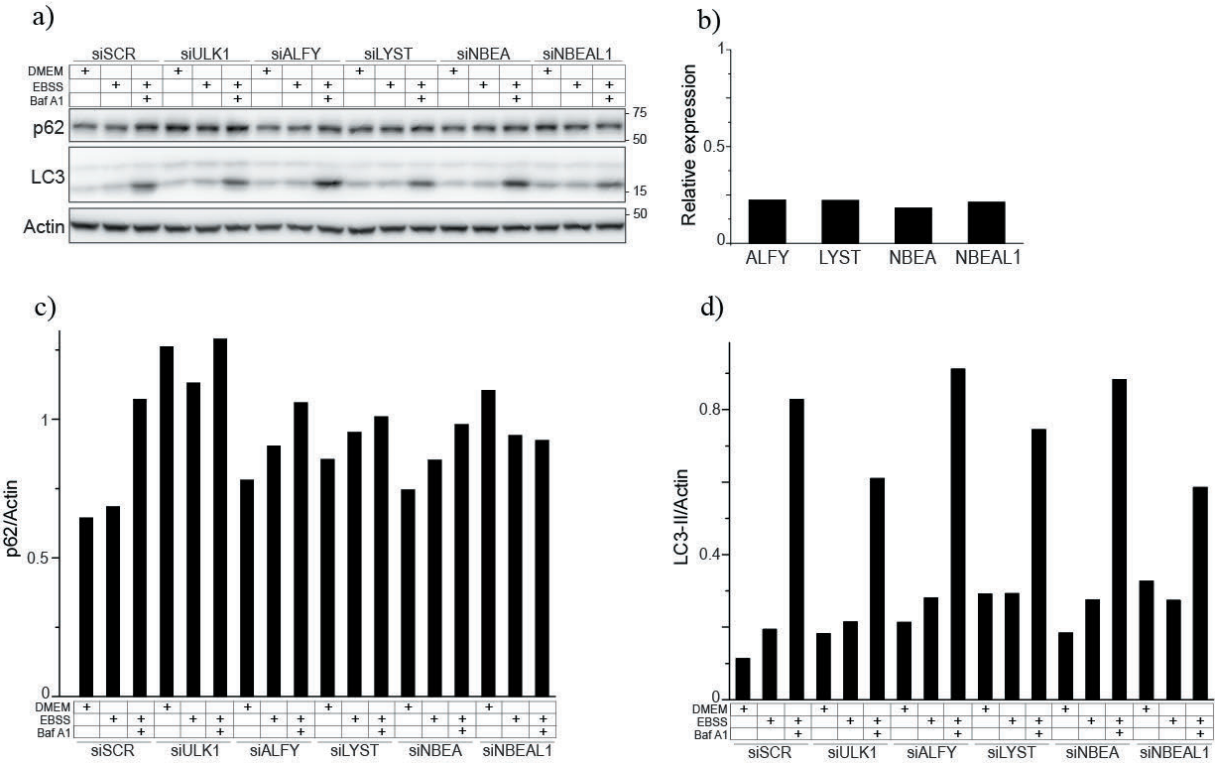

Figure 27: siRNA-mediated knockdown of BEACH proteins in HEK293 cells. All cells were seeded 24 hrs before a 72 hrs 40 nM smartpool siRNA transfection in DMEM. 2 hrs before lysing the cells, media was changed to DMEM, EBSS or EBSS+Baf A1 (100nM). From a separate set of samples that were treated identically as DMEM-only samples, RNA was isolated and qPCR was performed. Blots were quantified by ImageJ.

The knockdown screen was also performed in U2OS cells and in this case, all seven BEACH proteins studied in this project was included. For the HEK knockdown, 40 nM of the smartpool siRNAs was sufficient to achieve a good knockdown efficiency, while for U2OS we had to increase the siRNA concentrations to 100 nM to get an acceptable knockdown efficiency. The qPCR results showing a relative expression of WDFY4 of nearly 1 (Figure 28g) suggests that either WDFY4 has a low level of expression in U2OS cells, or alternatively that the WDFY4 qPCR primers used do not work as they should. The knockdown efficiency in U2OS cells was not as good (Figure 28g) as in HEK293 cells even after increasing the concentration of the siRNA oligos to 100 nM per well (compared to 40 nM used for HEK). However, as for HEK cells, knockdown of several of the BEACH proteins seem to result in an accumulation of p62 (Figure 28c, d). Especially knockdown of NBEA, NBEAL1 and NBEAL2 had a clear effect on p62 levels in normal media (fed) while p62 was clearly degraded upon starvation. This suggests that the mechanism of starvation-induced autophagy is preserved upon BEACH protein depletion while perhaps other, selective autophagy pathways that contribute to p62 degradation under normal conditions were attenuated. For U2OS, there is less change in LC3-II levels of EBSS+Baf A1 samples as compared to EBSS samples (Figure 28e, f), suggesting that the autophagic flux was less influenced by the BEACH protein knockdown as compared to HEK293 cells. This could be a consequence of the decreased knockdown efficiency in U2OS cells or it could be that the influence on LC3-II levels seen in the HEK knockdown was background variation.

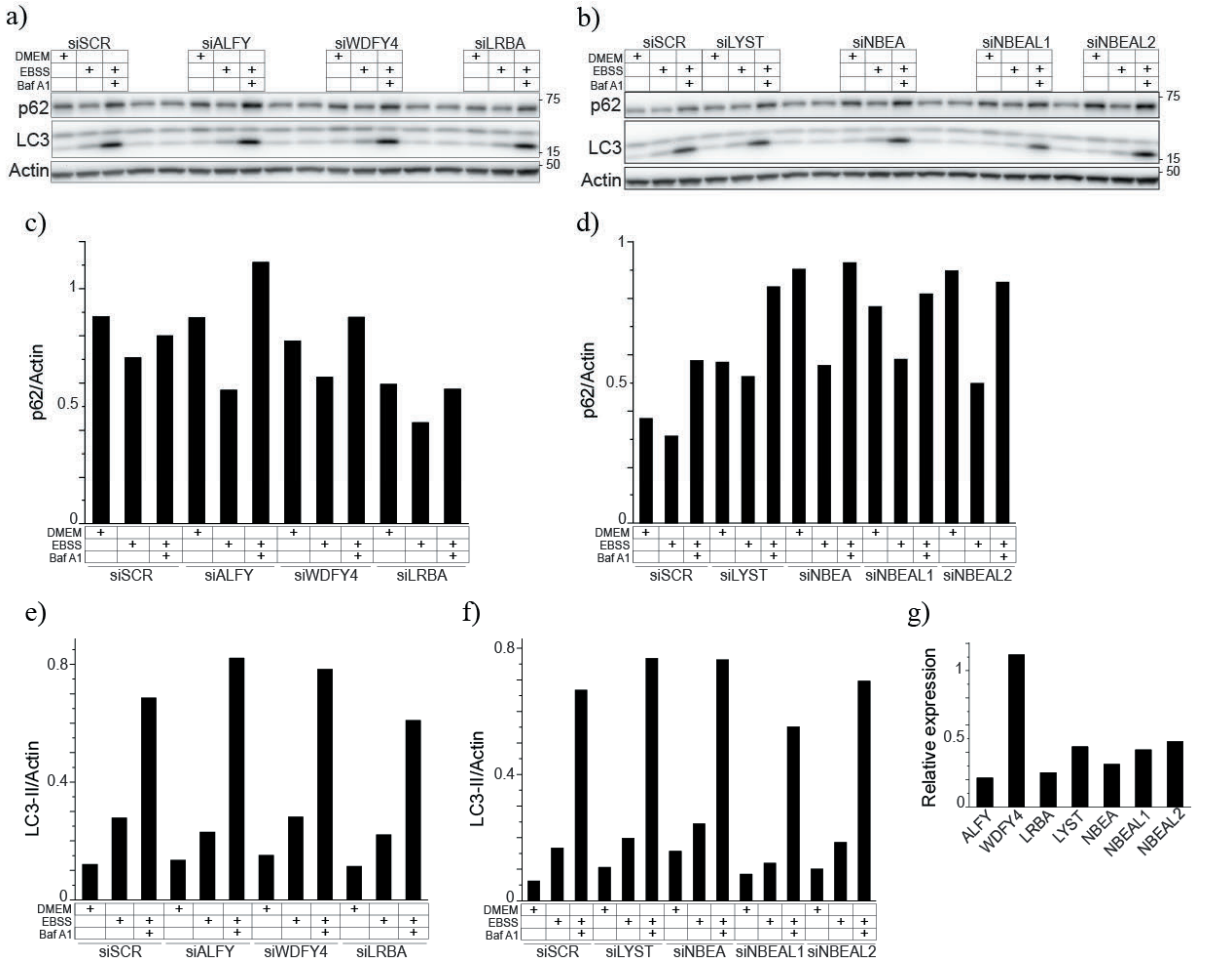

Figure 28: siRNA-mediated knockdown of BEACH proteins in U2OS cells. All cells were seeded 24 hrs before a 72 hrs 100 nM smartpool siRNA transfection in DMEM. 2 hrs before lysing the cells, media was changed to DMEM, EBSS or EBSS+Baf A1 (100nM). RNA was isolated from a replica plate of samples that were treated identically as the DMEM-only samples, RNA was isolated and qPCR analysis was performed. Blots were quantified by ImageJ.

To summarize the knockdown screen, it seems that depletion of several of the BEACH proteins are influencing the degradation of cargo in selective autophagy and possibly also autophagic flux. However, as the presented results are quantified from only one replicate in each cell line it is not possible to conclude anything from these experiments. Nonetheless, it is striking how knockdown of several of the BEACH proteins seem to cause a significant accumulation of p62 under normal conditions. Further studies to explore the involvement of the BEACH proteins in autophagy should repeat these experiments in several replicates before any conclusions can be made. Various inducers of selective autophagy can also be included to further investigate the suggested involvement in selective autophagy.

4.4.2 *Immunofluorescence analysis of endogenous BEACH proteins*

To further screen for a functional involvement of the BEACH proteins in starvation-induced or selective autophagy, the localization of endogenous BEACH proteins was analyzed in HeLa cells grown for 2 h in starvation media (EBSS) or incubated with drugs (puromycin and CCCP) known to stimulate selective autophagy. NBEAL2 was excluded from the endogenous localization studies because there were no commercially available antibodies. As mentioned above, p62 is an autophagy receptor playing an important role in selective autophagy, but because it is also a substrate for non-selective autophagy, increased formation of p62 foci is seen upon starvation. Puromycin is a chain-terminating amino acid analog and treatment by this drug is known to induce formation of p62 positive aggregates of ubiquitinated prematurely terminated misfolded proteins. ALFY is known to be recruited to puromycin-induced p62 bodies and is involved in the autophagic degradation of the ubiquitinated protein aggregates [70]. CCCP is a drug that induces decoupling of the mitochondrial membrane potential and thereby forms dysfunctional mitochondria that are degraded by autophagy [146]. Thus, all the treatments used are known to induce formation of p62 foci that are targeted for autophagic degradation and co-localization with endogenous p62 was therefore used as a marker for involvement in the induced autophagic processes.

The results show that in complete media (DMEM) or under CCCP treatment, there is no specific co-localization of any of the BEACH proteins with p62 (Figure 29). Starvation media (EBSS) causes some co-localization between p62 and ALFY, but none of the other BEACH proteins. In contrast, puromycin treatment causes a clear recruitment of ALFY to p62 foci and interestingly, all the investigated BEACH proteins except for NBEAL1 were also shown to be recruited to p62 foci upon puromycin treatment (Figure 29). This could mean that these proteins are recruited to p62 to aid in the selective autophagic degradation of the aggregates. Furthermore, it suggests that a common characteristic of the PH-BEACH domains is to mediate an interaction with p62 under certain conditions that are met upon puromycin treatment. The specific colocalization of the BEACH proteins with p62 upon puromycin treatment also show that the antibodies used most likely specifically recognize the endogenous proteins, although it can not be excluded that the antibodies also recongize non-specific proteins. A western blot analysis of the different anti-BEACH protein antibodies was performed, but as these proteins are all very large (more than 400 kDa) it was difficult to detect any specific bands. The lack of NBEAL1 colocalization with p62 in puromycin treated cells could therefore be due to a non-specific anti-NBEAL1 antibody, as the BEACH domain of NBEAL1 was found to colocalize with p62 when expressed as a GFP-tagged fusion protein in HeLa cells (Figure 22).

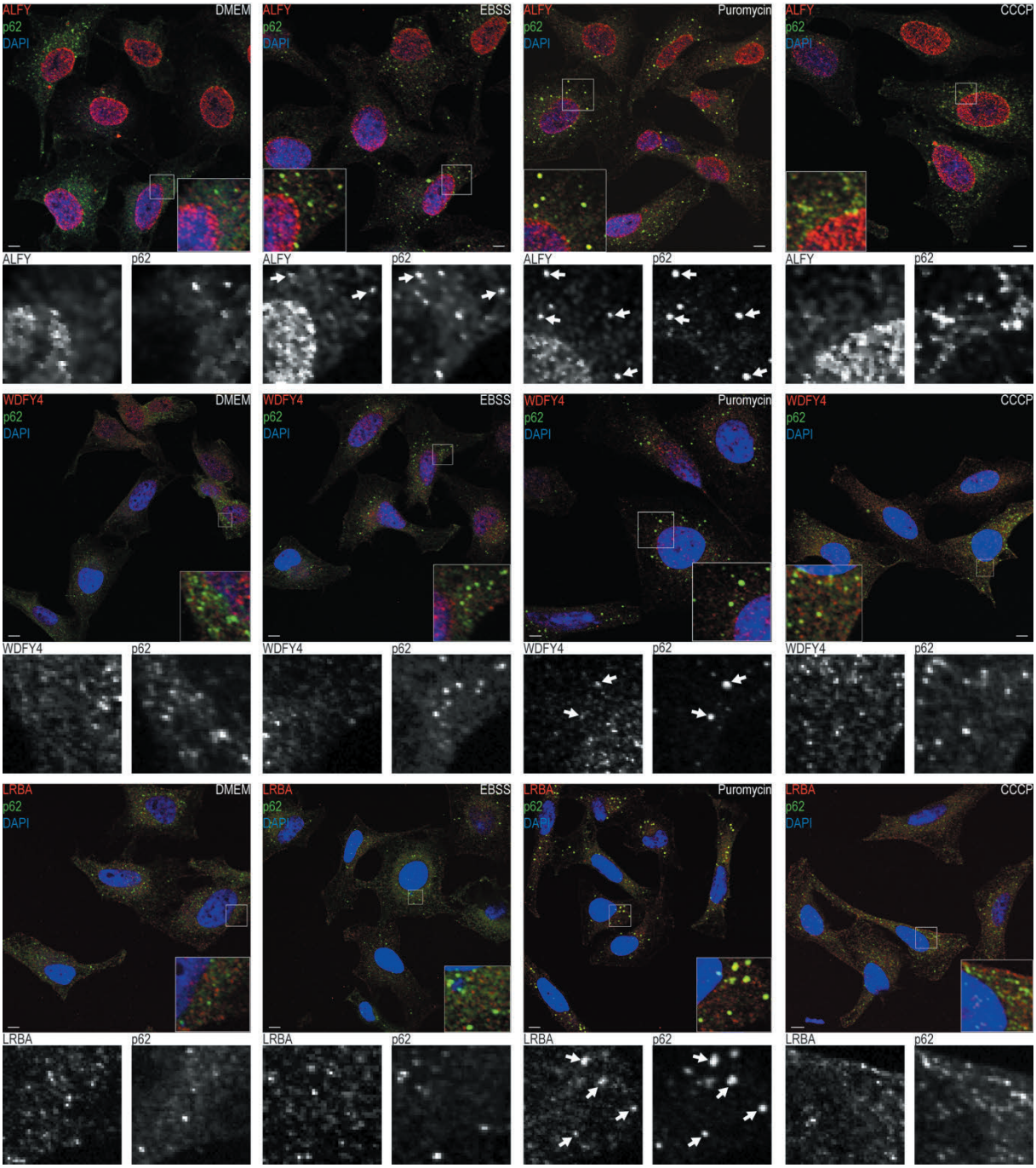
ALFY
p62
DAPI
DMEM
EBSS
Puromycin
CCCP
WDFY4
LRBA

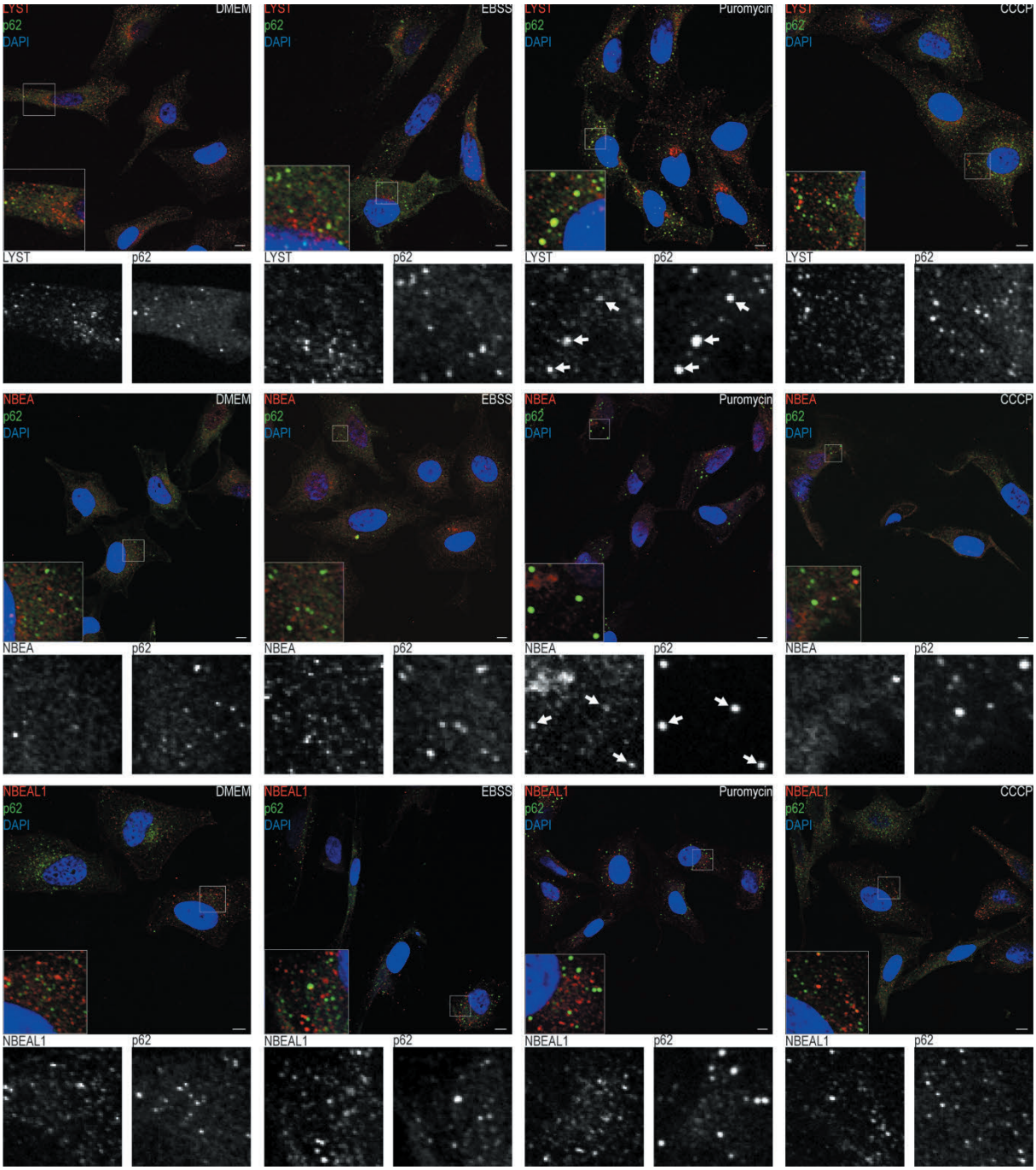

Figure 29: Screening for an involvement in autophagy for the BEACH proteins by studying localization upon different cell media and drug treatments. HeLa were grown in complete media (DMEM) until two hours before fixation when the media was changed to EBSS, DMEM+puromycin (10 µg/ml) or DMEM+CCCP (30 µM). The cells were stained for endogenous BEACH proteins (in red), p62 (in green) and DNA (DAPI, in blue) and analyzed by confocal immunoflouresence microscopy. Scale bar is 10 µm.

4.5 Contributions to other projects

During this project, work was also contributed to other, related projects in the same research group. My supervisor, Anne Simonsen was requested by Cell Death and Differentiation (CDD) to write a review on ALFY related to selective autophagy (Isakson, Holland and Simonsen, in press). For this review, a bioinformatics analysis of ALFY was performed to search for possible homologous sequence elements in the largely uncharacterized N-terminal part of the protein. The search identified three regions of ALFY that have considerable sequence homology to other unrelated proteins (Figure 30, [I], [II] and [III]). These sequences were found to be conserved in several of the proteins most closely related to ALFY. The degree of conservation of these regions of interest to other human BEACH proteins was also indicated in Figure 30. To the CDD review, the BEACH protein homology analysis for various species showed in Figure 6 in this thesis was also included and text was contributed related to the ALFY domain structure and homology.

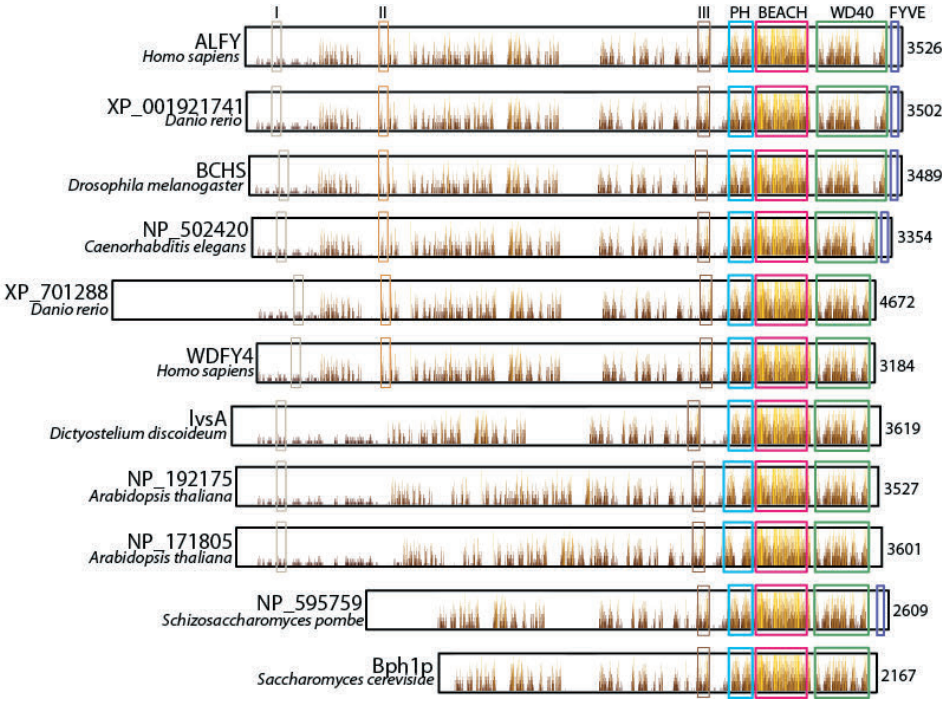

Figure 30: Domain structure and degree of sequence conservation in proteins most closely related to ALFY. Inside each protein box, bars illustrate the degree of sequence conservation throughout the indicated proteins, higher and more yellow bars indicate higher degree of conservation. Grey, light brown and dark brown boxes indicate regions of significant sequence homology to unrelated proteins, residues 247-351 (of ALFY) in grey [I] is similar to 'TBC1 domain family member 30', residues 842-923 in light brown [II] is similar to 'Origin recognition complex subunit 2' and residues 2281-2397 in dark brown [III] is similar to 'BCL-2 associated transcription factor 1'. Blue boxes indicate PH domains, red BEACH domains, green WD40 domains and purple FYVE domains.

There was also a contribution of bioinformatics work to another project in the group related to the WD40 domain of ALFY. Sequence analysis recognizes five WD40 repeats in ALFY that likely each form a β-sheet that can contribute to forming a β-propeller. WD40 domains are known to form seven-bladed β-propellers, but the structure of the ALFY WD40 domain has not been solved so we wanted to analyze the sequence of the WD40 domain to see if it is likely that sequence elements outside the WD40 repeats also form β-sheets that may contribute to forming a complete β-propeller. A RaptorX [144] structure prediction was performed based on the sequence of the ALFY WD40 domain (3077-3447). The results suggest that the WD40 domain of ALFY can form a complete β-propeller on its own even though it does not contain seven WD40 repeats (Figure 31). Such a computational structure prediction analysis is never sufficient to conclude anything about structure, but the information it gives can be useful if interpreted with care.

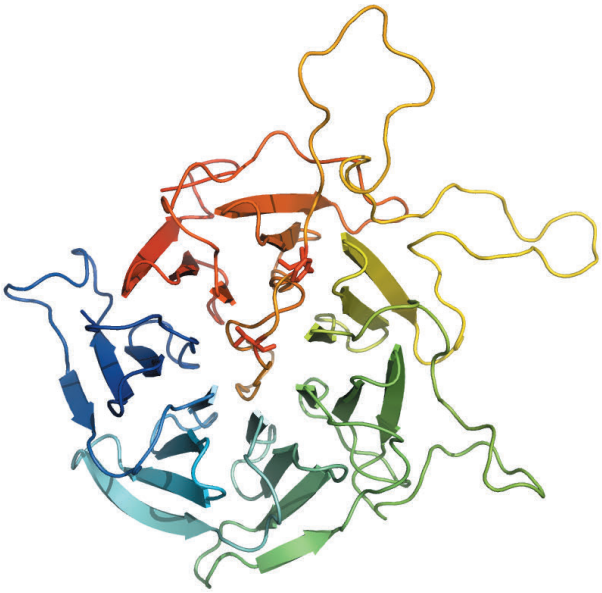

Figure 31: RaptorX structure prediction of the ALFY WD40 domain (3077-3447). The domain is colored by progressive color changes starting from blue from the N-terminal end of the domain and ending in red at the C-terminal end of the domain. The unstructured loop between yellow and orange β-sheets is unique to ALFY and its most closely related orthologs, as can be seen in the larger WD40 domains of these proteins in Figure 30.

5. Discussion

Based on a loosely characterized interaction between domains in the C-terminal end of ALFY and p62, we set out to get more information about which domains mediate this interaction. Previously published data indicated that the PH-BEACH domains of ALFY mediate this interaction so we wanted to investigate if the PH-BEACH domains of other BEACH proteins also interact with p62. Because p62 is a major autophagy receptor protein, any protein interacting with it might be involved in autophagy. We therefore set up screens to test for involvement in autophagy for several of the BEACH proteins.

5.1 Which domains of ALFY mediate the interaction to p62?

Previously, an in vitro translated deletion construct of ALFY containing its C-terminal domains has been shown to be pulled down by MBP-p62 [70]. Furthermore, the PH-BEACH domains of ALFY were shown to be required for recruiting ALFY to p62 bodies upon puromycin treatment [70]. We wanted to get more detailed information about this interaction, hoping to find that either the PH-like or BEACH domain, separately, or together are required for a direct interaction with p62. The results from transfection of GFP-tagged ALFY domains into HeLa cells (Figure 13) suggest that the BEACH domain alone can mediate the interaction with p62. In vitro translation pulldown assays (Figure 14) and purified recombinant protein pulldown assays (Figure 16) support this hypotesis although the interaction seen between the BEACH domain and p62 in pulldown assays is weak. Pulldown of p62 from cell lysate also showed an interaction between the BEACH domain and p62, but in this assay, the PH-like domain alone shows a higher affinity for p62 (Figure 15).

In addition to testing which of the PH-like or BEACH domains that mediate the interaction, we also wanted to see if we could identify the groove that is responsible for the interaction in the natural state of the domains, which is both domains together. Of the four conserved residue pairs that were tested (Figure 17e), two separate pairs were shown to both influence binding of p62 independently (Figure 18). Interestingly, all four residues that were shown to influence p62 binding all point into the same area, the deep end of the main groove that is formed between the PH-like and BEACH domains. We feel that the interpretation that best takes into account all the observed results regarding the ALFY to p62 interaction is that residues of the BEACH domain mediates a weak but direct interaction to p62, interacting in the main groove formed between the PH-like and BEACH domains. The PH-like domain probably modulates this interaction, either by regulating the availability of the BEACH domain for binding partners or by interacting with other binding partners of p62 or lipids. Further experiments to elucidate how p62 binds in the main groove can include combining mutations, especially patch 1 and 2 (Figure 17, 18) to see if p62 binding then is further increased. Building on the knowledge that there seems to be a dynamic regulation of p62 binding in the main groove, further residues can be chosen for site-directed mutagenesis in the areas surrounding the deep end of the main groove that are likely to be influenced by movement between the domains. Hopefully, such mutations can reveal residues where alanine mutations abolish the interaction to p62.

5.2 Do the PH-BEACH domains of other BEACH proteins interact with p62?

None of the human proteins containing PH-BEACH domains except for ALFY are previously known to interact with p62 or be involved in autophagy. Due to the very high degree of homology of the BEACH domain we therefore wanted to investigate if association with p62 is a common feature of the PH-BEACH domains found in these various proteins. Transfection of PH-like, BEACH and PH-BEACH domains from the BEACH proteins into HeLa cells showed that for WDFY4, LRBA, NBEAL1 and NBEAL2, similar to ALFY, the BEACH domain alone mediates a co-localization with p62 that is also seen for the PH-BEACH domains (Figure 13, 19-23). However, we were surprised to see that for LYST, the PH-like domain alone co-localizes with p62 and LC3 while the BEACH domain seems to have a lower affinity for p62. For LYST, the PH-BEACH domain also co-localizes strongly with LC3. For NBEAL2, there is also significant co-localization with both p62 and LC3 for the PH-BEACH domain. The observation that the PH-like domain of LYST co-localizes with p62 and also LC3 can be interpreted to support the hypothesis of the PH-like domain binding a protein or lipid that is found in complex with p62. It is also interesting to note that one of the sites in the BEACH domain that were chosen for mutagenesis on basis of being highly conserved and by further shown to have an effect on p62 binding is not conserved in LYST (Figure 17f, patch 2). Although the alanine mutations (M→A, T→A) used in the ALFY mutagenesis (Figure 18) actually increased p62 binding, in LYST these residues (M→T, T→K) might have more significant consequences on the binding surface on the main groove as compared with the relatively inert alanines. It would be interesting to test a T2714K (the most significant of the nonconserved residues in patch 2) mutation in ALFY to see if this would reduce p62 binding.

Pulldown assays of the isolated domains from the various BEACH proteins was also performed, adding HeLa lysate to various domains expressed as recombinant proteins and bound to beads (Figure 25). The results support the idea that interaction with p62 is a common feature of the BEACH domains in the studied proteins. In contrast to the ALFY PH-like domain, the PH-like domains of the other BEACH proteins do not pull down p62 from the lysate. These results correspond well to the immunoflouresence colocalization data except for the LYST PH-like domain. One possible interpretation is that PH-like domains interact with interaction partners of p62 to create a stable complex in the PH-BEACH domains but that the PH-like domains alone do not stably gain access to their binding partner under certain assays. Another possibility is that the interactions observed for the PH-like domain ALFY in lysate pulldowns and for the PH-like domain of LYST in immunoflouresence are due to unspecific contacts and/or aggregation and therefore are not physiologically relevant.

The BEACH domains of various BEACH proteins were also tested for a direct interaction to p62 to further confirm that the characteristics of the ALFY PH-BEACH to p62 interaction apply to other BEACH proteins as well. The results show that the BEACH domains of several BEACH proteins, but not all, mediate a direct interaction to p62 (Figure 26). Of the investigated proteins, the BEACH domains of ALFY, LRBA, NBEAL1 and NBEAL2 show a similar, relatively weak direct interaction to p62 while LYST and WDFY4 show no or little interaction with p62. This corresponds very well with the results of transfecting BEACH domains into HeLa cells for co-localization analysis (Figure 13, 19-23) where the BEACH domains of LYST and WDFY4 show less colocalization with p62 compared to the other BEACH proteins. Taken together, these results

strongly suggest that the observed co-localization of BEACH domains from various BEACH proteins with p62 is due to a specific direct interaction of the domains with p62 and not due to secondary effects such as transfection stress or aggregation and ubiquitination of the transfected proteins.

5.3 Are other BEACH proteins than ALFY involved in autophagy?

To look for an involvement of the BEACH proteins in autophagy, siRNA-mediated knockdown was performed and the generation of lipidated LC3-II and degradation of p62 was studied under various conditions. This assay can give information about a possible involvement of the depleted protein at various stages of the process of autophagic degradation. The most notable results from this assay was that depletion of several BEACH proteins seem to influence the rate of p62 degradation when the cells were grown in normal media (DMEM) (Figure 27, 28). The results need to be repeated for any conclusion to be drawn, but at this point it seems that depletion of BEACH proteins does not influence the rate of starvation-induced autophagy, with the possible exception of NBEAL1. Selective autophagy plays a basal housekeeping function in removal of damaged or dysfunctional cellular components such as aggregated proteins and depolarized mitochondria. Our results showing that several BEACH proteins are involved in binding to p62 and that their depletion cause an accumulation of p62 under conditions where selective autophagy is ongoing might indicate that they may promote degradation of specific autophagic cargo, similar to what is known for ALFY.

In an attempt to address whether BEACH proteins are involved in selective autophagy, cells in culture were treated with drugs known to cause accumulation of cargo for selective autophagy, protein aggregates and depolarized mitochondria induced by puromycin or CCCP treatment, respectively. Colocalization between endogenous BEACH proteins and p62 was then analyzed by confocal imaging (Figure 29). ALFY is known to be recruited to cytoplasmic p62 bodies upon puromycin treatment [70] and interestingly, we found that several of the other BEACH proteins are also recruited to p62 bodies upon puromycin treatment. Puromycin causes an accumulation of ubiqiutinated misfolded protein aggregates (also called p62 bodies) and ALFY is proposed to be recruited to these p62 bodies to aid their autophagic degradation. The observation that several BEACH proteins are recruited to these purmycin-induced p62 bodies could mean that they as well are involved in the autophagic degradation of such structures. Alternatively, they could be recruited to these structures to signal to or regulate other processes unrelated to autophagy. In contrast, we observed no colocalization between the BEACH proteins and p62 upon CCCP treatment. The recruitment of endogenous BEACH proteins to p62-bodies supplement the other assays in this project showing that several BEACH proteins can interact with p62 and it suggests that the PH-BEACH domain could have a general function of recruiting the containing proteins to p62 under conditions promoted by puromycin treatment.

5.4 Conclusion and future perspectives

To summarize, we have shown that several BEACH proteins can interact with p62 both in vitro and in vivo. The exact nature of the interaction between the PH-BEACH domains and p62 is still not clear, but it seems that there is a direct interaction between the BEACH domain and p62. There is no previously known function for the BEACH domain so the results presented here suggests that binding to p62 could be a major function of this domain. The functional role of this interaction remains unknown, but we found that siRNA-mediated depletion of BEACH proteins seem to inhibit p62 degradation under certain conditions and that puromycin treatment caused recruitment of several BEACH proteins to p62 bodies. These observations serve as indications that BEACH proteins may be involved in autophagic degradation of p62 its associated ubiquitinated cargo. Further studies are needed to confirm the siRNA-mediated depletion results and to elucidate the physiological significance of the puromycin-induced co-localization and the detailed effects of puromycin on the cell. It will also be interesting to test various other drugs and cell treatments that are known to induce formation of p62 bodies to try to elucidate what sort of stimuli causes the BEACH proteins to be recruited to p62, possibly leading to an understanding of the role of this inducible interaction in vivo.

Because BEACH proteins are involved in a variety of cellular processes and diseases, we hope that characterization of their interaction with p62 can potentially lead to treatment options for the related diseases. One obvious path forward related to this is to get a structural characterization of the PH-BEACH domain in complex with p62. Such detailed structural information can potentially be used in rational drug design to inhibit the interaction, giving a possible disease treatment. The uniqueness of the BEACH domain and the fact that only eight human proteins contain it could indicate that a drug specifically targeting this domain give limited off-target effects in the cell. In parallel with such a detailed characterization of the PH-BEACH and p62 interaction, studies will need to elucidate the functional significance of the interaction. Furthermore, if such functional studies confirm that BEACH proteins have a role in autophagy, modulation of autophagy can potentially also lead to treatment options for their associated diseases.

6. References

1. Yorimitsu, T. and D.J. Klionsky, *Autophagy: molecular machinery for self-eating.* Cell Death Differ, 2005. **12**(S2): p. 1542-1552.
2. Levine, B. and D.J. Klionsky, *Development by Self-Digestion: Molecular Mechanisms and Biological Functions of Autophagy.* Developmental Cell, 2004. **6**(4): p. 463-477.
3. Kuma, A., et al., *The role of autophagy during the early neonatal starvation period.* Nature, 2004. **432**(7020): p. 1032-1036.
4. Komatsu, M., et al., *Loss of autophagy in the central nervous system causes neurodegeneration in mice.* Nature, 2006. **441**(7095): p. 880-884.
5. Hara, T., et al., *Suppression of basal autophagy in neural cells causes neurodegenerative disease in mice.* Nature, 2006. **441**(7095): p. 885-889.
6. Komatsu, M., et al., *Impairment of starvation-induced and constitutive autophagy in Atg7-deficient mice.* The Journal of Cell Biology, 2005. **169**(3): p. 425-434.
7. Kim, I., S. Rodriguez-Enriquez, and J.J. Lemasters, *Selective degradation of mitochondria by mitophagy.* Archives of Biochemistry and Biophysics, 2007. **462**(2): p. 245-253.
8. Yokota, S., *Degradation of normal and proliferated peroxisomes in rat hepatocytes: Regulation of peroxisomes quantity in cells.* Microscopy Research and Technique, 2003. **61**(2): p. 151-160.
9. Kraft, C., et al., *Mature ribosomes are selectively degraded upon starvation by an autophagy pathway requiring the Ubp3p/Bre5p ubiquitin protease.* Nature Cell Biology, 2008. **10**(5): p. 602-610.
10. Gutierrez, M.G., et al., *Autophagy Is a Defense Mechanism Inhibiting BCG and Mycobacterium tuberculosis Survival in Infected Macrophages.* Cell, 2004. **119**(6): p. 753-766.
11. Nakagawa, I., et al., *Autophagy Defends Cells Against Invading Group A Streptococcus.* Science, 2004. **306**(5698): p. 1037-1040.
12. Pohl, C. and S. Jentsch, *Midbody ring disposal by autophagy is a post-abscission event of cytokinesis.* Nature Cell Biology, 2009. **11**(1): p. 65-70.
13. Ravikumar, B., R. Duden, and D.C. Rubinsztein, *Aggregate-prone proteins with polyglutamine and polyalanine expansions are degraded by autophagy.* Human Molecular Genetics, 2002. **11**(9): p. 1107-1117.
14. Hosokawa, N., et al., *Nutrient-dependent mTORC1 Association with the ULK1–Atg13–FIP200 Complex Required for Autophagy.* Molecular Biology of the Cell, 2009. **20**(7): p. 1981-1991.
15. Stenmark, H., R. Aasland, and P.C. Driscoll, *The phosphatidylinositol 3-phosphate-binding FYVE finger.* Febs Letters, 2002. **513**(1): p. 77-84.
16. Hanada, T., et al., *The Atg12-Atg5 Conjugate Has a Novel E3-like Activity for Protein Lipidation in Autophagy.* Journal of Biological Chemistry, 2007. **282**(52): p. 37298-37302.
17. Levine, B. and G. Kroemer, *Autophagy in the Pathogenesis of Disease.* Cell, 2008. **132**(1): p. 27-42.
18. Williams, A., et al., *Aggregate-Prone Proteins Are Cleared from the Cytosol by Autophagy: Therapeutic Implications*, in *Current Topics in Developmental Biology*, P.S. Gerald, Editor 2006, Academic Press. p. 89-101.
19. Rubinsztein, D.C., *The roles of intracellular protein-degradation pathways in neurodegeneration.* Nature, 2006. **443**(7113): p. 780-786.
20. Stefani, M. and C. Dobson, *Protein aggregation and aggregate toxicity: new insights into protein folding, misfolding diseases and biological evolution.* Journal of Molecular Medicine, 2003. **81**(11): p. 678-699.
21. Tompkins, M.M. and W.D. Hill, *Contribution of somal Lewy bodies to neuronal death.* Brain Research, 1997. **775**(1–2): p. 24-29.
22. Gutekunst, C.-A., et al., *Nuclear and Neuropil Aggregates in Huntington's Disease: Relationship to Neuropathology.* The Journal of Neuroscience, 1999. **19**(7): p. 2522-2534.

23. Arrasate, M., et al., *Inclusion body formation reduces levels of mutant huntingtin and the risk of neuronal death.* Nature, 2004. **431**(7010): p. 805-810.
24. Webb, J.L., et al., *α-Synuclein Is Degraded by Both Autophagy and the Proteasome.* Journal of Biological Chemistry, 2003. **278**(27): p. 25009-25013.
25. Goldberg, A.L., *Protein degradation and protection against misfolded or damaged proteins.* Nature, 2003. **426**(6968): p. 895-899.
26. Blommaart, E., J. Luiken, and A. Meijer, *Autophagic proteolysis: control and specificity.* The Histochemical Journal, 1997. **29**(5): p. 365-385.
27. Kuusisto, E.S., Antero ; Alafuzoff, Irina, *Ubiquitin-binding protein p62 is present in neuronal and glial inclusions in human tauopathies and synucleinopathies.* Neuroreport., 2001. **12**(10): p. 2085-2090.
28. Kuusisto, E., A. Salminen, and I. Alafuzoff, *Early accumulation of p62 in neurofibrillary tangles in Alzheimer's disease: possible role in tangle formation.* Neuropathology and Applied Neurobiology, 2002. **28**(3): p. 228-237.
29. Bjørkøy, G., et al., *p62/SQSTM1 forms protein aggregates degraded by autophagy and has a protective effect on huntingtin-induced cell death.* The Journal of Cell Biology, 2005. **171**(4): p. 603-614.
30. Komatsu, M., et al., *Homeostatic Levels of p62 Control Cytoplasmic Inclusion Body Formation in Autophagy-Deficient Mice.* Cell, 2007. **131**(6): p. 1149-1163.
31. Aita, V.M., et al., *Cloning and Genomic Organization of Beclin 1, a Candidate Tumor Suppressor Gene on Chromosome 17q21.* Genomics, 1999. **59**(1): p. 59-65.
32. Qu, X., et al., *Promotion of tumorigenesis by heterozygous disruption of the beclin 1 autophagy gene.* The Journal of Clinical Investigation, 2003. **112**(12): p. 1809-1820.
33. Schmelzle, T. and M.N. Hall, *TOR, a Central Controller of Cell Growth.* Cell, 2000. **103**(2): p. 253-262.
34. Tasdemir, E., et al., *Regulation of autophagy by cytoplasmic p53.* Nature Cell Biology, 2008. **10**(6): p. 676-687.
35. Maiuri, M.C., et al., *Self-eating and self-killing: Crosstalk between autophagy and apoptosis.* Nature Reviews Molecular Cell Biology, 2007. **8**(9): p. 741-752.
36. Martin, G.M., S.N. Austad, and T.E. Johnson, *Genetic analysis of ageing: role of oxidative damage and environmental stresses.* Nat Genet, 1996. **13**(1): p. 25-34.
37. Stadtman, E.R., *Protein Oxidation in Aging and Age-Related Diseases.* Annals of the New York Academy of Sciences, 2001. **928**(1): p. 22-38.
38. Brunk, U.T. and A. Terman, *The mitochondrial-lysosomal axis theory of aging.* European Journal of Biochemistry, 2002. **269**(8): p. 1996-2002.
39. Meléndez, A., et al., *Autophagy Genes Are Essential for Dauer Development and Life-Span Extension in C. elegans.* Science, 2003. **301**(5638): p. 1387-1391.
40. Bergamini, E., et al., *The anti-ageing effects of caloric restriction may involve stimulation of macroautophagy and lysosomal degradation, and can be intensified pharmacologically.* Biomedicine & Pharmacotherapy, 2003. **57**(5–6): p. 203-208.
41. Rubinsztein, David C., G. Mariño, and G. Kroemer, *Autophagy and Aging.* Cell, 2011. **146**(5): p. 682-695.
42. Simonsen, A., et al., *Promoting basal levels of autophagy in the nervous system enhances longevity and oxidant resistance in adult Drosophila.* Autophagy, 2008. **4**(2): p. 176-184.
43. He, C., et al., *Exercise-induced BCL2-regulated autophagy is required for muscle glucose homeostasis.* Nature, 2012. **481**(7382): p. 511-515.
44. Singh, R., et al., *Autophagy regulates lipid metabolism.* Nature, 2009. **458**(7242): p. 1131-1135.
45. Kouroku, Y., et al., *ER stress (PERK//eIF2[alpha] phosphorylation) mediates the polyglutamine-induced LC3 conversion, an essential step for autophagy formation.* Cell Death Differ, 2006. **14**(2): p. 230-239.

46. Park, Y.-E., et al., *Autophagic degradation of nuclear components in mammalian cells.* Autophagy, 2009. **5**(6): p. 795-804.
47. Kotoulas, O.B., S.A. Kalamidas, and D.J. Kondomerkos, *Glycogen autophagy in glucose homeostasis.* Pathology - Research and Practice, 2006. **202**(9): p. 631-638.
48. Vadlamudi, R.K., et al., *p62, a Phosphotyrosine-independent Ligand of the SH2 Domain of p56lck, Belongs to a New Class of Ubiquitin-binding Proteins.* Journal of Biological Chemistry, 1996. **271**(34): p. 20235-20237.
49. Pankiv, S., et al., *p62/SQSTM1 Binds Directly to Atg8/LC3 to Facilitate Degradation of Ubiquitinated Protein Aggregates by Autophagy.* Journal of Biological Chemistry, 2007. **282**(33): p. 24131-24145.
50. Lamark, T., et al., *Interaction Codes within the Family of Mammalian Phox and Bem1p Domain-containing Proteins.* Journal of Biological Chemistry, 2003. **278**(36): p. 34568-34581.
51. Zheng, Y.T., et al., *The Adaptor Protein p62/SQSTM1 Targets Invading Bacteria to the Autophagy Pathway.* The Journal of Immunology, 2009. **183**(9): p. 5909-5916.
52. Geisler, S., et al., *PINK1/Parkin-mediated mitophagy is dependent on VDAC1 and p62/SQSTM1.* Nature Cell Biology, 2010. **12**(2): p. 119-131.
53. Kim, P.K., et al., *Ubiquitin signals autophagic degradation of cytosolic proteins and peroxisomes.* Proceedings of the National Academy of Sciences, 2008. **105**(52): p. 20567-20574.
54. Kuo, T.-C., et al., *Midbody accumulation through evasion of autophagy contributes to cellular reprogramming and tumorigenicity.* Nature Cell Biology, 2011. **13**(10): p. 1214-1223.
55. Thurston, T.L.M., et al., *The TBK1 adaptor and autophagy receptor NDP52 restricts the proliferation of ubiquitin-coated bacteria.* Nat Immunol, 2009. **10**(11): p. 1215-1221.
56. Wild, P., et al., *Phosphorylation of the Autophagy Receptor Optineurin Restricts Salmonella Growth.* Science, 2011.
57. Novak, I., et al., *Nix is a selective autophagy receptor for mitochondrial clearance.* EMBO Rep, 2010. **11**(1): p. 45-51.
58. Jiang, S., C.D. Wells, and P.J. Roach, *Starch-binding domain-containing protein 1 (Stbd1) and glycogen metabolism: Identification of the Atg8 family interacting motif (AIM) in Stbd1 required for interaction with GABARAPL1.* Biochemical and Biophysical Research Communications, 2011. **413**(3): p. 420-425.
59. Lynch-Day, M.A. and D.J. Klionsky, *The Cvt pathway as a model for selective autophagy.* Febs Letters, 2010. **584**(7): p. 1359-1366.
60. Yoshihisa, T. and Y. Anraku, *A novel pathway of import of alpha-mannosidase, a marker enzyme of vacuolar membrane, in Saccharomyces cerevisiae.* Journal of Biological Chemistry, 1990. **265**(36): p. 22418-25.
61. Klionsky, D.J., R. Cueva, and D.S. Yaver, *Aminopeptidase I of Saccharomyces cerevisiae is localized to the vacuole independent of the secretory pathway.* The Journal of Cell Biology, 1992. **119**(2): p. 287-299.
62. Oda, M.N., et al., *Identification of a cytoplasm to vacuole targeting determinant in aminopeptidase I.* The Journal of Cell Biology, 1996. **132**(6): p. 999-1010.
63. Yorimitsu, T. and D.J. Klionsky, *Atg11 Links Cargo to the Vesicle-forming Machinery in the Cytoplasm to Vacuole Targeting Pathway.* Molecular Biology of the Cell, 2005. **16**(4): p. 1593-1605.
64. Shintani, T., et al., *Mechanism of Cargo Selection in the Cytoplasm to Vacuole Targeting Pathway.* Developmental Cell, 2002. **3**(6): p. 825-837.
65. Okamoto, K., N. Kondo-Okamoto, and Y. Ohsumi, *Mitochondria-Anchored Receptor Atg32 Mediates Degradation of Mitochondria via Selective Autophagy.* Developmental Cell, 2009. **17**(1): p. 87-97.
66. Kanki, T., et al., *Atg32 Is a Mitochondrial Protein that Confers Selectivity during Mitophagy.* Developmental Cell, 2009. **17**(1): p. 98-109.

67. Dunn, W.A., et al., *Pexophagy: the selective autophagy of peroxisomes.* Autophagy, 2005. **1**(2): p. 75-83.
68. Geng, J. and D.J. Klionsky, *Quantitative regulation of vesicle formation in yeast nonspecific autophagy.* Autophagy, 2008. **4**(7): p. 955-957.
69. Jogl, G., et al., *Crystal structure of the BEACH domain reveals an unusual fold and extensive association with a novel PH domain.* EMBO J, 2002. **21**(18): p. 4785-4795.
70. Clausen, T.H., et al., *p62/SQSTM1 and ALFY interact to facilitate the formation of p62 bodies/ALIS and their degradation by autophagy.* Autophagy, 2010. **6**(3): p. 330-344.
71. Filimonenko, M., et al., *The Selective Macroautophagic Degradation of Aggregated Proteins Requires the PI3P-Binding Protein Alfy.* Molecular Cell, 2010. **38**(2): p. 265-279.
72. Simonsen, A., et al., *Alfy, a novel FYVE-domain-containing protein associated with protein granules and autophagic membranes.* Journal of Cell Science, 2004. **117**(18): p. 4239-4251.
73. Nezis, I.P., & Stenmark, H., *p62 at the Interface of Autophagy, Oxidative Stress Signaling, and Cancer.* Antioxidants & redox signaling, 2012.
74. Duran, A., et al., *p62 Is a Key Regulator of Nutrient Sensing in the mTORC1 Pathway.* Molecular Cell, 2011. **44**(1): p. 134-146.
75. Moscat, J. and M.T. Diaz-Meco, *p62: a versatile multitasker takes on cancer.* Trends in Biochemical Sciences, 2012(0).
76. Rodriguez, A., et al., *Mature-onset obesity and insulin resistance in mice deficient in the signaling adapter p62.* Cell Metabolism, 2006. **3**(3): p. 211-222.
77. Sanchez, P., et al., *Localization of Atypical Protein Kinase C Isoforms into Lysosome-Targeted Endosomes through Interaction with p62.* Mol. Cell. Biol., 1998. **18**(5): p. 3069-3080.
78. Laurin, N., et al., *Recurrent Mutation of the Gene Encoding sequestosome 1 (SQSTM1/p62) in Paget Disease of Bone.* The American Journal of Human Genetics, 2002. **70**(6): p. 1582-1588.
79. Durán, A., et al., *The Atypical PKC-Interacting Protein p62 Is an Important Mediator of RANK-Activated Osteoclastogenesis.* Developmental Cell, 2004. **6**(2): p. 303-309.
80. Komatsu, M., et al., *The selective autophagy substrate p62 activates the stress responsive transcription factor Nrf2 through inactivation of Keap1.* Nature Cell Biology, 2010. **12**(3): p. 213-223.
81. Takamura, A., et al., *Autophagy-deficient mice develop multiple liver tumors.* Genes & Development, 2011. **25**(8): p. 795-800.
82. Inami, Y., et al., *Persistent activation of Nrf2 through p62 in hepatocellular carcinoma cells.* The Journal of Cell Biology, 2011. **193**(2): p. 275-284.
83. Sanz, L., et al., *The atypical PKC-interacting protein p62 channels NF-[kappa]B activation by the IL-1-TRAF6 pathway.* EMBO J, 2000. **19**(7): p. 1576-1586.
84. Xu, C. and J. Min, *Structure and function of WD40 domain proteins.* Protein & Cell, 2011. **2**(3): p. 202-214.
85. Wang, N., W.-I. Wu, and A. De Lozanne, *BEACH family of proteins: Phylogenetic and functional analysis of six Dictyostelium BEACH proteins.* Journal of Cellular Biochemistry, 2002. **86**(3): p. 561-570.
86. De Lozanne, A., *The Role of BEACH Proteins in Dictyostelium.* Traffic, 2003. **4**(1): p. 6-12.
87. Waterhouse, A.M., et al., *Jalview Version 2—a multiple sequence alignment editor and analysis workbench.* Bioinformatics, 2009. **25**(9): p. 1189-1191.
88. Sievers, F., et al., *Fast, scalable generation of high-quality protein multiple sequence alignments using Clustal Omega.* Mol Syst Biol, 2011. **7**.
89. Nagle, D.L., et al., *Identification and mutation analysis of the complete gene for Chediak-Higashi syndrome.* Nat Genet, 1996. **14**(3): p. 307-311.
90. Ward, D.M., et al., *Use of Expression Constructs to Dissect the Functional Domains of the CHS/Beige Protein: Identification of Multiple Phenotypes.* Traffic, 2003. **4**(6): p. 403-415.
91. Faigle, W., et al., *Deficient Peptide Loading and MHC Class II Endosomal Sorting in a Human Genetic Immunodeficiency Disease: the Chediak-Higashi Syndrome.* The Journal of Cell Biology, 1998. **141**(5): p. 1121-1134.

92. Rendu, F., et al., *Evidence that abnormal platelet functions in human Chediak-Higashi syndrome are the result of a lack of dense bodies.* The American Journal of Pathology, 1983. **111**(3): p. 307-14.
93. Zhao H, B.Y., Abdel-Malek Z, King RA, Nordlund JJ, Boissy RE., *On the analysis of the pathophysiology of Chediak-Higashi syndrome. Defects expressed by cultured melanocytes.* Lab Invest, 1994.
94. Introne, W., R.E. Boissy, and W.A. Gahl, *Clinical, Molecular, and Cell Biological Aspects of Chediak–Higashi Syndrome.* Molecular Genetics and Metabolism, 1999. **68**(2): p. 283-303.
95. Durchfort, N., et al., *The Enlarged Lysosomes in beigej Cells Result From Decreased Lysosome Fission and Not Increased Lysosome Fusion.* Traffic, 2012. **13**(1): p. 108-119.
96. Harris, E., et al., *Dictyostelium LvsB Mutants Model the Lysosomal Defects Associated with Chediak-Higashi Syndrome.* Molecular Biology of the Cell, 2002. **13**(2): p. 656-669.
97. Kypri, E., et al., *The BEACH Protein LvsB Is Localized on Lysosomes and Postlysosomes and Limits Their Fusion with Early Endosomes.* Traffic, 2007. **8**(6): p. 774-783.
98. Adam-Klages, S., et al., *FAN, a Novel WD-Repeat Protein, Couples the p55 TNF-Receptor to Neutral Sphingomyelinase.* Cell, 1996. **86**(6): p. 937-947.
99. Ségui, B., et al., *CD40 Signals Apoptosis through FAN-regulated Activation of the Sphingomyelin-Ceramide Pathway.* Journal of Biological Chemistry, 1999. **274**(52): p. 37251-37258.
100. Sánchez, C., et al., *The CB1 Cannabinoid Receptor of Astrocytes Is Coupled to Sphingomyelin Hydrolysis through the Adaptor Protein Fan.* Molecular Pharmacology, 2001. **59**(5): p. 955-959.
101. Ségui, B., et al., *Involvement of FAN in TNF-induced apoptosis.* The Journal of Clinical Investigation, 2001. **108**(1): p. 143-151.
102. Kreder, D., et al., *Impaired neutral sphingomyelinase activation and cutaneous barrier repair in FAN-deficient mice.* EMBO J, 1999. **18**(9): p. 2472-2479.
103. Werneburg, N., et al., *TNF-α-mediated lysosomal permeabilization is FAN and caspase 8/Bid dependent.* American Journal of Physiology - Gastrointestinal and Liver Physiology, 2004. **287**(2): p. G436-G443.
104. Möhlig, H., et al., *The WD repeat protein FAN regulates lysosome size independent from abnormal downregulation/membrane recruitment of protein kinase C.* Experimental Cell Research, 2007. **313**(12): p. 2703-2718.
105. Haubert, D., et al., *PtdIns(4,5)P-restricted plasma membrane localization of FAN is involved in TNF-induced actin reorganization.* EMBO J, 2007. **26**(14): p. 3308-3321.
106. Gebauer, D., et al., *Crystal Structure of the PH–BEACH Domains of Human LRBA/BGL†.* Biochemistry, 2004. **43**(47): p. 14873-14880.
107. Yang, W., et al., *Genome-Wide Association Study in Asian Populations Identifies Variants in ETS1 and WDFY4 Associated with Systemic Lupus Erythematosus.* PLoS Genet, 2010. **6**(2): p. e1000841.
108. Finley, K.D., et al., *blue cheese Mutations Define a Novel, Conserved Gene Involved in Progressive Neural Degeneration.* The Journal of Neuroscience, 2003. **23**(4): p. 1254-1264.
109. Rieger, K.-J., et al., *Large-scale phenotypic analysis—the pilot project on yeast chromosome III.* Yeast, 1997. **13**(16): p. 1547-1562.
110. Shiflett, S.L., et al., *Bph1p, the Saccharomyces cerevisiae Homologue of CHS1/Beige, Functions in Cell Wall Formation and Protein Sorting.* Traffic, 2004. **5**(9): p. 700-710.
111. Kwak, E., et al., *LvsA, a Protein Related to the Mouse Beige Protein, Is Required for Cytokinesis in Dictyostelium.* Molecular Biology of the Cell, 1999. **10**(12): p. 4429-4439.
112. Gerald, N.J., M. Siano, and A. De Lozanne, *The Dictyostelium LvsA Protein is Localized on the Contractile Vacuole and is Required for Osmoregulation.* Traffic, 2002. **3**(1): p. 50-60.
113. Su, Y., et al., *Neurobeachin Is Essential for Neuromuscular Synaptic Transmission.* The Journal of Neuroscience, 2004. **24**(14): p. 3627-3636.

114. Schwartz, J.H., *The many dimensions of cAMP signaling.* Proceedings of the National Academy of Sciences, 2001. **98**(24): p. 13482-13484.
115. Wang, X., et al., *Neurobeachin: A Protein Kinase A-Anchoring,beige/Chediak-Higashi Protein Homolog Implicated in Neuronal Membrane Traffic.* The Journal of Neuroscience, 2000. **20**(23): p. 8551-8565.
116. Niesmann, K., et al., *Dendritic spine formation and synaptic function require neurobeachin.* Nat Commun, 2011. **2**: p. 557.
117. Alvarez, V.A. and B.L. Sabatini, *Anatomical and Physiological Plasticity of Dendritic Spines.* Annual Review of Neuroscience, 2007. **30**(1): p. 79-97.
118. Castermans, D., et al., *The neurobeachin gene is disrupted by a translocation in a patient with idiopathic autism.* Journal of Medical Genetics, 2003. **40**(5): p. 352-356.
119. Castermans, D., et al., *SCAMP5, NBEA and AMISYN: three candidate genes for autism involved in secretion of large dense-core vesicles.* Human Molecular Genetics, 2010. **19**(7): p. 1368-1378.
120. Wang, J.-W., et al., *Identification of a Novel Lipopolysaccharide-Inducible Gene with Key Features of Both a Kinase Anchor Proteins and chs1/beige Proteins.* The Journal of Immunology, 2001. **166**(7): p. 4586-4595.
121. Wang, J.-W., et al., *Deregulated expression of LRBA facilitates cancer cell growth.* Oncogene, 2004. **23**(23): p. 4089-4097.
122. de Souza, N., et al., *SEL-2, the C. elegans neurobeachin/LRBA homolog, is a negative regulator of lin-12/Notch activity and affects endosomal traffic in polarized epithelial cells.* Development, 2007. **134**(4): p. 691-702.
123. Wech, I. and A.C. Nagel, *Mutations in rugose promote cell type-specific apoptosis in the Drosophila eye.* Cell Death Differ, 2005. **12**(2): p. 145-152.
124. Chen, J., et al., *Identification and characterization of NBEAL1, a novel human neurobeachin-like 1 protein gene from fetal brain, which is up regulated in glioma.* Molecular Brain Research, 2004. **125**(1-2): p. 147-155.
125. Gunay-Aygun, M., et al., *NBEAL2 is mutated in gray platelet syndrome and is required for biogenesis of platelet [alpha]-granules.* Nat Genet, 2011. **43**(8): p. 732-734.
126. Albers, C.A., et al., *Exome sequencing identifies NBEAL2 as the causative gene for gray platelet syndrome.* Nat Genet, 2011. **43**(8): p. 735-737.
127. Kahr, W.H.A., et al., *Mutations in NBEAL2, encoding a BEACH protein, cause gray platelet syndrome.* Nat Genet, 2011. **43**(8): p. 738-740.
128. Volders, K., K. Nuytens, and J. W.M. Creemers, *The Autism Candidate Gene Neurobeachin Encodes a Scaffolding Protein Implicated in Membrane Trafficking and Signaling.* Current Molecular Medicine, 2011. **11**(3): p. 204-217.
129. Introne WJ, W.W., Golas GA, Adams D, *Chediak-Higashi Syndrome*, ed. B.T. Pagon RA, Dolan CR, et al2009: Gene-reviews.
130. Blomberg, N., et al., *The PH superfold: a structural scaffold for multiple functions.* Trends in Biochemical Sciences, 1999. **24**(11): p. 441-445.
131. Smith, T.F., et al., *The WD repeat: a common architecture for diverse functions.* Trends in Biochemical Sciences, 1999. **24**(5): p. 181-5.
132. project, C. *High school biology resources*. Available from: http://www.copernicusproject.ucr.edu/ssi/HighSchoolBioResources/Genetic%20Engin%20Hum%20Genome/pcr.jpg.
133. online, B. *GATEWAY Cloning Technology—A Universal Cloning System*. 1999; Available from: http://www.bioresearchonline.com/doc.mvc/GATEWAY-Cloning-TechnologyA-Universal-Cloning-0001.
134. Technologies, A. *QuikChange Primer Design*. Available from: https://www.genomics.agilent.com/CollectionSubPage.aspx?PageType=Tool&SubpageType=ToolQCPD&PageID=15.

135. Technologies, A. *QuikChange I Site-Directed Mutagenesis Kits - Details & Specifications*. 2012; Available from: https://www.genomics.agilent.com/CollectionSubpage.aspx?PageType=Product&SubPageType=ProductData&PageID=388.
136. NCBI. *Basic Local Alignment Search Tool*. Available from: http://blast.ncbi.nlm.nih.gov/.
137. Hall, T.A., *BioEdit: a user-friendly biological sequence alignment editor and analysis program for Windows 95/98/NT.* Nucleic Acids Symposium Series, 1999. **41**: p. 95-98.
138. EMBI-EBI. *ClustalW2 Phylogeny*. Available from: http://www.ebi.ac.uk/Tools/phylogeny/clustalw2_phylogeny/.
139. Ashkenazy, H., et al., *ConSurf 2010: calculating evolutionary conservation in sequence and structure of proteins and nucleic acids.* Nucleic Acids Research, 2010. **38**(suppl 2): p. W529-W533.
140. Pupko, T., et al., *Rate4Site: an algorithmic tool for the identification of functional regions in proteins by surface mapping of evolutionary determinants within their homologues.* Bioinformatics, 2002. **18**(suppl 1): p. S71-S77.
141. EMBL-EBI. *MUSCLE Multiple Sequence Alignment*. Available from: http://www.ebi.ac.uk/Tools/msa/muscle/.
142. Schrodinger, LLC, *The PyMOL Molecular Graphics System, Version 1.3r1*, 2010.
143. Consurf, *python script for PyMOL, coloring atoms according to b-factor values.*
144. Peng, J. and J. Xu, *Raptorx: Exploiting structure information for protein alignment by statistical inference.* Proteins: Structure, Function, and Bioinformatics, 2011. **79**(S10): p. 161-171.
145. Szeto, J., et al., *ALIS are Stress-Induced Protein Storage Compartments for Substrates of the Proteasome and Autophagy.* Autophagy, 2006. **2**(3): p. 189-199.
146. Narendra, D., et al., *Parkin is recruited selectively to impaired mitochondria and promotes their autophagy.* J. Cell Biol., 2008. **183**(5): p. 795-803.